

Michael J. Schoning et. al. "Composition Measurement."

Copyright 2000 CRC Press LLC. <<http://www.engnetbase.com>>.

Michael J. Schöning

*Institut für Schicht-und Ionentechnik
Forschungszentrum Jülich*

Olaf Glück

*Institut für Schicht-und Ionentechnik
Forschungszentrum Jülich*

Marion Thust

*Institut für Schicht-und Ionentechnik
Forschungszentrum Jülich*

Mushtaq Ali

The National Grid Company plc

Behrooz Pahlavanpour

The National Grid Company plc

Maria Eklund

Nynas Naphthenics AB

E.E. Uzgiris

*General Electric Research and
Development Center*

J.Y. Gui

*General Electric Research and
Development Center*

Mushtaq Ali

The National Grid Company plc

C.K. Laird

*School of Applied Chemistry,
Kingston University*

Composition Measurement

- 70.1 Electrochemical Composition Measurement
Basic Concepts and Definitions • Voltammetry •
Potentiometry • Conductometry • Coulometry
- 70.2 Thermal Composition Measurement
Thermogravimetry • Measurement of α and $d\alpha/dt$ •
Thermometric Titrimetry • Thermomechanical Analysis •
Differential Thermal Analysis and Differential Scanning
Calorimetry • Specialized Techniques
- 70.3 Kinetic Methods
Theoretical Aspects • Experimental • Catalytic Reactions •
Noncatalytic Reactions
- 70.4 Chromatography Composition Measurement
Principles • Gas Chromatography • Liquid Chromatography •
Hyphenated Techniques • Applications in the Electricity
Industry

70.1 Electrochemical Composition Measurement

Michael J. Schöning, Olaf Glück, and Marion Thust

Electrochemical analysis in liquid solutions is concerned with the measurement of electrical quantities, such as potential, current, and charge, to gain information about the composition of the solution and the reaction kinetics of its components. The main techniques are based on the quantitative determination of reagents needed to complete a reaction or the reaction products themselves. Four traditional methods of electrochemistry are described here (Figure 70.1): potentiometry, voltammetry, coulometry, and conductometry. Potentiometry implies the measurement of an electrode potential in a system in which the electrode and the solution are in electrochemical equilibrium. Voltammetry is a technique in which the potential is controlled according to some prescribed function while the current is measured. Coulometry involves the measurement of charge needed to completely convert an analyte, and conductometry determines the electrical conductivity of the investigated test solution. The practical applications of these measurement techniques for analytical purposes range from industrial process control and environmental monitoring to food analysis and biomedical diagnostics. Both the analytical methods and their instrumentation as well as recent trends, such as electrochemical sensors are discussed.

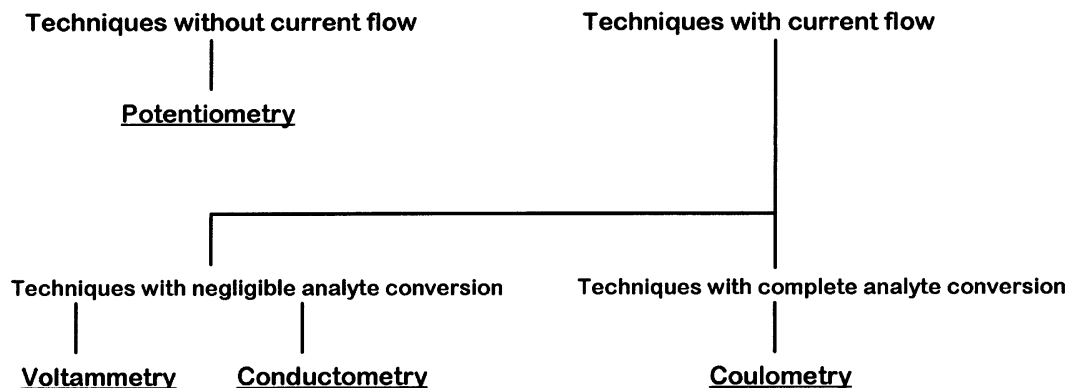


FIGURE 70.1 Electrochemical methods described in this section.

Basic Concepts and Definitions

Electrodes and the Electrical Double Layer

In electrochemistry, *electrodes* are devices for the detection of charge transfer and charge separation at phase boundaries or for the generation and variation of the charge transfer and separation with an impressed current across the phase boundary. One important feature of electrodes is a potential difference across the electrode/electrolyte phase boundary. At this interface, the conduction mechanism changes since electrode materials conduct the current via electrons whereas electrolytes conduct via ions. To understand the processes that lead to the formation of the potential difference, it is helpful to consider first an atomistic model, which was given by Helmholtz. It leads to the idea of an *electrical double layer*.

If an electrode is immersed in an electrolyte solution, the bulk regions of the two homogeneous phases — the electrode material and the electrolyte — are in equilibrium. This means that far away from the phase boundary ($>1 \mu\text{m}$), the sum of the forces on the particles is zero and charges are distributed homogeneously. Since the cohesion forces that bind the individual particles together in the bulk are significantly reduced at the surface of the electrode, particles in this region will have less neighbors or neighbors from the other phase. Thus, close to the phase boundary, the equilibrium conditions are drastically different from the equilibrium conditions in the bulk of the electrolyte. This change in the equilibrium of forces on particles at the interface can lead to an *interfacial tension*. In addition, the surface of a condensed phase usually has different electrical properties than the bulk phase, for example, due to the accumulation of free charge on the surface of an electrically charged solid. Besides, the orientation of dipoles in the surface region and adsorption of ions and dipoles from the electrolyte can lead to a change in the electrical properties. This excess charge from ions, electrons, and dipoles produces an electrical field that is accompanied by a potential difference across the phase boundary. The region in which these charges are present is termed the *electrical double layer*. The formation of an electrical double layer at interfaces is a general phenomenon but only the electrode/electrolyte interface will be considered here in more detail.

According to the hypothesis of Helmholtz, the electrical double layer has the character of a plate capacitor, whose plates consist of a homogeneously distributed charge in the metal electrode and ions of opposite charge lying in a parallel plane in the solution at a minimal distance from the surface of the electrode [1]. Modern conceptions are based on the assumption that the electron cloud in the metal extends to a certain degree into a thin layer of solvent molecules in the immediate vicinity of the electrode surface. In this layer, the dipoles of the solvent molecules (e.g., H_2O) are oriented to various degrees toward the electrode surface. Ions can accumulate in it due to electrostatic forces or be adsorbed specifically on the electrode through van der Waals and chemical forces. These substances are called *surface-active substances* or *surfactants*. The sum of oriented solvent molecules and surfactants in the immediate

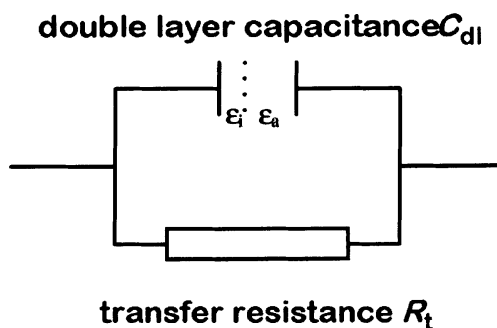
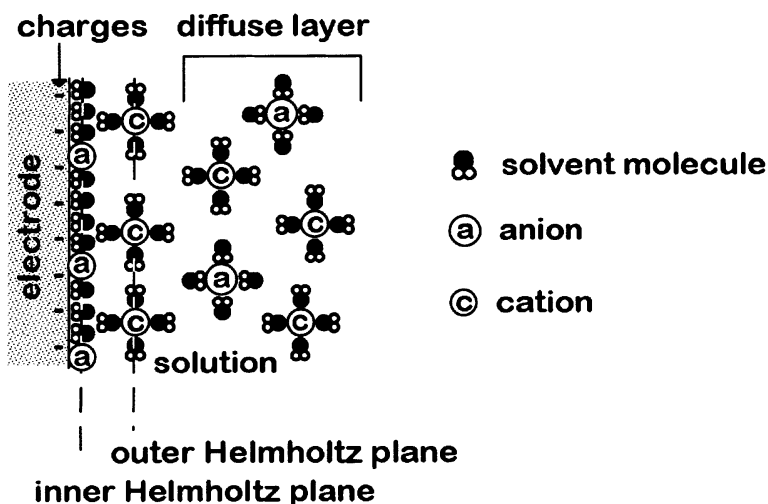


FIGURE 70.2 Electrical double layer according to the Helmholtz model and equivalent circuit representation.

vicinity of the electrode is considered as one layer. The plane through the centers of these molecules and ions parallel to the electrode surface is termed *inner Helmholtz plane* (Figure 70.2). If only electrostatic attraction is taken into account, ions from the solution can approach the surface to a distance given by their primary solvation sheaths. This means that at least a monomolecular solvent layer remains between the electrode and the solvated ion. The plane through the centers of these ions is called *outer Helmholtz plane*, and the solution region between the electrode surface and this outer Helmholtz plane is called *Helmholtz* or *compact layer*. In reality, electrostatic forces cannot retain ions at a minimal distance from the electrode surface. Due to thermal motion, the excess charge is smeared out in the direction of the electrolyte bulk to form a *diffuse layer*, also termed the *Gouy-Chapman layer*. It describes the region between the outer Helmholtz plane and the bulk of the solution. In concentrated electrolyte solutions (approx. 1 mol/L), the diffuse layer is as thin as the inner Helmholtz plane and may be considered as rigid. In highly dilute solutions, its thickness can be as large as 100 nm. As in the early model of Helmholtz, the double layer acts as a capacitor [2]. Here, two different dielectric layers with permittivities ϵ_i and ϵ_o represent the region between the electrode surface and the inner Helmholtz plane and the region between the inner and the outer Helmholtz plane, respectively (Figure 70.2).

In addition to these ideal electrostatic processes that lead to the formation of the electrical double layer, one has also to consider the transition of charge, ions and/or electrons from the electrode phase into the electrolyte phase or vice versa. In the equivalent circuit representation, such a charge transport through the double layer is symbolized as a transfer resistance R_t connected in parallel with the capacitor. If any charge transport through the double layer is excluded, the transfer resistance is nearly infinite. According to Ohm's law, any current impressed across the electrode surface leads to a high polarization voltage determining the electrode as *ideally polarizable*. One example of a polarizable electrode is the dropping mercury electrode, which is frequently used in polarography. In the opposite case with a nearly vanishing transfer resistance, the electrode is termed *ideally unpolarizable*. In the equivalent circuit representation, this corresponds to a short-circuit of the capacitor. The current flow then does not influence the voltage drop across the phase boundary. *Reference electrodes*, whose voltage have to be constant when immersed in an electrolyte, are nearly unpolarizable electrodes. Since every voltage measurement is accompanied by a small current flow, the difference between polarizable and unpolarizable electrodes is very important in measurement technique.

The Nernst Equation

If the electrode phase and the electrolyte phase contain a common ion, the potential difference across the phase boundary is determined by the effective concentration (activity) of this ion in the solution. This fact is described quantitatively by the *Nernst equation* and will be derived in the following. If one mole of ions of a species i has to be transferred from a given reference state outside into the bulk of an electrically charged phase work must be expended to overcome the chemical bonding forces and the electrical forces. This work is given by the electrochemical potential $\tilde{\mu}_i$. Since the chemical interactions of a species with its environment always possess electric components, generally the electrochemical potential cannot be separated into chemical and electrical parts. Nonetheless, the electrochemical potential is frequently given formally as a sum of the chemical potential μ_i and an electrostatic work $zF\phi$:

$$\tilde{\mu}_i = \mu_i + zF\phi \quad (70.1)$$

The chemical potential μ_i of an uncharged component of a system is the amount of Gibbs energy G inherent in 1 mol of that component [3]:

$$\mu_i = \left(\frac{\partial G}{\partial n_i} \right)_{p,T} \quad (70.2)$$

Here, n_i is the number of moles of the given component. In the case of a dilute solution, the chemical potential of a component i is

$$\mu_i = \mu_i^0 + RT \ln c_i \quad (70.3)$$

μ_i^0 denotes the standard chemical potential and c_i the concentration of the species i , R is the gas constant, and T is the absolute temperature. The values of standard chemical potentials can be found in standard textbooks of thermodynamics and in tables of physicochemical constants under the name standard molar Gibbs energies. μ_i^0 is independent of the concentration c_i . In concentrated electrolytes, the concentration c_i has to be replaced by the respective activity a_i . The activity a_i is given by the relationship $a_i = \gamma c_i$, where γ is the activity coefficient which is a correction factor for non-ideal behavior. In the second term of Equation 70.1, z denotes the charge number of the ion i , F is the Faraday constant, and ϕ is the *inner electric potential*, which is, in general, the electric work necessary for the transfer of a unit charge: for example, 1 coulomb, from infinity to a given site.

The inner electric potential may consist of two components, an *outer electric potential* ψ and a *surface electrical potential* χ . Whereas the outer electrical potential of a phase is produced by excess electric charge supplied from outside, the surface electric potential is an effect of electric forces at the interface which leads to the electrical double layer introduced above. The difference of the outer potentials of the electrode (e) and the solution (s):

$$\psi_e - \psi_s = \Delta\psi \quad (70.4)$$

is termed *Volta potential difference* and is the only measurable quantity. Neither the difference of the surface potentials of the appropriate phases $\Delta\chi$ nor the difference of the inner electric potentials:

$$\Delta\phi = \Delta\psi + \Delta\chi \quad (70.5)$$

defined as *Galvani potential difference*, can be measured directly. Strictly speaking, even the Volta potential difference between the solution and the electrode is a not measurable quantity since only the Volta potential difference between two electrodes can be measured. To determine the potential of the solution phase, one has to dip an electrode in the solution. This, however, creates a new electrode/solution interphase and, consequently, one measures the sum of two potential differences. This is the reason for the lack of absolute potentials in electrochemistry. Therefore, one uses a reference electrode that has a known potential relative to a standard electrode.

In thermodynamic equilibrium, the electrochemical potentials of the considered species are equal in both phases. For a charged particle i that may cross the phase boundary solution/electrode, this means

$$\mu_{i,s}^0 + RT \ln a_{i,s} + z_i F \phi_s = \mu_{i,e}^0 + RT \ln a_{i,e} + z_i F \phi_e \quad (70.6)$$

and therefore in equilibrium the Galvani potential difference is given by:

$$\Delta\phi = \phi_e - \phi_s = \frac{\mu_{i,s}^0 - \mu_{i,e}^0}{z_i F} + \frac{RT}{z_i F} \ln \frac{a_{i,s}}{a_{i,e}} \quad (70.7)$$

Since the chemical standard potential of the respective phases are constants, the first term in Equation 70.7 can be expressed as a standard Galvani potential difference $\Delta\phi^0$:

$$\Delta\phi = \Delta\phi^0 + \frac{RT}{z_i F} \ln \frac{a_{i,s}}{a_{i,e}} \quad (70.8)$$

For metal electrodes, the activity of the metal atoms M and that of the electrons in the electrode phase equal unity per definition. Thus, for an electrode reaction of type:



Equation 70.8 becomes the *Nernst equation*

$$\Delta\phi = \Delta\phi^0 + \frac{RT}{zF} \ln a_s \quad (70.10)$$

which gives the relation between the activity of the potential determining ion a_s and the Galvani potential difference $\Delta\phi$. Using base 10 logarithm, the Nernst equation is given as:

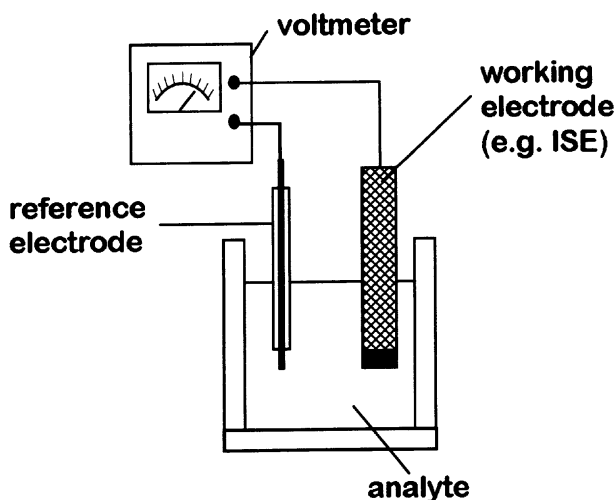


FIGURE 70.3 Schematic of an electrochemical cell with a working electrode and a reference electrode immersed in the test solution (electrolyte).

$$\Delta\phi = \Delta\phi^0 + \frac{RT \cdot 2.3}{zF} \log a_s = \Delta\phi^0 + k \cdot \log a_s \quad (70.11)$$

where k is called *Nernst constant*.

The classical form of the Nernst equation (Equation 70.10) can be formulated more generally for a redox reaction. If a_{ox} and a_{red} are the activities of the oxidized and reduced form of the considered ion, the Galvani potential difference is given as:

$$\Delta\phi = \Delta\phi^0 + \frac{RT}{zF} \ln \frac{a_{\text{ox}}}{a_{\text{red}}} \quad (70.12)$$

In *potentiometry*, the activity of a certain ion can be determined directly by the measurement of the equilibrium Galvani potential difference of a suitable electrode (*direct potentiometry*). On the other hand, changes of the activity of the detected ion and equivalence points can be detected in titration reactions (*potentiometric endpoint titration*).

After this rather theoretical definition of the Galvani potential difference, the question arises how to *measure* this potential difference between the bulk of the electrode and the solution. Since a potential difference cannot be measured with only one electrode, a second one must be immersed in the solution. Both are connected to a voltmeter, to complete the *electrochemical cell* (Figure 70.3). An electrochemical cell generally consists of two (or more) electrodes immersed in an analyte. Thus, in some of the old literature, a single electrode is often referred to as a *half-cell* and its potential is called *half-cell potential*. In modern electrochemistry, usually the term *electrode potential* is used. An electrochemical cell is in a current-free state during potentiometric measurements (e.g., with an *ion-selective electrode* (ISE)), but may also supply electric energy (a galvanic cell) or accept electric energy from an external source (an electrolytic cell). Since a second electrode potential arises at the phase boundary second electrode/electrolyte, only the sum of at least two Galvani potential differences can be measured. A separation into the two individual parts is impossible. Hence, the function of the second electrode, named reference electrode, is to act as an electrode of constant potential against which variations in the potential of the measuring electrode in various samples can be measured. In the Nernst equation, the Galvani potential ϕ is then replaced by E , the symbol for measurable voltages.

Classification of Electrodes

Electrodes are termed *reversible electrodes* if they transfer electrons and ions with negligible impedance. Therefore, under current, the electrochemical potential of electrons, ions, and neutral species do not change across the different interfaces that may exist in an electrode. Otherwise, the electrode is not suitable to measure thermodynamic (equilibrium) quantities such as ion activity. Since a distribution equilibrium of charged species is considered here, the electrode and the solution phase must have at least one charged species in common. Depending on the number of equilibria being involved in the forming of the electrode potential, reversible electrodes can be divided into different groups:

1. *Electrodes of the first kind.* These may be cationic or anionic electrodes at which equilibrium is established between the atoms or molecules in the electrode material and the respective cations or anions in the solution. According to the Nernst equation, the equilibrium Galvani potential difference is here determined by the activity of the considered ion in the solution. Examples for electrodes of the first kind are ISEs including metal and amalgam electrodes and the hydrogen electrode.
2. *Electrodes of the second kind.* These electrodes consist of three phases. A metal wire is covered by a layer of its sparingly soluble salt which usually has the character of a solid electrolyte (e.g., Ag and AgCl). This wire is immersed in a solution containing a soluble salt of the anions of this solid electrolyte (e.g., KCl). Here, the equilibrium between the Ag atoms in the metal and the anions in the solution is established through two equilibria: The first one is given between the metal and the cation in its sparingly soluble salt; for example,



and the second one between the anion in the sparingly soluble salt and the anion in the solution; for example,



The electrode potential of electrodes of the second kind is rather insensitive to small current flows. Thus, they are often used as reference electrodes.

3. *Electrodes of the third kind.* In this electrode, the sparingly soluble salt contains a second cation that also forms a sparingly soluble compound with the common anion but with a higher solubility product than the electrode metal compound (e.g., Ag₂S and PbS). Here, the electrode potential depends on the activity of this cation in the solution.
4. *Oxidation-reduction (redox) electrodes.* They consist of an inert metal such as Pt, Au, or Hg that is immersed in a solution of two soluble oxidation forms of a single substance (e.g., Fe³⁺ and Fe²⁺). Thus, for the electrode reaction:



the Nernst equation is:

$$E_{\text{Fe}^{3+}/\text{Fe}^{2+}} = E_{\text{Fe}^{3+}/\text{Fe}^{2+}}^0 + \frac{RT}{F} \ln \frac{a_{\text{Fe}^{3+}}}{a_{\text{Fe}^{2+}}} \quad (70.16)$$

according to Equation 70.10. Here, E is termed the *electrode potential* and E^0 is designated the *standard electrode* (or *redox*) *potential* of the electrode reaction if it is measured versus the *standard hydrogen electrode* (SHE). The subscripts of E and E^0 denote the redox couple of the considered

TABLE 70.1 Some Standard Electrode Potentials and Redox Potentials

Electrode or Half-Cell Reaction	E^0 (V)
$\text{Li}^+ + \text{e}^- \leftrightarrow \text{Li}$	-3.0403
$\text{K}^+ + \text{e}^- \leftrightarrow \text{K}$	-2.931
$\text{Ca}^{2+} + 2\text{e}^- \leftrightarrow \text{Ca}$	-2.868
$\text{Mg}^{2+} + 2\text{e}^- \leftrightarrow \text{Mg}$	-2.372
$\text{Al}^{3+} + 3\text{e}^- \leftrightarrow \text{Al}$	-1.662
$\text{Zn}^{2+} + 2\text{e}^- \leftrightarrow \text{Zn}$	-0.762
$\text{Fe}^{2+} + 2\text{e}^- \leftrightarrow \text{Fe}$	-0.447
$\text{Pb}^{2+} + 2\text{e}^- \leftrightarrow \text{Pb}$	-0.1264
$\text{AgCl} + \text{e}^- \leftrightarrow \text{Ag} + \text{Cl}^-$	0.22216
$\text{Hg}_2\text{Cl}_2 + 2\text{e}^- \leftrightarrow 2\text{Hg} + 2\text{Cl}^-$	0.26791
$\text{Cu}^{2+} + 2\text{e}^- \leftrightarrow \text{Cu}$	0.3417
$\text{I}_2 + 2\text{e}^- \leftrightarrow 2\text{I}^-$	0.5353
$\text{Fe}^{3+} + \text{e}^- \leftrightarrow \text{Fe}^{2+}$	0.771
$\text{Ag}^+ + \text{e}^- \leftrightarrow \text{Ag}$	0.7994
$\text{Tl}^{3+} + 2\text{e}^- \leftrightarrow \text{Tl}^+$	1.2152
$2\text{Cl}^- \leftrightarrow \text{Cl}_2 + 2\text{e}^-$	1.35793
$\text{Ce}^{4+} + \text{e}^- \leftrightarrow \text{Ce}^{3+}$	1.610

electrode reaction. The standard redox potential is a measure of the reducing or oxidizing ability of a substance. If one considers, for example, two systems 1 and 2 with their respective standard redox potentials E_1^0 and E_2^0 , system 1 is a stronger oxidant than system 2 if $E_1^0 > E_2^0$. This means that in a mixture of the solutions of these two systems where originally the activities of the reduced forms equal that of the oxidized forms ($a_{\text{red}}^1 = a_{\text{ox}}^1$ and $a_{\text{red}}^2 = a_{\text{ox}}^2$), an equilibrium will be established with $a_{\text{ox}}^2 > a_{\text{red}}^2$ and $a_{\text{red}}^1 > a_{\text{ox}}^1$. The experimentally determined standard potentials of well-known redox systems are listed in Reference 4. Table 70.1 gives some examples. In redox electrodes, the metal acts as a medium for the electron transfer between the two forms. In contrast to electrodes of the first kind, the solution should not contain ions of the electrode metal in order to avoid an additional Galvani potential difference at the electrode determined by the activity of the electrode metal ions in the solution. This disturbing ion activity is negligible if the standard potential of the electrode metal is a few 100 mV higher than the redox potential to be measured. Thus, mainly platinum electrodes ($E_{\text{Pt}^{2+}/\text{Pt}}^0 = 1.20$ V) and gold electrodes ($E_{\text{Au}^+/\text{Au}}^0 = 1.42$ V) are used as redox electrodes.

Reference Electrodes

The potential of an ion-selective electrode (ISE) is always measured with respect to a reference electrode. Ideally, the reference electrode should not cause chemical changes in the sample solution, or vice versa. It should maintain a constant potential relative to the sample solution, regardless of its composition. In practice, any changes of its potential with composition should be at least as small as possible and reproducible. Reference electrodes with liquid junctions, strictly speaking reference electrode *assemblies*, consist of a reference element immersed in a filling solution (often called bridge solution) contained within the electrode. This reference element should possess a fixed activity of the ion defining the potential of the element with respect to the filling solution. The electric contact between the electrode and the sample solution is made by the liquid junction consisting of a porous plug or a flow restriction which permits the filling solution to flow very slowly into the sample.

At the junction between the two electrolyte solutions, ions from both solutions diffuse into each other. Since different ions have different mobilities, they will diffuse at different rates. Thus, a charge separation will occur related in size to the difference in mobilities of the anions and cations in the two solutions. This charge separation produces a potential difference across the junction called the *liquid junction potential* [5]. In reference electrodes, usually the bridge solution is given a slightly higher pressure than the sample so that the solution, often concentrated potassium chloride, flows out relatively rapidly into

the sample, and diffusion of the sample back into the salt bridge is impeded. If the bridge solution is concentrated enough, it is assumed that variations in the liquid junction potential due to the varying composition of the sample are suppressed. This is the basis on which the reference electrode assembly is used. Since the potential of the whole assembly E_{ref} is the sum of the potential of the reference element E_r in the bridge solution and the liquid junction potential E_j :

$$E_{\text{ref}} = E_r + E_j \quad (70.17)$$

any change in the liquid junction potential appears as a change in the potential of the assembly. An extra liquid junction potential must be included if a *double junction* reference electrode is considered. When an analysis using a cell with an ion-selective electrode is carried out, standard solutions are used to calibrate the ISE. A change in the liquid junction potential that occurs when the standard solutions are replaced by the sample is termed the *residual liquid junction potential* and constitutes an error in the analytical measurement. The needed constancy of the potential can be approached by a suitable choice of standards and/or sample pretreatment, and by the use of a proper bridge solution and the best physical form of the liquid junction.

Several types of liquid junctions exist from which the best ones with regard to stability and reproducibility are complicated to realize in practice, and the worst ones are easy to use but much less stable and reproducible. Most of the commercial reference electrodes with adequate properties possess *restrained diffusion junctions* where the most common junctions available are the ceramic plug, the asbestos wick or fiber, two types of ground sleeve junction, and the palladium annulus junction (Figure 70.4). For a very large majority of applications with ion-selective electrodes, a ceramic plug will perform adequately. The flow rate of the bridge solution into the sample solution is sometimes called leak rate and is given

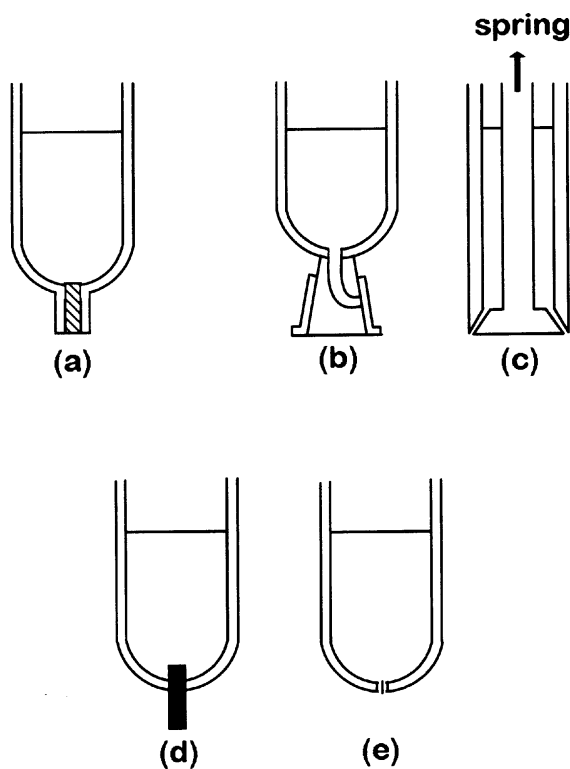


FIGURE 70.4 Different types of liquid junctions: (a) ceramic plug, (b) ground glass sleeve (type 1), (c) ground glass sleeve (type 2), (d) asbestos wick, (e) palladium annulus.

in mL per 5 cm head of bridge solution per day. The head of bridge solution is measured as the height of the surface of the bridge solution above the surface of the sample. In order to work satisfactorily, the surface of the bridge solution of all these restricted junction devices has to be at least 1 cm above the sample solution. Otherwise, if the bridge solution falls too low, the junction and the bridge will become contaminated by species diffusing from the sample. The bridge solution has then to be replaced. For the same reason, reference electrodes should be stored, when not in use, with the junction immersed in bridge solution.

Whereas the ceramic plug and the asbestos wick and fiber (Figure 70.4(a) and (d)) have relatively slow flow rates of about 0.01 to 0.1 mL per 5 cm head of bridge solution per day, ground sleeve junctions of type (b) have a flow rate of 1 to 2 mL. On the other hand, the flow rates of different asbestos wick junctions may vary by a factor up to 100 and the liquid junction potential may have a day-to-day (in)stability of ± 2 mV under the favorable conditions of a junction between strong potassium chloride solution and an intermediate pH buffer. Under the same conditions, ground glass sleeve junctions of type (b) and the little-used palladium annulus junction show stabilities of ± 0.06 mV and ± 0.2 mV, respectively. It is worth mentioning that palladium annulus junctions may partly respond as a redox electrode in strong oxidants (e.g., 0.2 M KMnO_4 in 0.05 M H_2SO_4) and mild or strong reductants (e.g., 0.5 M SnCl_2 in 1 M HCl). In such samples, reference electrodes with palladium or platinum annulus junctions should not be used. Although ground glass sleeve junctions have inconveniently high flow rates and the bridge solution needs to be replenished frequently, these junction types have found particular use in applications where the junction has the tendency to clog, such as measurements in protein solutions. However, the stability of the liquid junction potential appears to be relatively poor in fast-flowing sample solutions and may be very sensitive to sample flow rate. Asbestos wick junctions are particularly liable to blockage and should consequently be used in clear solutions only.

In *double-junction reference electrodes*, the filling solution in which the reference element is immersed (reference solution) makes contact with another solution, the bridge solution, by means of a liquid junction. A second liquid junction enables contact to be made between the bridge solution and the sample. Such electrodes are useful when it is essential that contamination of the sample by the inner filling solution must be kept at a very low level. The outer bridge solution can be selected to be compatible with the sample. In order to minimize the liquid junction potentials that can drift and cause instability, the bridge solution should be equitransferent; that is, the transport numbers of its anion and cation should be nearly equal. However, the complication of a second liquid junction in the cell should be avoided if possible.

The Standard Hydrogen Electrode.

Aqueous solutions are of major concern in electrochemistry because of their hydrogen ion content. Thus, it is advantageous to use a reference electrode where a reaction occurs that involves the participation of hydrogen ions. One of this reactions is:



Figure 70.5 shows a hydrogen electrode. A hydrogen electrode usually consists of a platinum sheet covered by a thin layer of sponge-like structured platinum, so-called platinum black, that has a high specific surface area. This electrode is rinsed with pure gaseous hydrogen in order to form a complete layer of adsorbed H_2 molecules at the surface. If this electrode is immersed in an electrolyte, it acts as an electrode consisting of hydrogen at which the gaseous hydrogen is oxidized to hydronium ions or the hydronium ions are reduced to hydrogen, respectively, according to Equation 70.18. The real mechanism of this electrode process is rather complicated because the platinum electrode is in contact with the hydronium ions in the solution as well as with the gaseous hydrogen that is bubbled through it. Thus, the final equilibrium between the gaseous hydrogen, the dissolved hydronium ions, and the electrode phase consists of several successive equilibrium steps which can be found in Reference 6. To calculate the

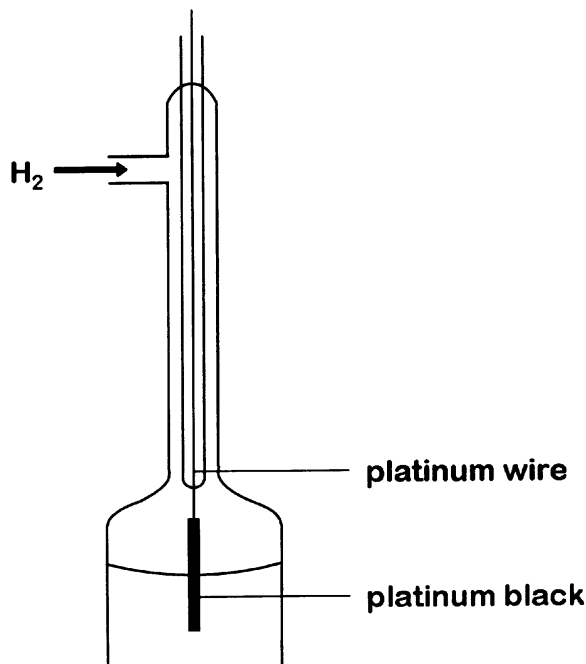


FIGURE 70.5 Schematic of a hydrogen electrode.

potential of a hydrogen electrode, which is strictly speaking the difference between the potential of the electrode and that of the solution, one has to consider the electrochemical potentials of the respective phases. The chemical potential of gases is usually expressed in terms of the pressure p instead of the molar concentration c . Due to the elementary relationship $pV = nRT$ for ideal gases, where V is the volume of the gas and n is the amount of moles the pressure, p is proportional to the molar concentration $c = n/V$. Thus, according to Equation 70.3:

$$\mu_{\text{H}_2} = \mu_{\text{H}_2}^0 + RT \ln \frac{p_{\text{H}_2}}{p_{\text{H}_2}^0} \quad (70.19)$$

where μ_{H_2} and $\mu_{\text{H}_2}^0$ are the pressure and standard pressure of hydrogen, respectively. In the case of moderate ion concentrations, the chemical potential of the solvent water is equal to its standard chemical potential. Hence, the potential difference between the electrode and the solution is, according to Equation 70.7:

$$\Delta\phi = \frac{\mu_{\text{H}_3\text{O}^+}^0 - \frac{1}{2}\mu_{\text{H}_2}^0 - \mu_{\text{H}_2\text{O}}^0}{F} + \frac{RT}{F} \ln c_{\text{H}_3\text{O}^+} - \frac{RT}{2F} \ln \frac{p_{\text{H}_2}}{p_{\text{H}_2}^0} \quad (70.20)$$

This equation is generally valid for hydrogen electrodes. The electrode is called *standard hydrogen electrode* (SHE) if the molar concentration is such that the activity of the hydronium ions is unity ($a_{\text{H}_3\text{O}^+} = 1$) and the pressure of hydrogen is equal to its standard pressure. Hence, for an SHE, the second and third term in Equation 70.20 vanish. The combination of standard chemical potentials in the first term of Equation 70.20 is defined as zero. Consequently, the total potential difference across the interface SHE/electrolyte is equal to zero *by definition* at any temperature. Since standard hydrogen electrodes are very difficult to prepare, they are not used as reference electrodes in practice. However, electrode potentials are usually standardized with respect to the SHE and their values are thus called “on the hydrogen scale.”

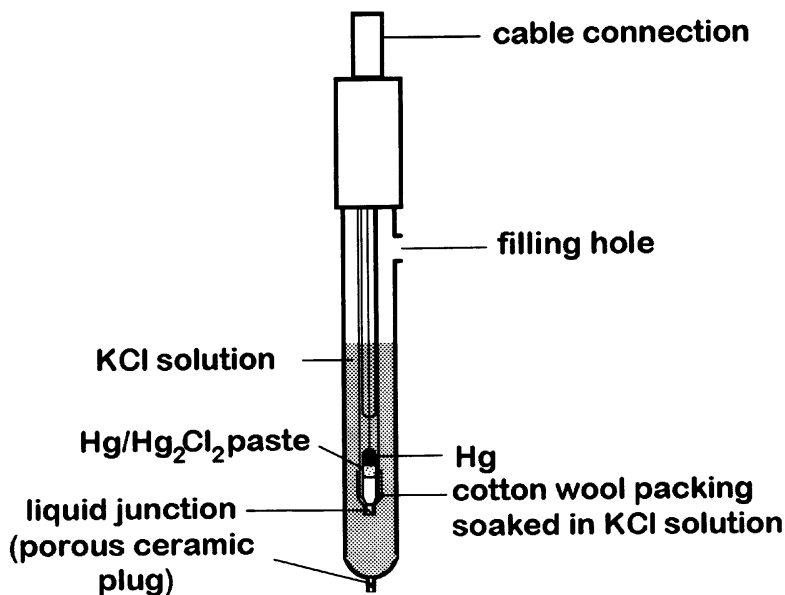


FIGURE 70.6 Schematic of a calomel reference electrode.

The Calomel Electrode.

The calomel electrode is the most common of all reference electrodes. It consists of a pool of mercury that is covered by a layer of mercurous chloride (calomel, Hg_2Cl_2). The calomel is in contact with a reference solution that is nearly always a solution of potassium chloride, saturated with mercurous chloride. Thus, the calomel electrode is a typical electrode of the second kind. Figure 70.6 shows a typical arrangement of a commercial calomel electrode assembly where the electrode is inverted, with the mercury uppermost, and packed into a narrow tube. Depending on the strength of the potassium chloride solution used, the electrode is called saturated calomel electrode (SCE), 3.8 *M* or 3.5 *M* calomel electrode, respectively. Potassium chloride is used as reference solution because it gives rise to a small liquid junction potential at the outer liquid junction of the electrode, i.e., the liquid junction with the sample. Hence, potassium chloride is a suitable reference solution as well as a good bridge solution. Furthermore, mercurous chloride has a very low solubility in potassium chloride solutions, regardless of concentration. The electrode reaction of a calomel electrode is:



Its standard potential, including the liquid junction, is 0.2444 V vs. SHE at 25°C for the SCE, and 0.2501 V for the 3.5 *M* calomel electrode according to Reference 7. Further data are given, for example, in Reference 8.

The components of a calomel electrode are chemically stable except for the mercurous chloride, which significantly disproportionates at temperatures above 70°C according to the equation:



Hence, potential drift occurs and life time decreases with increasing working temperature. On the other hand, calomel electrodes can be used at temperatures down to -30°C if 50% glycerol is added to the potassium chloride solution.

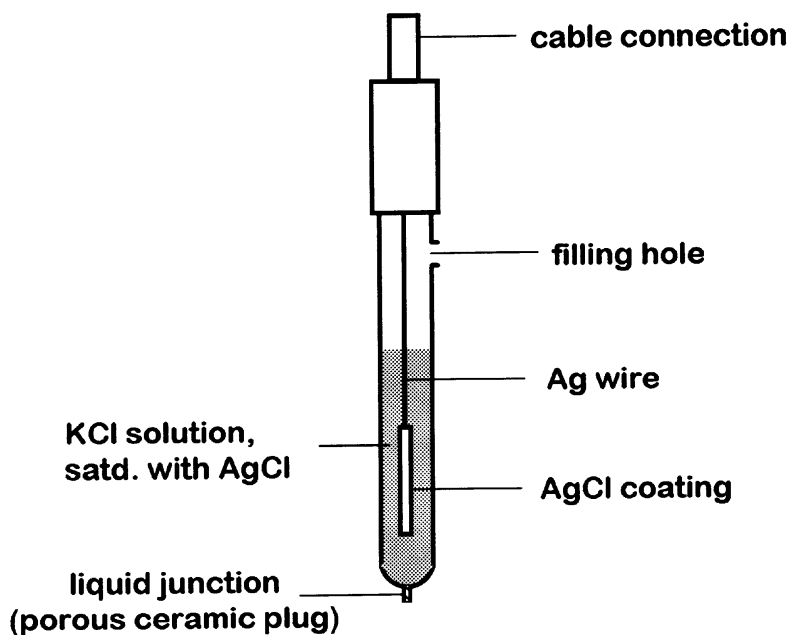


FIGURE 70.7 Schematic of a Ag/AgCl reference electrode.

Impurities in the potassium chloride solution, such as bromide and sulfide ions as well as redox agents and complexants, cause a small shift in the electrode potential. Nevertheless, the measurement of potential differences is not affected. However, the most unsatisfactory feature of the performance of the calomel electrode is its thermal hysteresis that occurs if the electrode filling material is not in thermal equilibrium or if the electrode and the sample have different temperatures. Thus, temperature stability during the storage and measurements is very important. In any cases where the temperature of the reference electrode or the sample has to be varied, it is thus usually better to use a silver/silver chloride electrode instead of a calomel electrode.

The Silver/Silver Chloride Electrode.

The silver/silver chloride electrode consists of a silver wire or plate that is coated with silver chloride. For the same reasons as with the calomel electrode, this phase is in contact with a strong potassium chloride solution, here saturated with silver chloride. [Figure 70.7](#) shows the diagram of a typical Ag/AgCl reference electrode. Since this kind of reference electrode is the simplest and for many applications the most satisfactory one, it is commonly used as internal reference electrode of pH electrodes and other ion-selective electrodes. Besides, Ag/AgCl electrodes can be easily prepared in the laboratory. In contrast to mercury-based electrodes, the Ag/AgCl electrode does not contain toxic chemicals and is therefore recommendable for measurements in food.

The major problem with the Ag/AgCl electrode is the considerably high solubility of AgCl in concentrated potassium chloride solution. Thus, especially for the use at high temperatures, a sufficient excess of solid silver chloride must be present in the reference solution. This can be achieved, for example, through the addition of a few drops of diluted silver nitrate solution. Otherwise, silver chloride will dissolve off the electrode until saturation is reached. As a consequence, the electrode potential will drift and the lifetime of the electrode will be shortened. However, in contrast to the calomel electrode, the Ag/AgCl electrode can be used successfully up to 125°C. Its electrode potential is very stable in the long term in pure potassium chloride solutions, but is affected by impurities like redox reagents and species that react with the silver chloride, as with the calomel electrode. Unlike the calomel electrode, in the Ag/AgCl electrode, the concentration of the electrode coating in the bridge solution is rather high. Thus, a greater amount of reaction products (e.g., solid silver sulfide) may arise in the reference solution and

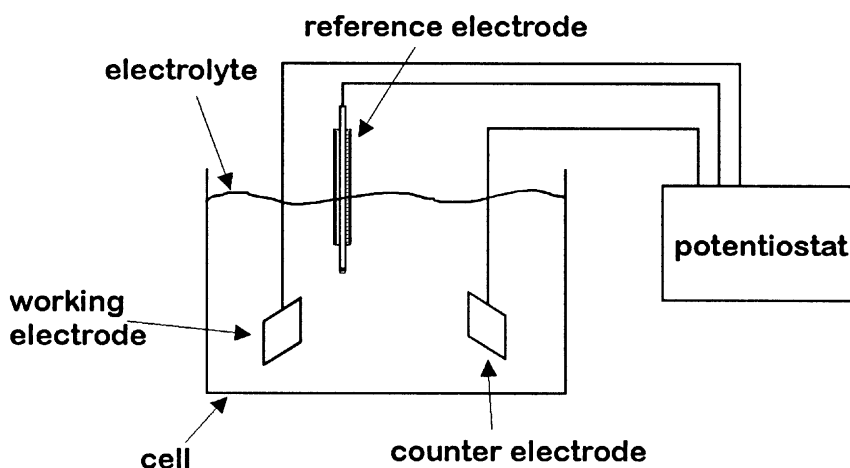


FIGURE 70.8 For voltammetric measurements a three electrode arrangement is usually employed.

block the liquid junction causing drift and instability of the electrode potential. In contrast to the calomel electrode, the silver/silver chloride electrode shows only very small thermal hysteresis effects that are usually negligible. Hence, this kind of electrode is suitable for measurements in samples with varying temperatures. Ag/AgCl electrodes are relatively insensitive to polarization. The standard potentials, including the liquid junction potentials of saturated and 3.5 M silver/silver chloride electrodes, at 25°C are 0.1989 V and 0.2046 V, respectively according to Reference 9. As with the calomel electrode, the nomenclature of the electrodes is derived from the potassium chloride concentration of the respective reference solution.

Voltammetry

The basic concept of *voltammetry* is the measurement of the current i at a redox electrode as a function of the electrode potential E . During the experiment, the electrode is immersed in a solution that contains an electroactive species; that is, a species that can undergo an electrode reaction (standard redox potential E^0). The electrode potential is changed from a value $E_1 < E^0$ to a value $E_2 > E^0$ or vice versa in a manner that is predetermined by the operator. Thus, during the measurement, the electrochemical equilibrium shifts from the oxidized (reduced) form of the analyte to the reduced (oxidized) form. The resulting charge transfer across the interface electrode/solution can be observed as a current flow, which is termed *faradaic*.

Instrumentation

Voltammetric measurements are usually performed with a cell arrangement of three electrodes (Figure 70.8). The redox electrode at which the electrode processes occurs is called *working electrode*. Its potential is measured against a suitable reference electrode, often Ag/AgCl or calomel. To adjust the potential difference between the working and the reference electrode to a certain value, a current is forced through the working electrode. Because the current and the electrode potential are related functionally, this current is unique. However, the current through the reference electrode must be kept as small as possible. Therefore, a third electrode called *auxiliary electrode* or *counter electrode* is usually employed to close the current circuit. It should be emphasized that there are two circuits: one in which the current flows and which contains the working and the auxiliary electrode and another, and a current-free one in which the potential difference between the working and the reference electrode is measured. Since almost no current flows through the reference electrode, its potential can be regarded as constant and the measured change in potential equals the potential change of the working electrode. The current

through the working electrode, and thus its potential, can be adjusted by controlling the voltage between the working and the auxiliary electrode. This task is performed by an instrument called a *potentiostat*, which basically consists of a voltage source and a high-impedance feedback loop. With a function generator, that may be integrated into the potentiostat, the potential–time course can be predetermined. Modern potentiostats are controlled by a PC and offer the possibility to program many different potential–time courses. Thus, they allow the performance of several voltammetric techniques, as are discussed below. The measured current can be displayed as a function of the electrode potential or of time using a strip-chart or *xy*-recorder or a PC.

There are two possibilities to operate an electrochemical cell. In so-called *batch cells*, the electrolyte solution rests stationary during the measurement, whereas in *flow-through cells*, it flows across the electrode. Between two measurements with different solutions the cell must be cleaned in order to remove residues of the preceding measurement's solution that could disturb the new measurement. The electrochemical cell is usually built of glass or teflon because of these materials' chemical inertness.

The chemical inertness is also important for the choice of the working electrode because the electrode must not change during the measurement. Common materials are gold, platinum, and mercury. Several kinds of carbon electrodes (e.g., glassy carbon) are also used but are often covered with gold or mercury. An advantage of the solid-state electrodes is their easy handling. They can be employed as planar or as wire electrodes. Further, with the noble metal electrodes, substances having a more positive redox potential than mercury can be investigated [10]. However, the use of mercury electrodes offers distinct advantages and the voltammetric techniques using mercury electrodes are extremely well developed. These techniques play a major role in electroanalytical methods and are summarized under the term *polarography*.

In polarography, mercury is either used as a *thin mercury film electrode* (TMFE) or as a *hanging mercury drop electrode* (HMDE). The HMDE can be a *stationary mercury drop electrode* (SMDE) or a *dropping mercury electrode* (DME). The drop is produced from a thin capillary with an inner diameter that can range from several ten to a few hundred micrometers. The size of an SMDE is held constant during the measurement, whereas a DME constantly grows during its lifetime until it falls from the capillary due to its weight.

The main advantages of mercury drop electrodes are their good reproducibility and their high *overpotential* for the hydrogen evolution; that is, the fact that hydrogen evolution is inhibited and thus occurs at much higher potentials than would be expected from the standard potential. The good reproducibility is achieved because a new drop can easily and rapidly be produced from the capillary for each measurement. Hence, the contamination of the electrode with substances from a preceding measurement and from impurities in the solution is near zero. However, a drawback of HMDEs is their relative mechanical instability, which can be a problem in flow-through cells, in field measurements, and if the solution is stirred.

Stirring of the solution is often applied during the measurement if the supply of reactive species at the electrode should be enhanced. However, this forced convection affects the electrode current. Moreover, the electrolyte is often stirred and bubbled with an inert gas like nitrogen or argon before voltammetric measurements are carried out to remove dissolved oxygen. This is usually necessary to reduce background currents from oxygen reduction and to prevent undesirable oxidation or precipitation of solution components. Because the electrode currents, especially in trace and ultra-trace analysis, can be quite small, it is common to place the cell in a Faradaic cage to shield it from electromagnetic stray fields. Coaxial cables are then used for the electric connections from the cell to the instruments.

Principles of Voltammetry

Actually, the electrode current measured in voltammetry is a sum of two currents that arise due to different processes. Besides the faradaic current i_f , a capacitive current i_c results from changes in the *double layer charging*. Although the faradaic current is a direct measure for the rate of the electrode reaction, several effects usually occur that have to be considered.

Diffusion Limitation of the Faradaic Current.

The decrease of the analyte concentration at the electrode surface due to an electrode reaction must be balanced by the diffusion of species from the bulk solution. In most measurements, the consumption of reactive species is faster than the supply by diffusion and the effect of *diffusion limitation* of the faradaic electrode current is observed. To understand this important point, the time-dependent concentration profile of the analyte has to be calculated using *Fick's laws*. The electrode current can then be derived as a function of time. According to Fick's first law, the flux j of the analyte at the point r and at the time t is proportional to the gradient of the analyte concentration c :

$$j(r, t) = -D\nabla c(r, t) \quad (70.23)$$

The proportionality factor D is called the *diffusion coefficient*. At the electrode surface, the flux must be equal to the number of moles N converted per unit of time and surface area by the electrode reaction:

$$j(0, t) = dN/dt \quad (70.24)$$

The faradaic current i_f is related to dN/dt according to:

$$i_f = nFAdN/dt \quad (70.25)$$

where n is the number of electrons involved in the reaction of a single analyte particle, F is the Faraday constant, and A is the surface area of the working electrode. The *Nernst diffusion layer* model assumes that within a layer of thickness δ , the analyte concentration depends linearly on the distance from the electrode surface until it reaches the bulk concentration c_0 . For simplicity, the diffusion problem is often considered to be one-dimensional as it is the case for a planar working electrode in a cylindrical cell. The combination of Equations 70.23 to 70.25 then gives:

$$i_f = nFAD\left((c_0 - c_e)/\delta\right) \quad (70.26)$$

where c_e is the concentration at the electrode surface. For a sufficiently large difference between the applied potential and the standard potential of the analyte's redox couple, all species reaching the electrode surface by diffusion are immediately converted and the faradaic current reaches a maximum. In this case, the analyte concentration c_e at the electrode surface can be regarded as zero.

The diffusion profile and thus the dependence of δ from time can be obtained by solving the differential equation that is known as Fick's second law:

$$\frac{\partial c(r, t)}{\partial t} = D\nabla^2 c(r, t) \quad (70.27)$$

where ∇^2 is the Laplacian operator. For *linear diffusion* — that is, one-dimensional diffusion as it was considered in Equation 70.26 — the solution of Equation 70.27 with the appropriate boundary conditions ($c_e(t = 0) = c_0$; $c_e(t > 0) = 0$; $c(x > \delta) = c_0$) yields:

$$\delta = \text{sqrt}(\pi Dt) \quad (70.28)$$

Combination with Equation 70.26 leads to the *Cottrell equation*:

$$i_f(t) = nFAC_0\text{sqrt}(D/\pi t) \quad (70.29)$$

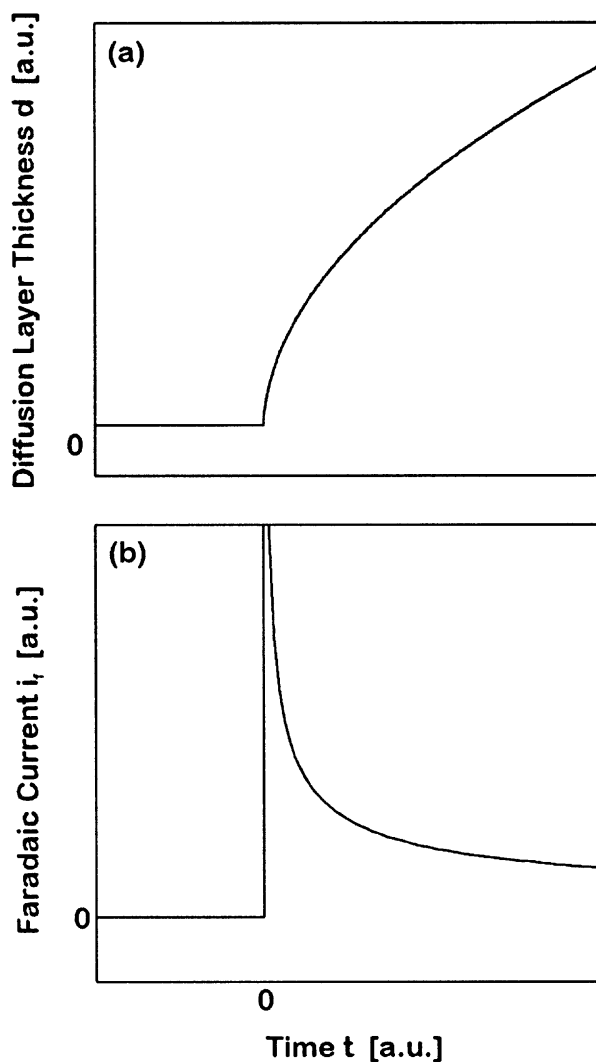


FIGURE 70.9 At a planar electrode, the diffusion-layer thickness increases with $t^{1/2}$ (a) whereas the diffusion-limited current decreases with $t^{-1/2}$ (b).

After reaching a maximum value, the current decreases with $t^{-1/2}$ and is proportional to c_0 , whereas the diffusion layer thickness increases with $t^{1/2}$ (Figure 70.9).

For a spherical electrode of radius r_0 , as it is the case for HMDEs, one has to change to spherical coordinates and Fick's second law becomes:

$$dc(r,t)/dt = D \left[d^2c(r,t)/dr^2 + 2/r dc(r,t)/dr \right] \quad (70.30)$$

where $r > r_0$ is the radial distance from the electrode center. The solution of Equation 70.30 with the appropriate boundary conditions $c(r,0) = c_0$, $\lim(r \rightarrow \infty) c(r,t) = c_0$, $c(r_0, t > 0) = 0$ yields the current-time relation

$$i_f(t) = nFADc_0 \left[1/(\pi Dt)^{1/2} + 1/r_0 \right] \quad (70.31)$$

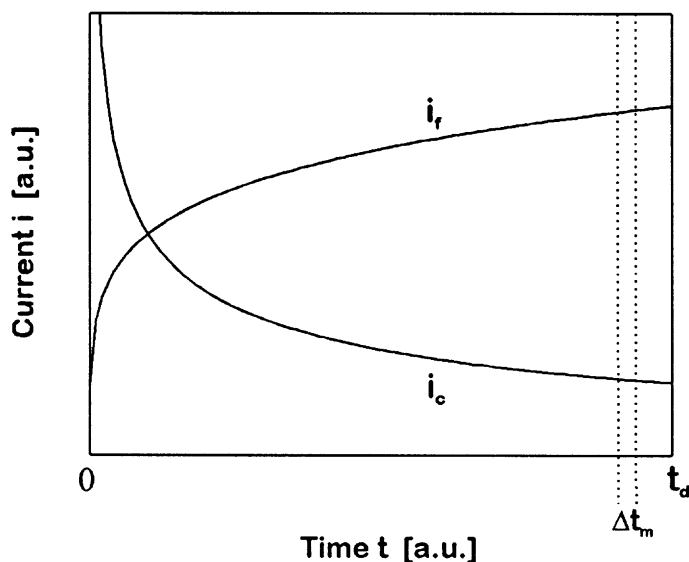


FIGURE 70.10 At a DME the measurement is performed during a time interval Δt_m at the end of the drop's lifetime when the ratio i_r/i_c is very large.

The first term in brackets equals that for the linear case; the second, constant term reflects the fact that the surface of the spherical diffusion layer grows and thus can draw an increasing number of reactive species.

The situation is even more complicated for DMEs because in addition to the surface of the diffusion layer, the surface and the radius of the drop are growing during the drop's lifetime. At any time, the growing electrode surface forces the depletion layer to stretch over a still larger sphere, which makes the layer thinner than it otherwise would be. A rigorous mathematical approach to this is rather difficult [11] because the relative convective movement between the solution and the electrode during drop growth must be considered. However, a simplified approach that is valid when the second term in Equation 70.31 is negligible, and the diffusion problem can be regarded as linear, yields the *Ilkovic equation*

$$i_r(t) = 708nDcm^{2/3}t^{1/6} \quad (70.32)$$

where m is the mercury flow rate (mass/time) from the capillary. Consequently, the current increases during the lifetime t_d of the drop (*drop time*), whereas it decreases with time in the other arrangements that have been described. **Figure 70.10** depicts this current–time relation of a DME with the characteristic current plateau at the end of the drop's lifetime.

In the considerations that have been made above, analyte transport by convection and migration in the electric field have been neglected. Convection can be regarded as absent if the solution is unstirred and if the working electrode rests motionless. However, in longer-lasting measurements, convective mass transport can play a role due to arising inhomogeneities in the density of the solution. Furthermore, if a DME is employed, the growth of the drop may cause a considerable convection of the solution. When the drop falls off, it stirs the surrounding solution and the depletion effect almost vanishes. Consequently, every drop is born in an almost homogeneous environment. The migration of electrically charged analyte particles due to the electric field in the solution can easily be suppressed using an inert supporting electrolyte with a concentration that is much larger than the analyte concentration. Since all charged species contribute to the migration current, the migration of the analyte species can then be neglected.

Double-Layer Charging Current.

A process that affects all kinds of voltammetric measurements is the flow of *capacitive current*. The accumulation of charge on one side of the electrode/solution interface causes the necessity of a mirror charge on the other side. Hence, a change of the electrode potential (i.e., in the electrode charging) causes a corresponding flux of charged particles between the double layer and the bulk solution. Therefore, the interface has a certain capacitance that is called the double-layer capacitance. The resulting *double-layer charging current* i_c is superimposed on the faradaic current and often perturbs its measurement. In analytical techniques, one is often concerned with the reduction of the capacitive/faradaic current ratio. However, the actual measurement of the double-layer capacitance is demanding and requires the technique of *impedance spectroscopy*, as described, for example, in References 12 and 13.

Irreversible Electrode Processes.

Another assumption that has been made implicitly is that the rate of the electrode reaction is very fast in comparison to the supply of analyte by diffusion (*reversible electrode process*). Under this condition, all analyte species reaching the electrode are immediately converted. However, if the reaction rate is too slow, the consumption of reactive species is compensated by the diffusion of the analyte (*irreversible electrode process*) and thus, the concentration at the electrode surface never drops to zero. The electrode current is then determined by the reaction rate and the calculations above do not hold. In practice, the situation is sometimes complicated if so-called *quasi-reversible* electrode processes with intermediate reaction rates occur. Although this concept of electrochemical *reversibility* is a simplification, it is a suitable working basis and can be summarized in the following statement: In a given electrochemical experiment, an electrode process that follows the *Nernst equation at any time* is called *reversible*.

Influence of Adsorption, Catalysts, and Chemical Reactions.

Besides the diffusion and reaction rate, some other processes can influence the electrode current. *Adsorption* of the analyte or its reaction product on the electrode changes the double-layer capacitance or can passivate the electrode surface and thus lower the current. Moreover, if a species serves as a *catalyst*, it may shift the equilibrium potential. In the case that the catalyst returns the product of the electrode reaction back into the initial form of the analyte, the analyte concentration at the electrode surface will always be large and thus increases the limiting current and shifts the equilibrium. All these *catalytic currents* are subject to analytical studies. Besides adsorption and catalysis, complicated scenarios occur if the electrode reaction is followed by a chemical reaction whose product itself undergoes an electrode reaction within the observed potential range.

Techniques

The several voltammetric (i.e., *potential-controlled*) techniques differ just in the manner in which the electrode potential is varied with time. The potential can be changed in distinct steps, in a continuous sweep, or it can be pulsed or superimposed with an ac signal. In addition, the rate of potential change can be varied. The characteristics, advantages, and drawbacks of the most important techniques will be discussed in the following sections. Special attention will be given to polarography due to its practical importance in electroanalysis. Besides, the emphasis will be on reversible electrode processes because only they allow the realization of *analytical* investigations, on which this chapter is focused.

Amperometry.

If in a *potential step* experiment the working electrode potential is abruptly changed from a constant value E_1 where faradaic processes do not occur to another constant value E_2 where the electrochemical equilibrium is on the side of the oxidized or reduced form of the analyte, then a faradaic current begins to flow (Figure 70.11 (a)). In the case that the difference between the applied potential and the standard potential E^0 of the analyte's redox couple is sufficiently large, the effect of *diffusion limitation* sets in and a further increase of the potential difference yields no increase in the electrode current. The current is then called *limiting current*. The current–time relationship follows the Cottrell equation (Equation 70.29), with the current decreasing while the diffusion layer thickness increases.

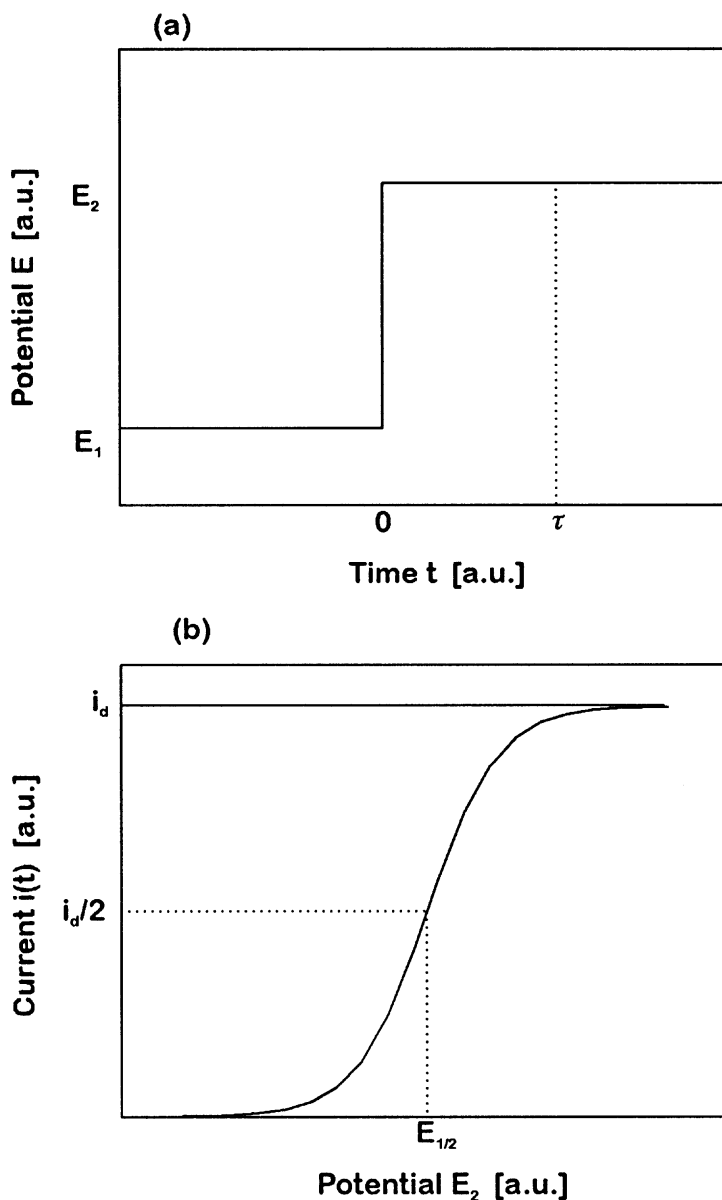


FIGURE 70.11 In potential step techniques, the current is measured a fixed time τ after the potential step (a). The measurement of $i(\tau)$ for different potential steps ΔE yields a wave-shaped current–potential relation with a half-wave-potential $E_{1/2} \approx E^0$ (b). The maximum current is proportional to the analyte's bulk concentration c_0 .

If the diffusion layer thickness could be held constant, then from Equation 70.26, it follows that the current would not decrease with time but remain at a constant value. This can be accomplished if the solution is stirred or flows across the electrode in a proper way. According to Equation 70.26 (with $c_e = 0$), the current then is proportional to the analyte concentration in the solution.

The described method corresponds to the electroanalytical technique called *amperometry* [14], with the exception that in this the potential step is omitted and the electrode current is measured at a fixed potential E at which the analyte undergoes an electrode reaction and the faradaic current is in the limited region. The solution usually crosses the electrode in a laminar flow, keeping the diffusion layer thickness constant.

Because the electrode current is proportional to the concentration of the analyte, only two measurements are needed for calibration. The base current is measured in an analyte-free solution and a second measurement is performed at a known analyte concentration. It should be mentioned that amperometry cannot only be used to determine liquid and ionic components of a solution but also to measure the amount of dissolved gas in a liquid. Moreover, with modified electrochemical cells, even gas analysis can be accomplished.

The main disadvantage of amperometry is its poor selectivity. Given a certain analyte and operating at a higher potential than the corresponding standard potential E^0 , all components of the solution with a standard potential smaller than E also contribute to the faradaic current. Operating at a potential $E < E^0$, the same problem occurs if substances with a standard potential larger than E are present in the solution. For this reason, amperometry is preferably carried out in solutions containing only one electroactive substance or, if possible, at a potential at which only one substance is involved in an electrode reaction. If this is impossible, the selectivity can often be enhanced by covering the working electrode with a membrane which, in comparison to the diffusion rate of the analyte through the membrane, is virtually impermeable for the interfering substances.

In addition to analytical purposes, amperometric methods can also be used to investigate reaction constants of chemical reactions. In *reversed potential step techniques*, the first potential step is followed by a second one in the opposite direction, often back to the initial value. The reaction product B of the first step is then reconverted into the original analyte A . However, if the first electrode reaction is followed by an additional chemical reaction, a certain part of B is converted into a product C before the reversed step is applied. Therefore, the current during the reversed step is reduced. The ratio of the electrode currents during the forward and reversed steps depends on the reaction constant of the chemical reaction. Because the reversion of B into A is required, batch arrangements without convection of the electrolyte are used for reversed step methods. Otherwise, a large part of B would be flushed away from the electrode surface and could not be reconverted.

Amperometric Titration.

In *amperometric titration techniques* [15], a titrant that reacts with the analyte is added to the analyte solution. During the titration, the limiting current is measured as a function of the volume of titrant added. The titrant has to be chosen such that the reaction product is not reducible or oxidizable at the applied potential and, hence, does not contribute to the current.

If the analyte as well as the titrant are electroactive at the applied potential, then the current flow will be large at the beginning of the measurement and decreases linearly with the volume of the titrant added, because both, the analyte and the titrant, are consumed by the reaction. The concentration of electroactive species then diminishes until the analyte is totally consumed. Further addition of titrant leads to a linearly increasing current because the titrant is no longer consumed. In the plot of the current versus the volume of titrant added, the point where the slope changes is called *endpoint* of the titration. From the corresponding amount of titrant added and the stoichiometry of the reaction the original volume of analyte can be computed. If only the analyte is electroactive, then from the endpoint the current will not increase but remain zero. If only the titrant undergoes an electrode reaction, the current will be zero until all analyte is consumed and then will linearly increase from the endpoint. In practical operation, the slope of the current does not change abruptly due to background currents and the endpoint has to be determined by extrapolation of the two linear regions.

In contrast to the majority of other electrochemical techniques, amperometric titration offers the advantage that even analytes which are not reducible or oxidizable can be determined using the oxidation-reduction characteristics of the titrant. Moreover, it is possible to analyze systems that have no measurable standard potential but can be electrolyzed.

Sampled-Current Voltammetry.

Consider a *potential step* experiment like the one in the section next to previous one. If the potential difference between E_2 and E^0 is too small, the electrode reaction is not so efficient that the analyte concentration at the electrode surface becomes zero (i.e., $c_e > 0$ in Equation 70.26). Within this region,

the current depends on the applied potential. However, even in this situation, a depletion effect occurs so that the current always decreases with time. Recording the current i for different values of E_2 at a fixed time τ after switching the potential (*sampled-current voltammetry*), a sigmoidal (wave-shaped) curve is obtained (Figure 70.11(b)).

The shape of this curve can also be calculated by exactly solving the diffusion problem. A wave rising from a baseline to the diffusion-limited current i_d is obtained. In the common case, the diffusion coefficients of the analyte and its redox partner are nearly equal the *half-wave potential* $E_{1/2}$, where $i = i_d/2$ is almost identical with the standard potential E^0 . Therefore, $E_{1/2}$ is often used in qualitative analysis to determine the analyte. Quantitative information about the analyte concentration is obtained from the maximum current (Cottrell current), which according to Equation 70.29 is proportional to c_0 .

The influence of the double-layer charging current has been neglected thus far, but is worth considering. It obeys the equation:

$$i_c = \Delta E / R_s \exp\left(-t / (R_s C_{dl})\right) \quad (70.33)$$

where ΔE is the potential step width, R_s the solution resistance, and C_{dl} is the double-layer capacitance. Although the measurement of R_s and C_{dl} is not trivial, one can obtain qualitative information from this formula. Comparison of Equations 70.33 and 70.29 yields that the capacitive current decreases exponentially while the faradaic current decreases according to $t^{-1/2}$. Consequently, the electrode current is measured a sufficiently long time after the potential step when the capacitive current has largely decayed, whereas the faradaic current is still significant. In polarography with DMEs, the growth of the electrode surface alters the temporal decrease of the double-layer charging current according to:

$$i_c \sim m^{2/3} t^{-1/3} \quad (70.34)$$

whereas the faradaic current increases according to $t^{1/6}$ (Equation 70.32). The current is measured shortly before the drop falls off (Figure 70.10).

The lower detection limit amounts to 10^{-5} to 10^{-6} mol/L for the determination of organic and inorganic analytes. The half-wave potential of different substances should be at least 100 mV apart for a simultaneous determination.

Linear Sweep and Cyclic Voltammetry.

In *linear sweep voltammetry* (LSV), the electrode potential is changed *continuously* from an initial to a final value at a constant rate $v = dE/dt$, such that $E(t) = E_1 \pm vt$. Starting at a potential E_1 where no faradaic process occurs, a current begins to flow when the electrode potential comes into the vicinity of E^0 . The current rises to a maximum and then decreases due to the depletion effect (Figure 70.12). The solution of the diffusion equations, which yields the shape of the i - E wave, can only be found numerically. For the electrode process to always follow the Nernst equation and thus be reversible, the sweep rate must not be too high (e.g., $v < 100$ mV s $^{-1}$). The peak potential E_p can then be calculated to be:

$$E_p = E_{1/2} \pm 1.1 \cdot (RT/nF) = E_{1/2} \pm (28.0/n) \text{ mV (at } 25^\circ\text{C)} \quad (70.35)$$

The positive sign in Equation 70.35 applies to an anodic sweep (from negative to positive potential with $v > 0$) and the negative sign to a cathodic one (from positive to negative potentials with $v < 0$). The peak current is given by:

$$i_p = 0.446 n F A \left(n F / RT \right)^{1/2} D^{1/2} c_0 v^{1/2} \quad (70.36)$$

Thus, the peak current is proportional to the bulk concentration c_0 of the analyte and depends on the sweep rate according to $v^{1/2}$.

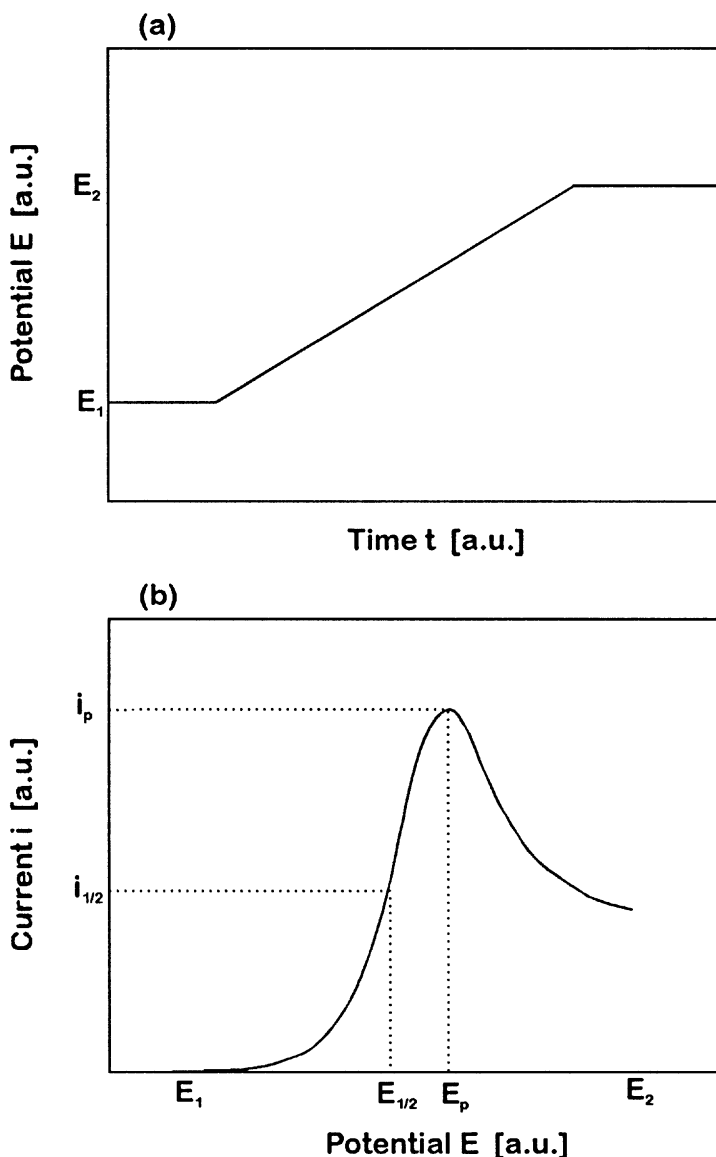


FIGURE 70.12 In LSV the potential varies linearly with time (a). The current–potential relation yields a peak-shaped curve with a half-wave potential $E_{1/2} \approx E^0$ (b). The peak current is proportional to the analyte's bulk concentration c_0 .

Another contribution to the measured current is the capacitive double-layer-charging current i_c , which always flows in LSV due to the continuous change of potential. It can be calculated using the equation:

$$i_c = C(dE/dt) = Cv \quad (70.37)$$

which yields a proportionality to v while the faradaic peak current is proportional to $v^{1/2}$. Thus, for the faradaic current to dominate the measurement, the sweep rate should not be chosen too large. A sweep rate of 100 mV s^{-1} can be regarded as an upper limit. Moreover, the surface area of the working electrode must be taken into consideration. Rough electrodes have a much larger active than geometric surface area and thus a very large capacitance. Therefore, small, very smooth electrodes should be chosen.

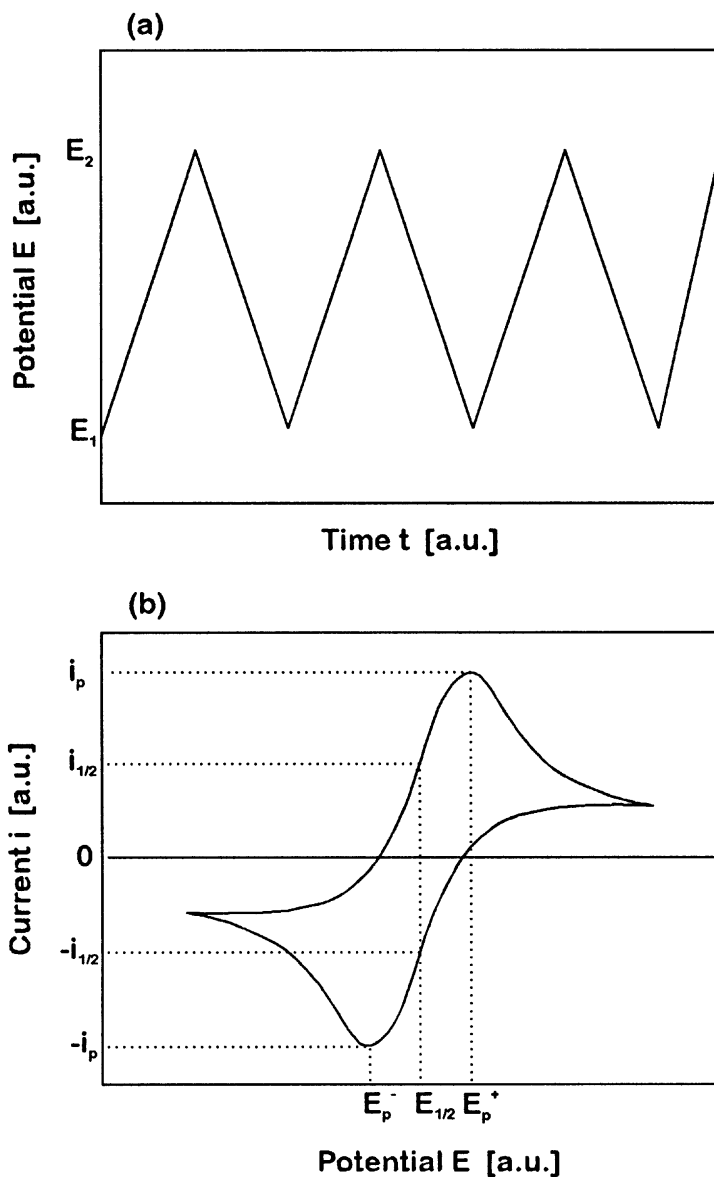


FIGURE 70.13 In CV, the potential is swept forth and back between two fixed values (a). The current–potential relation yields a peak-shaped curve with a half-wave potential $E_{1/2} \approx E^0$ (b). The peak current is proportional to the analyte’s bulk concentration c_0 . For totally reversible systems, the peak currents of the forward and the backward sweep are equal in magnitude but of opposite sign.

A variation of LSV is a technique called *cyclic voltammetry* (CV). Here, the electrode potential is swept forth and back between two potentials E_1 and E_2 (Figure 70.13(a)). Although the bulk concentration of the reaction product is essentially zero, its concentration at the electrode surface after the first sweep is quite large. In the backward sweep, the reaction product of the analyte is converted into the analyte again. The current flows in the opposite direction and using an xy -recorder, an i – E curve is obtained (Figure 70.13(b)). From Equation 70.35, it follows that for reversible processes, the peak potentials of the forward and backward sweep have a distance of $(56/n)$ mV at room temperature. Therefore, cyclic voltammetry is a favorable method for the investigation of the reversibility of a system. If the electrode current totally decays in the forward sweep, the analyte concentration has dropped to zero and the product

concentration at the electrode surface is about c_0 . Ideally, the peak current during the reverse scan should be equal (with reversed sign) to the peak current of the forward sweep.

Although the theory of LSV and CV measurements is very promising, the methods have several practical limitations. One is the frequently insufficient stability of the i - E characteristic during the first cycles in CV. However, after 5 to 10 cycles, it tends to become highly reproducible. Yet, one must be careful deriving quantitative information from these later cycles because the initial and boundary conditions of the diffusion problem have changed and convective mass transport may already play a role. Thus, the equations developed for LSV cannot be used. Another problem that concerns both LSV and CV is the potential drop that occurs in the solution between the working and the reference electrode and which leads to a distortion of the shape of the i - E wave. This error increases with increasing current flow. Thus, the rate of change v of the electrode potential is not really constant, as has been assumed in the boundary conditions for solving the diffusion equations. Furthermore, the quantitative information is usually obtained from the position E_p and the height i_p of the current peak where the error is maximum. Finally, the determination of the peak height itself is sometimes problematic due to difficulties in the extrapolation of the baseline. For all these reasons, it may be advisable to verify the results of quantitative analysis with additional methods. Nevertheless, on easy terms, the lower detection limit of LSV and CV in quantitative analysis can amount to 10^{-7} mol/L with a resolution of about 50 mV.

Besides the analysis of faradaic processes, LSV and CV are favorable techniques for the investigation of the adsorption of species on the electrode surface [16]. In such adsorption processes, the current is called *pseudocapacitive current*. Although it is a charge transfer across the interface, it exhibits many of the properties of a pure capacitive current. The current-potential wave has a very similar shape as for faradaic processes. If Θ denotes the coverage ($0 \leq \Theta \leq 1$) and q_1 the charge that is required to form a monolayer of a species, the pseudocapacitive current i_a can be expressed as:

$$i_a = q_1 \left(\frac{d\Theta}{dt} \right) = q_1 \left(\frac{d\Theta}{dE} \right) \left(\frac{dE}{dt} \right) = C_a v \quad (70.38)$$

where C_a is called the *adsorption pseudocapacitance*. The calculation of C_a yields that the pseudocapacitance does not depend on v . Therefore, at any potential the current is proportional to the sweep rate ($i \sim v$). The peak potential gives information about the adsorption kinetics. In contrast to faradaic CV, it has the same value for the forward and the backward sweep.

Pulse Techniques.

Voltammetric pulse techniques are derived from potential step experiments to suppress the capacitive currents during the measurement. A potential step that can vary in amplitude and sign is periodically repeated and superimposed with a potential ramp. The current is measured at the end of the step when the double-layer charging current has largely decayed.

Normal Pulse Voltammetry. In *normal pulse techniques*, periodic voltage pulses with an increasing amplitude from pulse to pulse are superimposed on a constant potential. A typical pulse duration is about 50 ms and the current is measured during a time interval Δt_m of about 10 to 15 ms at the end of each pulse. Between two pulses there is a waiting period of a few seconds (Figure 70.14). In polarography with a DME, each drop is dislodged directly after the pulse and thus used for just one measurement.

Because normal pulse voltammetry equals a series of potential-step measurements with increasing step widths, the current obeys to Equation 70.29 and the evaluation of the measured current values can be carried out using the sampled-current method. In comparison with the step technique, the lower detection limit is enhanced for one to two orders of magnitude up to 10^{-6} and 10^{-7} mol/L [17]. The peak resolution is about 100 mV.

Square-Wave Voltammetry. In *square-wave techniques*, a periodic rectangular voltage is superimposed on a linearly rising potential ramp. The measuring interval lies at the end of a pulse when the capacitive current can be neglected (Figure 70.15(a)). Typical pulses have frequencies between 200 Hz and 250 Hz and an amplitude of $\Delta E_p = 5$ to 30 mV [17]. The capacitive current is suppressed even more effectively if the pulse is tilted to decrease during the pulse period. No pulse tilt is required if the potential ramp is

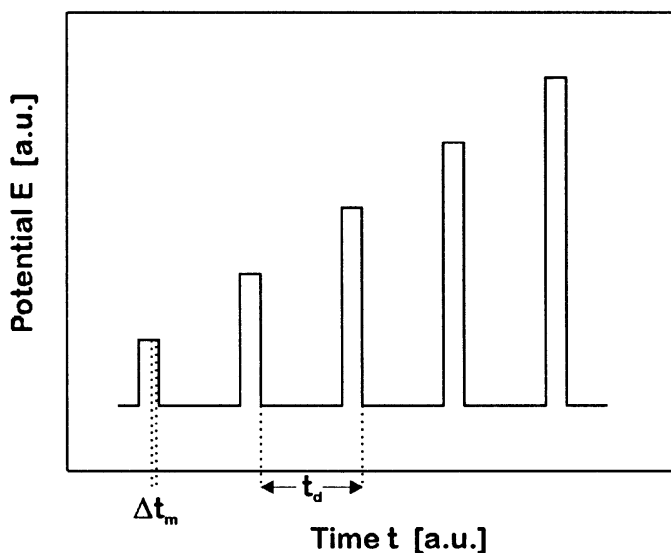


FIGURE 70.14 Normal pulse voltammetry equals a series of potential-step measurements with increasing step widths. The current is measured during a time interval t_m near the end of the pulse. In polarography with a DME, the drop is dislodged after each measurement. The drop's lifetime is denoted by t_d .

stepped (staircase ramp) instead of a linear ramp. The voltage pulse is then applied on the plateau of the stepped ramp (Figure 70.15(b)).

After rectification of the measured current values, one obtains peak-shaped i - E -curves. The peak potential corresponds to the half-wave potential of LSV and, thus, to the standard potential of the analyte's redox couple. The peak current i_p depends on the frequency and amplitude ΔE of the voltage pulses and obeys:

$$i_p \sim n^2 D \Delta E c_0 \quad (70.39)$$

where the frequency dependence is included in the proportionality constant. The lower detection limit is in the range of 10^{-8} mol/L and the peak resolution amounts to 40 to 50 mV.

Shorter analysis times are achieved if very short and relatively large rectangular pulses with a duration $t_p = 5$ to 10 ms and an amplitude of $\Delta E = 50$ mV are superimposed on a stepped potential ramp with the same duration but smaller potential steps of about 10 mV. The potential can then be scanned at extremely high rates of up to 1200 mV s^{-1} . However, the sensitivity decreases because the ratio of faradaic to capacitive currents is lowered by the short pulse times.

Differential Pulse Voltammetry. *Differential pulse methods* are the most important ones in analytical voltammetry. Periodically repeated rectangular voltage pulses with a constant amplitude ΔE of several 10 mV are superimposed on a stepped potential ramp (Figure 70.16). The pulse duration Δt_p is about 5 to 100 ms [17]. Between two pulses, the potential is held constant for a few seconds. The current is measured in a short time interval ($\Delta t_m \approx 1$ to 20 ms) directly before a pulse is applied and for the same duration near the pulse end. If a DME is used, the drop is knocked off mechanically between two pulses and each drop serves for just one measurement.

For the evaluation, the difference between the two measured current values Δi that corresponds to one pulse is recorded as a function of the base potential. A peak-shaped curve is obtained with a maximum very close to the half-wave potential $E_{1/2}$. The peak height is proportional to the analyte concentration in the bulk:

$$\Delta i_p \sim nFA \left(D / \pi t_p \right)^{1/2} c_0 \quad (70.40)$$

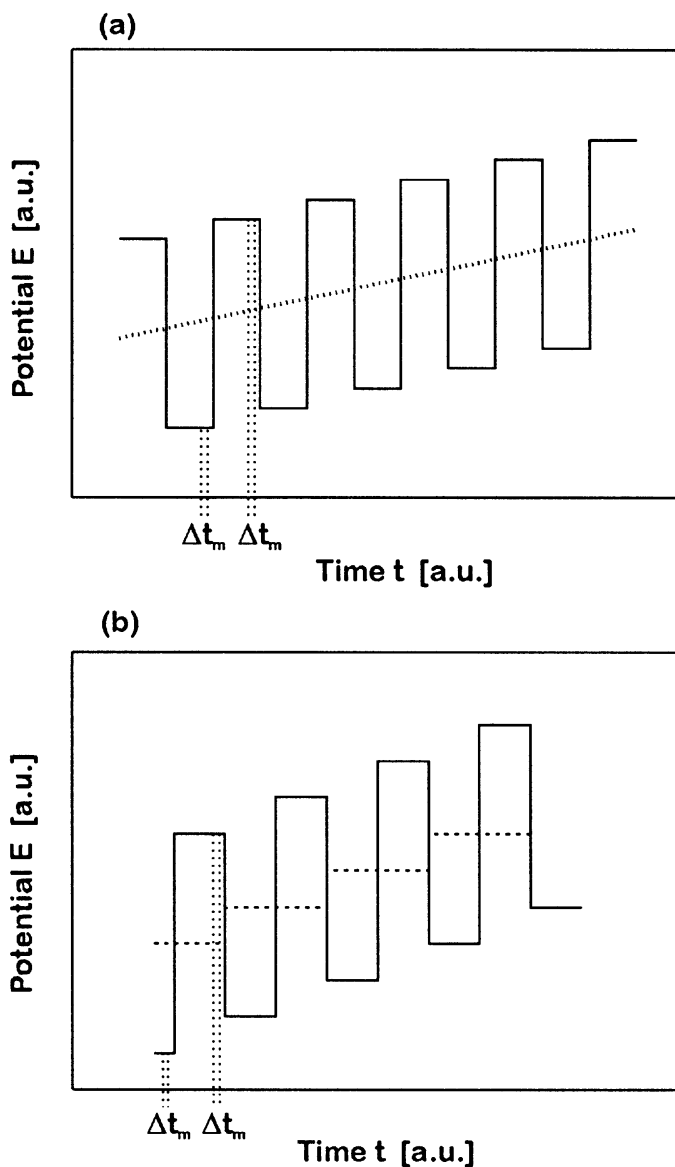


FIGURE 70.15 In square-wave voltammetry, a periodic rectangular voltage pulse is superimposed on (a) a linearly changing potential ramp (dotted line) or (b) on a stepped ramp (dashed curve). The current is measured during a time interval Δt_m at the end of each pulse.

With differential pulse measurements, a lower detection limit of 10^{-8} mol/L and a resolution of 50 to 100 mV can be achieved.

Alternating Current Voltammetry.

Alternating current techniques are similar to differential pulse methods. A linear potential ramp is modulated with a low frequency ($f \sim 50$ Hz) sinusoidal alternating voltage of small amplitude ($\Delta E \sim 50$ mV) [17]. The amplitude of the resulting alternating current is plotted against the base potential. A peak-shaped curve is obtained with a maximum that is proportional to the bulk concentration of the analyte:

$$i_p \sim \Delta E f^{1/2} c_0 \quad (70.41)$$

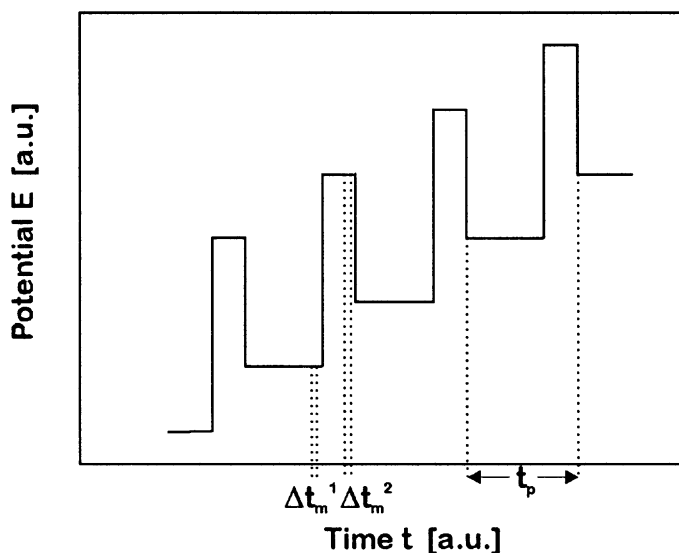


FIGURE 70.16 In differential pulse voltammetry, periodic rectangular pulses are superimposed on a stepped potential ramp. The difference between the current measured in a time interval Δt_m^1 directly before each pulse and during a time interval Δt_m^2 at the end of each pulse is plotted against the base potential. In polarography with a DME, the drop is dislodged after each pulse. The drop's lifetime is denoted by t_d .

The lower detection limit is 10^{-5} mol/L due to the large capacitive currents. It can be enhanced by phase-selective rectification because the capacitive and the faradaic currents have a phase shift of 90° and 45° , respectively. The peak resolution amounts to 50 to 100 mV.

Stripping Voltammetry.

Stripping techniques can be performed with analytes whose reaction products adsorb on the electrode surface. For accumulation, the electrode potential is held at a value at which the electrochemical equilibrium is on the product's side. Accumulation times usually amount up to several minutes. During this period, the solution is stirred to prevent the depletion of the analyte at the electrode surface. The accumulation is followed by a rest period of 2 to 30 s, during which the solution remains unstirred and the current falls to a small residual value. In the subsequent *stripping step*, the electrode potential is shifted to a value at which the adsorbed product is reconverted into the analyte by oxidation or reduction. Depending on whether an oxidation or reduction process occurs, the method is called *anodic stripping voltammetry* (ASV) or *cathodic stripping voltammetry* (CSV), respectively. The stripping step can be performed in various manners [18] of which the linear sweep method shall be exemplarily discussed here. It yields a peak-shaped i - E curve with a maximum at:

$$E_p = E_{1/2} - 1.1 \frac{RT}{nF} \quad (70.42)$$

and a peak height that is proportional to the bulk analyte concentration according to:

$$i_p \sim n^{3/2} v^{1/2} c_0 \quad (70.43)$$

Different substances can be determined in successive experiments with an adequate choice of the accumulation potentials. For the first measurement, the accumulation potential is chosen to allow adsorption of only one species; in the next experiment, the first and one further analyte adsorb, and so on. For the simultaneous determination of two or more substances their peak potentials should be at least 150 mV apart.

A special case of the stripping techniques is *adsorptive stripping voltammetry* (AdSV). Here, the analyte is deposited in the form of metal chelates or organic molecules. For the formation of metal chelates, a complexing agent is added to the electrolyte or the surface of a solid-state electrode is modified with it. The stripping current is then due to the oxidation or reduction of the central atom or the ligand of the metal chelate complex. With this method, organic and organometallic compounds can be determined in the ultratrace range.

A crucial point in stripping analysis is the reproducibility. All experimental parameters have to be selected very carefully. In particular, the electrode surface must not be changed significantly by the adsorption and dissolution processes. Therefore, HMDEs are frequently employed for stripping analysis. A new drop is produced for each measurement. Another advantage of mercury electrodes is the fact that not only their surface but rather the hole bulk is used for the accumulation of analyte species. Consequently, more material can be collected. This leads to an enhanced lower determination limit which can be below 10^{-8} mol/L. Comprehensive monographs about stripping techniques are given in References 18 and 19.

Applications

Analytical applications of voltammetry concern the determination of (heavy) metal cations, typical anions (halides, pseudohalides), organometallic, and organic compounds in the 10^{-4} to 10^{-9} mol/L concentration range. Therefore, they are established in several fields like environmental, medical, food, and water analysis. A disadvantage is the usually labor-intensive sample preparation necessary, for example, to disintegrate ions from complexes, to adjust the pH of the solution, or to remove interfering species like oxygen and organic molecules. Principally, the preparation of the electrode (surface) is also crucial. However, commercially available equipment is well developed not only to enhance determination limits, sensitivity, selectivity, and reproducibility, but also to reduce the expense for electrode and cell preparation. Moreover, sample and electrode preparation can be automated to a certain degree by devices which pump different solutions for cleaning, conditioning and analysis through the cell setup. A further improvement of the instrumentation is the use of *microelectrodes* with dimensions of 1 to 100 μm . Because their dimensions are small in comparison with the diffusion length of the analyte, even for planar microelectrodes the diffusion is rather hemispherical than linear. Therefore, the depletion effect is less strong and the faradaic current is increased. Moreover, planar microelectrodes can be rotated (*rotating disk electrode*, RDE) to intensify convection and the solution can be stirred with ultrasound. Another advantage of microelectrodes is the possibility to realize several electrodes in a close neighborhood, so-called *electrode arrays*. They serve as *one* electrode if they are held at *one* potential and exhibit an improved signal-to-noise ratio due to the better diffusion conditions. In contrast, if different potentials are applied at different electrodes, the simultaneous determination of different species is possible. These techniques have just become commercially available as electrochemical detectors, for example, for high performance liquid chromatography (HPLC). In this arrangement, the different species in the solution are separated by the HPLC and flow through the detector cell one after the other. Thus, interference between different analytes is minimized. The selectivity can often be further improved by the use of membrane-covered microelectrodes. The well-known *Clark oxygen sensor* and different biochemical sensors represent promising examples of this application in amperometry. Moreover, it opens up new possibilities for the creation of microelectrode arrays.

Due to the high analytical potential and the relatively low costs of voltammetric methods in comparison with spectroscopic techniques, all aspects of voltammetry are still subject of intense research. Current efforts concern the *miniaturization* of the whole cell, including microchannels, microvalves, micropumps, and microelectrodes by means of precision mechanics and *micromachining techniques* [20]. They employ fabrication methods of silicon planar technology and LIGA technique (Lithographie, Galvanoformung, Abformung). Thin-film techniques like physical and chemical vapor deposition (PVD, CVD) allow the fabrication of electrodes with a thickness in the submicrometer range and with lateral dimensions from the micrometer to the nanometer range. One goal is the realization of a *microsystem* with the sensitive components (i.e., the electrodes) and microelectronics integrated on a single chip. The electronics could

serve as a first stage of signal amplification and information processing. Although first demonstrator devices have already been presented [21] it is still quite a long way to commercially available systems.

Potentiometry

Potentiometry implies the measurement of an electrode potential in a system in which the electrode and the solution are in electrochemical equilibrium. Thus, the potential becomes the dependent variable, for example, as a function of time. In potentiometry, the current is attempted to be kept as small as possible; ideally, it should be zero. Potentiometry implies known fluxes (i.e., concentration gradients at the electrode surface) and thus information on the composition of the sample. In this section, potentiometry is related to the measurement of potentials, where the voltage source is a form of a galvanic cell, consisting of a measuring electrode and a reference electrode (in general, electrodes of the second kind). The principles of *direct potentiometric measurements* as well as *potentiometric titrations* will be described.

Ion-Selective Electrodes

The equipment required for potentiometric analysis includes a measuring electrode, also called an *ion-selective electrode* (ISE) or *indicator electrode*, and a reference electrode. In addition to the sensitivity, the most important characteristic of the ISE is given by its *selectivity*. Depending on the type of membrane, ISEs can be classified into four different groups: *glass electrodes*, *solid-state electrodes*, *liquid-membrane electrodes*, and miscellaneous *combined electrodes*. For all ISEs, the validity of the Nernst equation could be proved.

Glass Electrodes.

The most common *glass electrode* is the *pH electrode*, widely used for hydrogen ion determination. The pH glass electrode consists of a thin, pH-sensitive *glass membrane* sealed to the bottom of an ordinary glass tube. The tube is filled with a solution of hydrochloric acid (e.g., 0.1 M HCl) that is saturated with silver chloride. A silver wire, connected to an external potential-measuring device, is immersed in this solution. Note that the internal HCl concentration is constant and, thus, the internal potential (inner surface of glass membrane) of the pH electrode is fixed. Only the potential that occurs between the outer surface of the glass bulb and the test solution responds to pH changes. To measure the hydrogen ion concentration of the test solution, the glass electrode (indicator electrode) must be combined with an external reference electrode, which is required for all kinds of ISE determination. Often, pH glass electrodes are available as a combination of the indicator electrode and an internal reference electrode (e.g., Ag/AgCl in saturated KCl solution) as schematically shown in [Figure 70.17](#).

The composition of the glass membrane clearly influences the sensitivity of the pH electrode. Usually, three-component systems of, for example, SiO₂/Na₂O/CaO are employed [22]. The pH dependence can be expressed by the Nernst equation (Equation 70.11). At room temperature (T = 25°C), Equation 70.11 can be simplified by:

$$E = E^0 + 59.1 \text{ mV pH} \quad (70.44)$$

where E^0 is the standard Galvani potential with respect to the SHE. Thus, the measured potential is a linear function of pH within an extremely wide range (10 to 14 decades). The selective pH response of the pH ISE is due to the ion exchange process, in particular, due to the replacement of sodium ions in the glass membrane (m) by protons in the solution (s), and vice versa:



The sodium ion exchange is also responsible for the *alkaline error* of pH electrodes in solution with pH greater than 10. In spite of the high resistance of the glass membrane against chemical attack, one

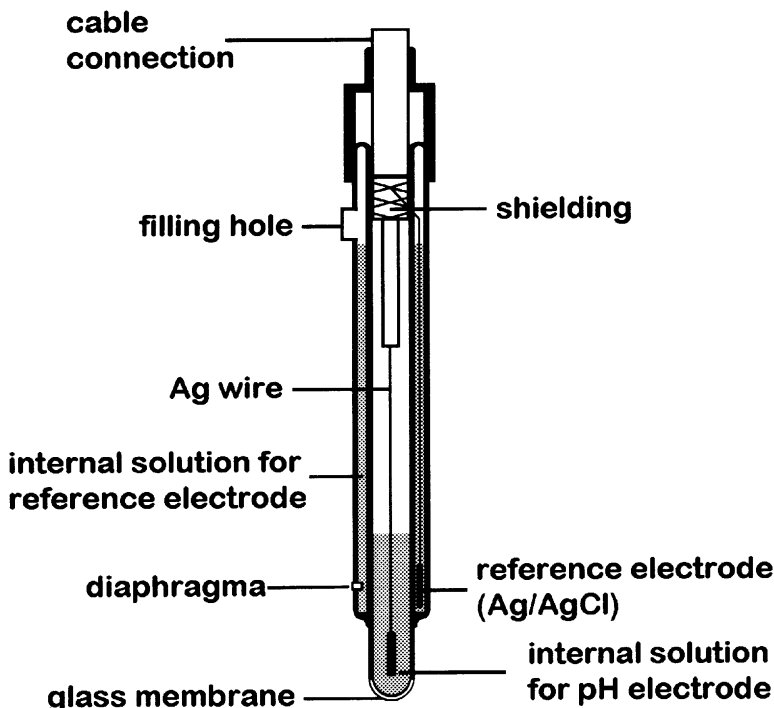


FIGURE 70.17 Combination pH glass electrode with an integrated Ag/AgCl reference electrode.

has to deal with deviations (alkaline error) from the linear pH dependence. This error (i.e., the sensitivity toward alkali-metal ions) can be greatly reduced if Na_2O is replaced by LiO_2 . Because pH glass electrodes can be used in the presence of substances that interfere with other electrodes (e.g., proteins, oxidants, reductants, and viscous media), they have a wide range of applications. Typical fields are the clinical and food analysis, environmental monitoring (e.g., industrial waste, acidity of rain), and process control (e.g., fermentation, boiler water, galvanization and precipitation).

The employment of glass membranes prepared with different glass compositions allows an electrode response sensitive to cations. For example, sodium-, potassium-, and ammonium-selective glasses consist of a mixture of Na_2O , Al_2O_3 , and SiO_2 in various proportions (aluminosilicate glasses). Using specific compositions and mixtures of chalcogenides, ion-selective *chalcogenide glass electrodes* with sensitivities toward monovalent ions (e.g., Ag^+ , Tl^+ , F^- , Cl^- , Br^- , I^-) and double-charged species (e.g., Cu^{2+} , Pb^{2+} , Cd^{2+} , Hg^{2+} , S^{2-}) can be prepared [23]. However, in all cases, some sensitivity to charged species (e.g., H^+ ions) remains. The electrode potential under these conditions is described by the *Nikolsky-Eisenmann* equation

$$E = E^0 \pm \frac{RT}{zF} \ln \left(a_i + K_{ij} a_j^{z_i/z_j} \right) \quad (70.46)$$

where z_i , z_j , and a_i , a_j are the ionic charge and activity of the primary or determined (i) and the interfering (j) ion. K_{ij} is the *selectivity coefficient*. It is a measure of the ISE ability to discriminate against the interfering ion. A small value of K_{ij} indicates an ISE with a poor selectivity.

Solid-State Electrodes.

The glass membrane of an ISE can be replaced by a single or a mixed crystal, or a polycrystalline (pressed) pellet (Figure 70.18(a)). With respect to their membrane composition, *solid-state electrodes* are divided into *homogeneous* and *heterogeneous membrane electrodes*.

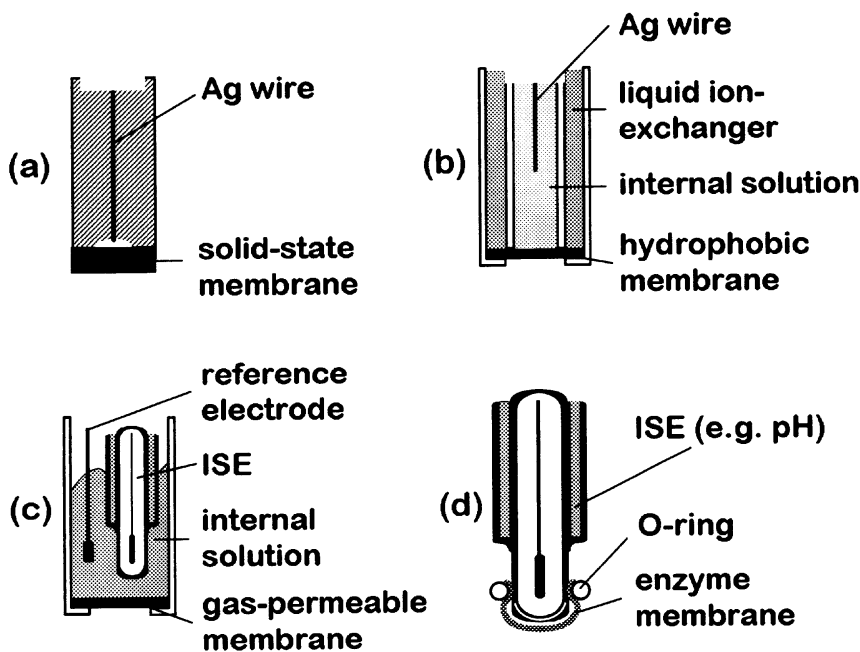


FIGURE 70.18 Typical membrane electrode types: solid-state electrode (a), liquid-membrane electrode (b), gas-sensing electrode (c), and enzyme-based electrode (d).

A typical single-crystal electrode (homogeneous membrane electrode) is the fluoride-sensitive ISE, which contains a LaF_3 crystal doped with Eu^{2+} . The crystal with a thickness of about 2 mm is sealed into the bottom of a plastic tube. The internal solution (0.1 M of NaF and NaCl) controls the potential at the crystal inner side by means of an Ag/AgCl wire as reference electrode. In contact with the test solution at the crystal outer side, an electrochemical equilibrium is established, proportional to the fluoride ion activity. This is due to an ion exchange process at the phase boundary membrane/electrolyte. In particular, fluoride ions from the membrane are replaced by fluoride ions from the solution and vice versa, where the fluoride ions can migrate from one lattice defect to another inside the crystalline membrane. Further homogeneous membrane electrodes are silver halide electrodes, where the respective silver halide (AgCl , AgI , AgBr , Ag_2S) is pressed into a pellet, placed in a tube, and contacted via a silver wire. In these substances, silver ions are accordingly able to migrate. Such electrodes have been successfully used for the selective determination of chloride, bromide, iodide, silver, and sulfide ions. Likewise, if the pellets contain Ag_2S together with the silver halides or mixtures of PbS , CdS , and CuS , solid-state electrodes sensitive toward Pb^{2+} , Cd^{2+} , Cu^{2+} , and SCN^- can be realized. Moreover, the general problem of light sensitivity and high membrane resistance can be reduced by the additional use of Ag_2S .

Instead of the pressed pellets, the ion-selective material can be incorporated into an organic polymer matrix, like silicon rubber, carbon paste, or paraffin. In heterogeneous membrane electrode preparation, a mixture of the precipitate (e.g., $\text{AgI}/\text{Ag}_2\text{S}$) and polysiloxane is homogenized, and the polymerization is carried out. The resulting disks are fixed on the end of a tube and the internal solution (e.g., 0.1 M KI) is contacted via a Ag/AgCl wire. *Coated-wire electrodes* represent another possibility. They can be manufactured by coating an appropriate polymeric membrane onto a conducting wire. Often, the conductor (Pt, Ag, Cu, or graphite) is dipped in a solution of polymer (e.g., polyvinylbenzylchloride (PVC) or polyacrylic acid) and the active substance. These electrodes allow the determination of K^+ , Na^+ , amino acids, and some drugs (e.g., cocaine). In addition to their simple miniaturization, the preparation is easy and inexpensive. However, further work is necessary to improve their analytical performance with regard to reproducibility and long-term stability.

Liquid-Membrane Electrodes.

Liquid-membrane electrodes base on two different membrane-active components, *solid ion-exchanger* and *complex-forming neutral-charged carriers*. They permit the determination of several polyvalent cations as well as certain anions. The sensor membrane (10 to 100 μm thickness) is usually prepared of a plasticized PVC containing the organic sensor-active component that is insoluble in water. A Ag/AgCl wire is immersed into the internal reference solution. The liquid-membrane electrode differs from the glass electrode only in that the test solution is separated from the solution with the known target ion activity by a hydrophobic membrane, instead of the glass layer (Figure 70.18(b)). As membrane materials besides PVC, teflon, sintered glass, filtering textile, or disks can be employed to hold the organic layer.

Liquid-membrane electrodes with ion-exchangers have been realized for the determination of, for example, Ca^{2+} , K^+ , BF_4^- , ClO_4^- , IO_4^- , SCN^- , I^- , Br^- , Cl^- , HCO_3^- , H_2PO_4^- , and NO_3^- . On the other hand, the synthesis of compounds containing individual cavities of molecule-sized dimensions results in complex-forming neutral-charged carriers. These *ionophores* (e.g., crown ethers like cyclic polyether, depsipeptides like valinomycin, and macrotetrolides like nonactin and monactin) are capable of enveloping various target ions reversibly in their pockets. For example, valinomycin membranes show a high K^+ selectivity. Many cyclic and monocyclic carriers with remarkable ion selectivities have been successfully developed for the determination of Li^+ , Cs^{2+} , Ca^{2+} , Na^+ , NH_3^+ , Mg^{2+} , Ag^+ , Hg^{2+} , SCN^- , and H_2PO_4^- [24]. For all kind of membranes, a high molecular weight (i.e., a slight overpressure) prevents the quick intrusion of the test solution inside. Hence, the electrode's lifetime is limited as a consequence of diffusion of the sensor-active component into the analyte (*leaching out*).

Combined Electrodes.

Two different types of *combined electrodes* will be presented here: *gas-sensing electrodes* and *enzyme-based electrodes*. Gas-sensing electrodes can be used to determine solutions of gases. They consist of an inner sensing element, normally a suitable ISE with an electrolyte solution (0.1 M), surrounded by a gas-permeable membrane (Figure 70.18(c)). On immersion of this ISE, the gas-permeable membrane contacts the liquid of the gas which diffuses through it, and the resultant internal solution will be examined with the ISE. The partial pressure of the gas attains an equilibrium between the test solution/membrane and the membrane/ISE phase boundary. For example, the determination of carbon dioxide, which diffuses through the semipermeable membrane, lowers the pH values of the inner solution:



Such pH changes are detected by the ISE, in this case by a pH-sensitive glass electrode. Semipermeable membrane materials are polytetrafluorethylene, polypropylene, or silicone rubber. The internal solution contains sodium chloride and an electrolyte with the corresponding ion that is determined. Gas-sensing electrodes have been realized for gases dissolved in solution, such as NH_3 , NH_4Cl , CO_2 , H_2CO_3 , NaHCO_3 , NO_2 , NaNO_2 , SO_2 , H_2SO_3 , $\text{K}_2\text{S}_2\text{O}_5$, CN , SCN , Cl_2 , Br_2 , I_2 , and H_2S .

Enzyme electrodes are based on the coupling of an enzymatic membrane with any type of appropriate ISE. The enzyme converts (*catalyzes*) the analyte (*substrate*) to be determined extremely selective into an ionic product. The latter can be detected by the known ISE (Figure 70.18(d)). The coupling of the enzyme can be carried out by several *immobilization procedures*, such as entrapping in a gauze or gel, adsorptive or covalent binding, and cross-linking. A typical example for the operation of an enzyme electrode is given by the urea electrode. The enzyme urease hydrolyzes urea in order to liberate ammonium ions:



Either the alteration of the pH by a pH ISE or the variation of the NH_4^+ concentration by an ammonium-sensitive gas electrode can be detected. Likewise, penicillin, glucose, lactate, phenol, creatinine, cholesterol, salicylate, or ethanol will be catalyzed by means of the respective enzyme. Using different biological

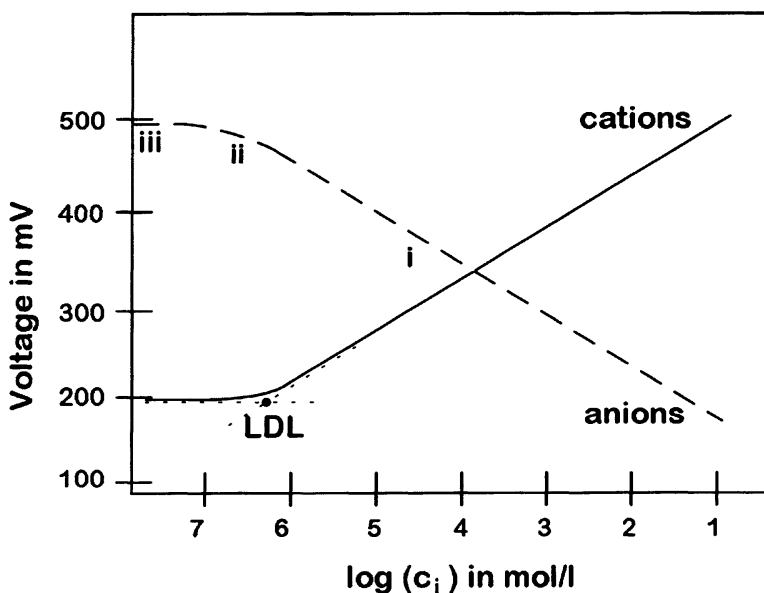


FIGURE 70.19 Schematic calibration curves for anions and cations (LDL: lower detection limit).

components (enzymes, cells, tissues, antibodies, receptors, or nucleic acids), a wide variety of analytically important substances for clinical, environmental, and food analysis can be determined. However, disadvantages of this type of electrode are its slow response time (several minutes) and the insufficient stability in the long term.

Instrumentation and Measurement.

For potentiometric measurements, one uses an indicator electrode (ISE) versus a reference electrode and a *potentiometer*, also called *pH meter* or *ion meter*. Owing to the high resistance of the ISE membranes (e.g., 5 to 500 M Ω for the glass membrane), a potentiometer with a high input resistance is required. Modern potentiometers consist of an electronic digital voltmeter with a suitable operational amplifier, scaled directly to pH units or mV, with a resolution of better than ± 0.002 pH and ± 0.1 mV. They may range from simple hand-held instruments for field applications to more convenient laboratory models. Frequently, potentiometers include a bias control that can be adjusted to correspond to the temperature of the test solution (*automatic temperature compensation*).

Direct Potentiometry. *Direct potentiometric* measurements can be performed for the determination of ionic species for which an appropriate ISE is available. A schematic measuring set up for direct potentiometry is shown in Figure 70.3. The measuring technique is quite simple: comparing the potential of the ISE in the test solution with its potential in a known *standard solution*. That means, before the determination, the ISE must be calibrated in solutions of known concentration of the chosen ionic species. Thus, for the ion determination to be made, at least two to three reference solutions are necessary which differ by two to five concentration decades. Typical resulting *calibration curves* for anions and cations are plotted in Figure 70.19. The curves can be separated into three distinct regions: (1) the straight part corresponding to the Nernstian slope (i.e., the sensitivity of the ISE), (2) the curve portion, and (3) the horizontal part below the lower detection limit, where almost no sensitivity exists. The *lower detection limit* (LDL) of the ISE is defined as the concentration at which the extrapolated horizontal portion of the graph intersects the extrapolated Nernstian portion of the graph.

For practical applications, there are two aspects to be dealt with: often a *total ionic strength adjuster buffer* (TISAB) is added to both the standard solutions and the test solution (same temperature) to achieve comparable ionic strengths. Then, the potential difference can be assigned to the equivalent concentration of the calibration curve. Various methods for calibration calculations are described by, for

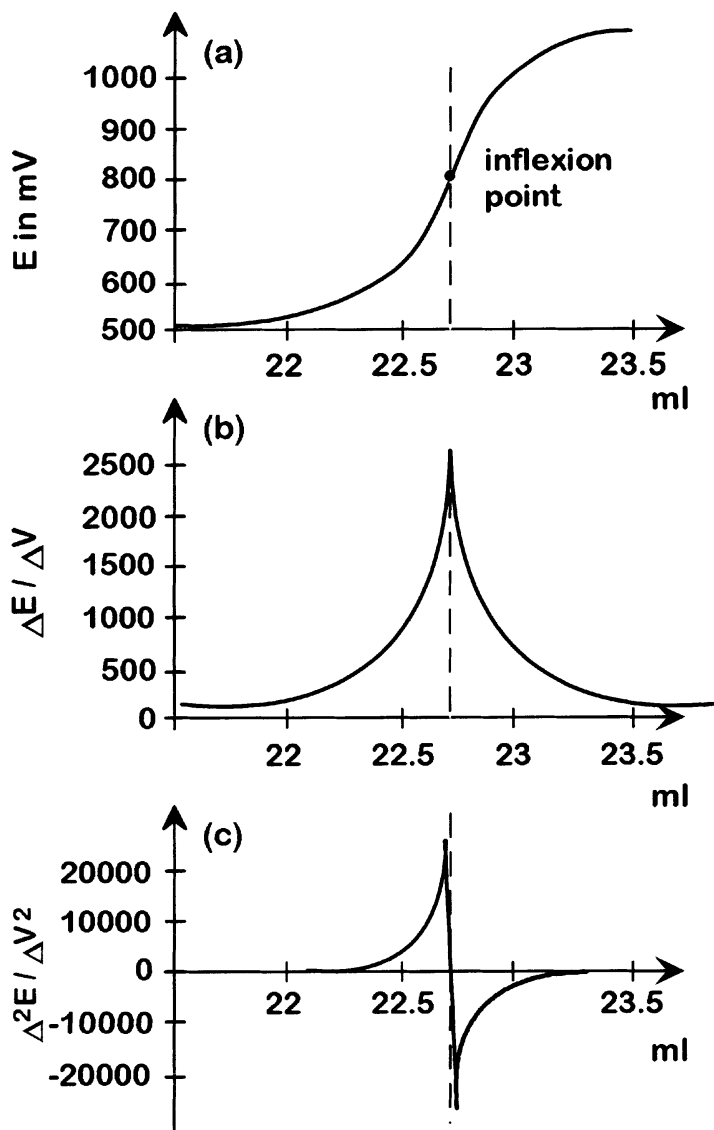


FIGURE 70.20 Characteristic potentiometric titration curve (a), first-derivative curve (b), and second-derivative curve (c).

example, Gran's plot or the standard addition method [25]. Because all measurements take place in dilute solutions ($\leq 0.1 M$), ion concentrations can be used in the Nernst equation instead of ion activities.

Potentiometric Titrations. *Potentiometric titrations* can be applied in the fields of *acid-base*, *precipitation*, *complex-formation*, and *redox reactions*. Therefore, the ISE is used in combination with a reference electrode in order to establish the *equivalence point* in a titration curve. A typical S-shaped potentiometric titration curve, where the electrode potential is plotted versus the reagent volume (*titrant*) is given in [Figure 70.20\(a\)](#). The titrant is added to the initial solution which is stirred, and the ISE records the potential value at equilibrium. The equivalence point (*endpoint*) of the reaction is reached when a sudden change in the potential of the ISE occurs. The midpoint in the curve (i.e., the steeply rising portion) is termed *endpoint* or *inflexion point*. It can be evaluated by analytical methods, namely the first- and second-derivative curve ([Figure 70.20\(b\) and \(c\)](#)). The first-derivative curve gives the potential change per unit change in volume of reagent and depicts the endpoint at the maximum of the inflexion point.

The second-derivative curve is zero where $\Delta E/\Delta V$ reaches its maximum. The greater the slope at the endpoint, the smaller should be the volume increment in order to reduce titration errors.

For practical applications, modern microprocessor-controlled titrators are commercially available (*auto-titrator*), coupled to a chart recorder to produce the titration curve directly. Such instruments also allow to evaluate the first- and second-derivative curves, and provide Gran's plot. Acid-base (neutralization) titrations are performed with a glass/calomel electrode system and can be used to titrate a mixture of acids that differ greatly in their strengths (e.g., acetic (ethanoic) and hydrochloric acids). For precipitation titrations, the ISE consists of an electrode (e.g., a silver or a platinum wire) that quickly reaches equilibrium with the ions to be precipitated. A typical precipitate reagent represents silver nitrate for the determination of halogens, halogenides, mercaptans, sulfides, arsenates, phosphates, and oxalates. For complex formation titrations, membrane electrodes can be used that involve the formation of soluble complexes, like EDTA (ethylene-diaminetetraacetic acid) or silver cyanide ($\text{Ag}(\text{CN})_2^-$). Oxidation-reduction titrations are performed by a platinum indicator electrode to any redox couples where the potential depends on the concentration ratio of the reactants. Some experimental details for potentiometric titration are described in Reference 26.

As an alternative principle, *chronopotentiometry* is based on the observation of the change in potential of a working electrode as a function of time during electrolysis. Usually, this electrolysis is performed with a constant current, whereas the time is measured that is necessary for the potential to go from one level to another. Since chronopotentiometry is disappointing at concentrations below 10^{-4} mol/L, it is only a powerful tool for studying electrode processes at higher concentrations. Consequently, this method is not very important for practical applications.

Ion-Sensitive Field-Effect Sensors

The integration of thin ion-selective membranes with solid-state electronics leads to miniaturized *chemically sensitive solid-state devices* (CSSDs). They can be distinguished into two different types: *chemically sensitive field-effect transistors* and *chemically sensitive capacitors*. These field-effect devices are based on the technology used for manufacturing microelectronic chips and thus offer the possibility of mass production. However, the techniques and miniaturized sensors presented in this section are in the most cases still in the state of research and development.

Chemically Sensitive Field-Effect Transistors.

Chemically sensitive field-effect transistors (ChemFET) can react sensitive to some ions (*ISFET: ion-sensitive FET*), biomolecules (*BioFET: biologically sensitive FET*), or gases (*GasFET: gas-sensitive FET*) in aqueous media, or they can be insensitive (*ReFET: reference FET*). They incorporate the sensor membrane directly on the gate area of a field-effect transistor (FET). A schematic of an ISFET with an SiO_2 gate insulator (about 100-nm thickness), mounted in a measuring cell and contacted via a reference electrode, is given in [Figure 70.21\(a\)](#). When the sensor membrane is placed into contact with the test solution of the ion to be detected, a potential shift (ΔV) occurs. The charge density at the interface solution/membrane changes because of the chemical interaction with the ions, and this potential affects the drain current (I_D) flowing between source (S) and drain (D) of the transistor. After calibration of the ISFET with standard solutions of known ion activity, the variation of I_D can be used to determine the ion concentration in the test solution ([Figure 70.21\(b\)](#)). Often, the ISFET is operated in a feedback loop (e.g., the *constant charge mode*, [Figure 70.21\(c\)](#)) and the voltage V_M needed to maintain I_D at a fixed value represents the sensor response. The sensor response can be described by the same Nernst and Nikolsky equations that characterize conventional ion-selective electrodes.

The operation principle of ChemFETs can be derived from the essential electronic behavior of *MOSFET* (*metal-oxide-semiconductor FET*) devices [27], where the drain current I_D is expressed by:

$$I_D = K_d \left((V_G - V_T) V_D - \frac{V_D^2}{2} \right) \quad (70.49)$$

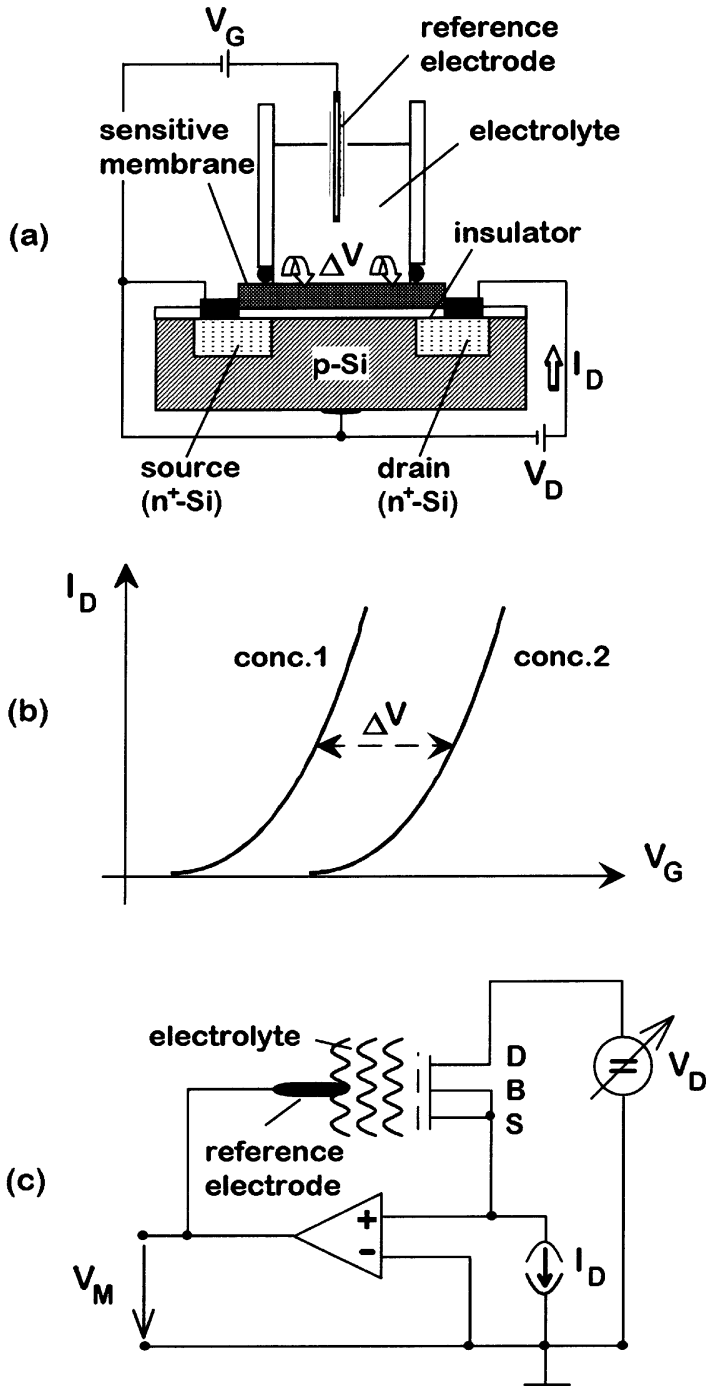


FIGURE 70.21 ISFET configuration (a), input characteristic (b), and schematic circuit of CCM (c). The metallic gate from a MOSFET (metal-oxide-semiconductor FET) is replaced by the arrangement sensitive membrane/test solution/reference electrode (V_G : gate-source voltage, V_D : drain-source voltage).

for the *nonsaturated “triode” region* ($V_D < V_G - V_T$), and

$$I_D = K_d \frac{(V_G - V_T)^2}{2} \quad (70.50)$$

for the *saturated region* ($V_D > V_G - V_T$), with:

$$K_d = \mu \frac{\epsilon_i}{d_i} \frac{b}{L} = \mu C_1 \frac{b}{L} \quad (70.51)$$

The proportionality constant K_d includes the geometric factors that influence the signal characteristic of the MOSFET. μ is the mobility of the electrons in the channel between source and drain, b is the width, and L is the length of the channel. C_1 represents the gate capacitance of the insulator per unit area. The *threshold voltage* V_T is the gate voltage to create a conductive channel between source and drain (i.e., when an inversion layer at the surface of the semiconductor is formed). For example, a positive gate voltage V_G is applied in Figure 70.21(a) that causes an n -inversion layer between the two n^+ -regions (highly n -doped silicon) S and D. The additional positive drain-source voltage V_D controls the measured current in a kind that the FET is operated in the saturated region. Thus, a small change in V_G results in a significant change in I_D .

Like with the ISEs, the most attention is gained to pH-sensitive ISFETs, built up of SiO_2 and an additional layer of Si_3N_4 , Al_2O_3 , IrO_2 , or Ta_2O_5 . The additional layer is necessary because the pH response of SiO_2 , initially used as pH-sensitive dielectric, is poor (20 to 40 mV/pH) and the material was indeed found to be unstable and to suffer from considerable drift of the sensor signal. Therefore, different insulating materials have been investigated with respect to their stability and sensitivity. For example, a double layer of $\text{SiO}_2/\text{Si}_3\text{N}_4$ shows a sensitivity of about 45 to 55 mV/pH. The sensitivity can be improved by using $\text{SiO}_2/\text{Al}_2\text{O}_3$ or $\text{SiO}_2/\text{Ta}_2\text{O}_5$ with 53 to 57 mV/pH and 55 to 59 mV/pH, respectively. Also, the reported drift values are less than 1 mV per hour. Usually, after thermal oxidation of the silicon to realize the SiO_2 layer, the pH-sensitive Al_2O_3 and Ta_2O_5 layers (about 30 to 100 nm) are deposited by means of chemical vapor deposition or sputtering. The chemical sensitivity of these gate insulating materials can be explained by the site-binding theory, which is exemplary discussed for SiO_2 in Reference 28.

Several methods and membrane types were developed to realize ISFETs sensitive toward various ions. By implantation of high doses of B, Al, Ga, In, Ti, Li, or Na, potassium- and sodium-sensitive ISFETs were achieved. Also, the deposition of thin layers of modified chalcogenide glasses offers the determination of heavy metal ions for biological investigations and industrial applications [23]. By means of vacuum evaporation, ion-sensitive films of LaF_3 , Ag_2S , or AgX ($X = \text{Cl}, \text{Br}, \text{I}$) for the determination of F^- , Cl^- , Br^- , I^- , Ag^+ , and S^{2-} can be prepared. A chemical surface modification of the original gate insulator (e.g., the covalent linking of hydrophilic layers that contain the sensing molecule), leads to organic gate materials for the determination of different ions, such as Ca^{2+} , NH_4^+ , K^+ , Cl^- , NO_3^- , Na^+ , Ag^+ , etc. [29]. Similar results were obtained for homogeneous polymeric membranes, containing solid ion-exchanger or neutral-charged carriers (see section on ISE). In order to achieve well-defined and highly ordered sensor membranes, the gate can be coated with ultrathin Langmuir-Blodgett films [30].

BioFETs (biologically sensitive FET) have been mainly realized as ISFET-based enzyme sensors, so-called *EnFETs* (*enzyme FET*). The EnFET directly corresponds to the enzyme ISE and detects the potentiometric response to either the concentration change in one of the products or reactants catalyzed by the enzyme. Frequently, EnFETs consist of a pH ISFET with the individual enzyme layer for the determination of, for example, glucose, penicillin, urea, creatinine, adenosin, acetylcholine, etc. Dual pH-sensitive FETs on the same chip can be formed as an ISFET and an EnFET, where the latter one is loaded with the active enzyme. The ISFET serves as reference and the differential output signal is insensitive to pH changes. The demand of compatibility with integrated circuit technology provides enzymatic membranes that can be photolithographically patterned (e.g., photocrosslinkable materials). A review of

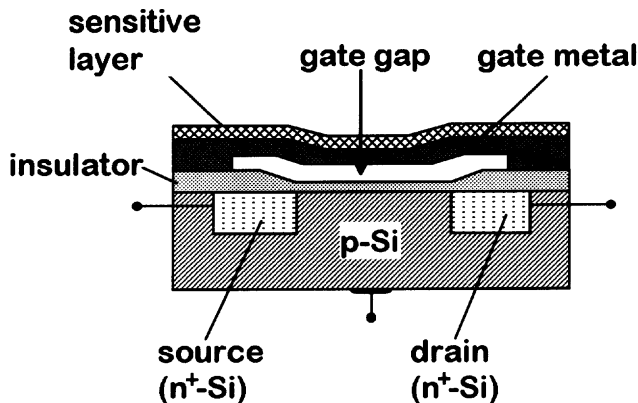


FIGURE 70.22 Schematic of a suspended gate FET (SGFET).

different categories of sensitive films and coatings and basic concepts of chemically sensitive field-effect transistors are given in Reference 31.

ReFETs (reference FETs) consist of a sensor surface that is as insensitive as possible to all kinds of substances in the test solution. Thus, a differential pair of an ISFET and a ReFET eliminates perturbations, like temperature and potential of the analyte. Appropriate materials to cover the ISFET surface with an insensitive layer are blocking materials, such as teflon or different polymers (e.g., parylene, polyacrylate, PVC). However, not well-defined potential processes as well as some ion exchange will result in nonideal behavior. Alternative concepts use nonblocking polymer membranes with a fixed membrane potential or quasi-ReFETs with a delayed pH response. The most promising approaches are the application of an inert metallic layer or wire in a differential ISFET setup as a *quasi-reference electrode*, and the miniaturization of conventional reference electrodes. For example, by means of physical vapor deposition methods, Ag/AgCl electrodes were miniaturized on silicon chips inside anisotropically etched cavities [31].

The basic mechanism of gas-sensitive FETs (GasFETs) is due to the chemical modification of the *electron work function* of a metal-insulator-semiconductor field-effect structure, for example, of a *suspended gate FET (SGFET)* as schematically shown in Figure 70.22. The SGFET contains an additional insulator, the “gap” within the gate structure, which consists of a vacuum, a gas or a nonconducting liquid. As gate metal, usually a platinum layer or mesh is used. The chemically sensitive layer on top of this structure, for example palladium, exhibits sensitivity toward hydrogen. The hydrogen molecules adsorb and dissociate atoms (H_a) on the metal surface (Pd), depending on their partial pressure, as well as desorb from the metal surface by recombination into H_2 and reacting with oxygen to form water:



The adsorbed atoms diffuse rapidly to the inner surface gap/insulator where they become polarized and form an interface dipole layer, resulting in a potential drop. For example, SGFETs with Pd, operated at 100 to 140°C, are sensitive to H_2 , CO, and H_2S in the ppm range, whereas an increased operating temperature up to 240°C allows the detection of alcohols (methanol, ethanol, propanol, buthanol). To achieve selectivity, the surface of the suspended gate can be modified by inorganic or organic layers. Ammonia sensitivity can be achieved by catalytic metals such as Pt, Ir, Ru, or Rh. By the deposition of organic layers like polypyrrole, sensitivities to alcohols and aromatic hydrocarbons are achieved. Several related devices based on SGFETs are explained in Reference 32.

Chemically Sensitive Capacitors.

Sensors on the basis of capacitive field-effect structures are much simpler to fabricate than chemically sensitive FETs, and consequently they are favorable for laboratory use. Such *EIS (electrolyte-insulator-semiconductor) structures* correspond to *MIS (metal-insulator-semiconductor) capacitors* and their operation

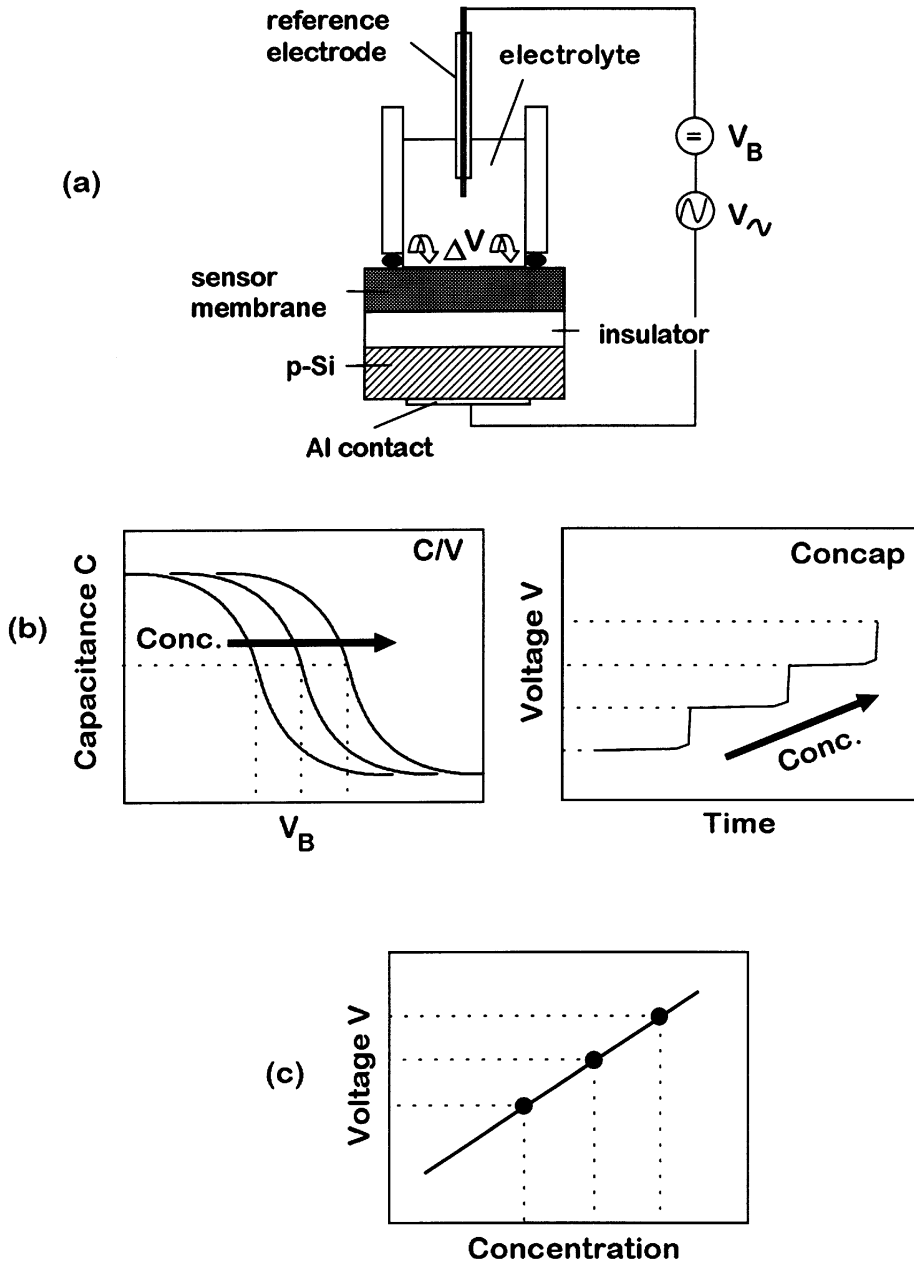


FIGURE 70.23 Schematic of an EIS (electrolyte-insulator-semiconductor) structure (a). Measurement of the EIS sensor in the C/V (capacitance/voltage) and the Concap (constant capacitance) mode (b), and resulting calibration curve (c).

principle can be derived from the fundamental MIS devices [33]. A schematic build-up of an EIS structure and the measuring principle is given in Figure 70.23(a). The sensor consists of a *p*- or *n*-type semiconductor (silicon) covered by a thermally grown SiO₂ insulating layer (<100 nm) and the sensor membrane that is directly immersed into the test solution. Usually, the sensor is contacted via a reference electrode.

Its physical properties can be explained by the charge carrier distribution at the insulator/semiconductor interface, which is controlled by both an external dc voltage (V_B) and an electrochemical interaction between the test solution and the sensor membrane (ΔV). For a *p*-Si substrate, a negative V_B ($V_B < 0$)

on the reference electrode accumulates mobile charge carriers (i.e., positive holes) at the Si/SiO₂ interface (*accumulation*). When V_B becomes positive ($V_B > 0$), the holes are displaced from the interface, forming a space charge region (*depletion*) at the semiconductor surface. If the potential gets more positive ($V_B \gg 0$), an inversion layer of accumulated electrons at the interface is created (*inversion*). The electrical behavior is given by the small-signal capacitance of the EIS structure. Depending on the applied V_B and a superimposed ac voltage (e.g., 1 kHz, 20 mV), a characteristic C/V (*capacitance/voltage*) curve results (Figure 70.23(b), left). The integral capacitance C , corresponding to V_B , is given by:

$$\frac{1}{C} = \frac{1}{C_M} + \frac{1}{C_I} + \frac{1}{C_S} \quad (70.53)$$

where C_M , C_I , and C_S are the capacitance values of the sensor membrane, the insulator, and the space charge region, respectively, with:

$$C = \frac{\epsilon_0 \epsilon_r A}{d} \quad (70.54)$$

where A is the area, d the thickness, ϵ_r the dielectric permittivity, and ϵ_0 the dielectric constant. Due to the electrochemical interaction (ΔV), a horizontal shift of the C/V curve is provided, depending on the change of the ion concentration in the test solution. As resulting measuring signal (calibration curve), the shift can be evaluated at a fixed capacitance value within the linear region of the C/V curves (e.g., 60% of the maximum capacitance, Figure 70.23(c)). Using a feedback circuit, the measured capacitance can be adjusted at a fixed value in the *Concap* (*constant capacitance*) mode (Figure 70.23(b), right). Thus, potential shifts can be recorded directly.

Chemical and biological sensing EIS structures with different organic and inorganic sensor membranes have been developed within the last few years. They consist of nearly identical sensor membrane materials and compositions as ISFETs, ranging from inorganic pH-sensitive layers (e.g., Si₃N₄, Al₂O₃, Ta₂O₅) or crystalline films (e.g., LaF₃, silver halides) over organic Langmuir-Blodgett films to enzymatic layers (e.g., urease, penicillinase). Much effort has been done in order to improve the limiting long-term stability that is often disclosed by FET devices in permanent contact with the analyte. Novel approaches pursue a further optimization with regard to the preparation (e.g., due to specific immobilization procedures) or the deposition of the sensor membrane in order to raise the sensor performance. For example, an extremely long-term stable pH sensor was developed by the suggestion of the pulsed laser deposition (PLD) process as the thin-film preparation method. The EIS structure consists of a layer sequence of Al/*p*-Si/SiO₂/Al₂O₃, where no degradation of the pH sensitivity during a measurement period of 2 years was found [34].

Like GasFETs, MIS (metal-insulator-silicon) capacitors and *MIS Schottky diodes* are also available as gas-sensitive devices. For the MIS capacitor, a concentration-dependent dipole layer is detected as a shift of the C/V curve. To reduce the drift of these devices, additional insulating layers, such as Al₂O₃, Si₃N₄, or Ta₂O₅ can be deposited between the metal layer and the SiO₂ insulator. Experimental results of Pd/Al₂O₃/SiO₂/Si structures show sensitivities of 25 mV ppm⁻¹ around 1 ppm [35]. Schottky barrier diodes consist of a thin insulating layer (e.g., 2 nm SiO₂) between the metallic gate (e.g., Pd) and the semiconductor, in order to allow the current to pass through it. By variation of the metallic gate films, different sensitivities can be achieved, comparable to those of the SGFETs.

Practical Applications and Limitations.

ChemFETs possess significant advantages over classical ISEs, such as a high-input impedance that consequently eliminates the need of shielding wires and the need for voltmeters. The small sensor area includes the possibility of multiple sensor applications (*sensor arrays*) on a single chip. Moreover, temperature compensation is possible. However, most of these sensors are exposed to a chemically very reactive environment and therefore, a highly long-term stable protection (encapsulation) of the electronics

from the analyte is required. The instability of the materials used induces sensor drifts of several millivolts per day. In some cases, attachment and fixation of the sensor membranes must be improved. To take the advantage of miniaturized FET devices, there is also the necessity of a small reference electrode. For ChemFETs, there exist two approaches for successful commercialization: dealing with small sample volumes for biomedical use (e.g., intracellular measurements) and the high-volume fabrication for a low-price market (e.g., environmental and process monitoring, agriculture and food analysis, leak detectors). The employment of capacitive EIS and MIS sensors offers besides the more easier manufacturing technique distinct advantages concerning the improved mechanical and electrochemical stability and sensor lifetime.

Conductometry

In addition to potentiometry, *conductometric analysis* represents the most important nonfaradaic method. *Conductometry* is based on the measurement of the electrical conductance of an electrolyte solution, which directly depends on the number of positively and negatively charged species in the solution. This analysis method is limited due to its nonselective nature, because all ions in the solution will contribute to the total conductance. Nevertheless, *direct conductance measurements* play an important role in the analysis of binary water/electrolyte mixtures, for example, in chemical water monitoring. The technique can also be applied to ascertain the endpoint detection in *conductometric titrations* for the determination of numerous substances.

Measurement of Conductance and Instrumentation

The *conductance* G of a solution is the reciprocal of the electrical resistance R and has the units of siemens (S) that correspond to ohm^{-1} (Ω^{-1}). The conductance of a uniform sample with the length l and cross-sectional area A is given by:

$$G = \kappa \frac{A}{l} \quad (70.55)$$

where the proportionality constant $\kappa = 1/\rho$ (ρ : resistivity) describes the *conductivity (specific conductance)* of the solution, expressed in units of S cm^{-1} . The *equivalent conductivity* Λ (*molar conductivity*) of a solution is defined as the conductivity due to one mole, measured between two electrodes which are spaced 1 cm apart, and is:

$$\Lambda = \frac{1000 \kappa}{c} \quad (70.56)$$

where c corresponds to the concentration of the solution in mol L^{-1} . The units of Λ are $\text{S cm}^{-1}\text{mol}^{-1}$. Equation 70.55 permits the calculation of the molar conductivity for a solution of known concentration by considering the experimental values of κ . The molar conductivity Λ , i.e., the mobility of ions in solution, is mainly influenced by interionic effects for strong electrolytes and the degree of dissociation for weak solutions. For strong electrolytes, the molar conductivity increases as the dilution is increased. By linear graphical extrapolation for diluted solutions of strong electrolytes, a limiting value is defined as *molar conductivity at infinite dilution* Λ_0 . At infinite dilution, the interionic attraction is nil, the ions are independent of each other, and the total conductivity is:

$$\Lambda_0 = \lambda_+^0 + \lambda_-^0 \quad (70.57)$$

where λ_+^0 and λ_-^0 are the ionic molar conductivities of the cations and anions, respectively, at infinite dilution. For weak electrolytes, due to the nonlinear relationship between Λ and c , a graphical extrapolation cannot be made. Typical values for the limiting molar conductivities for various species in water are listed in [Table 70.2](#).

TABLE 70.2 Molar Conductivity at Infinite Dilution Λ_0 ($\Omega^{-1} \text{ cm}^2 \text{ mol}^{-1}$)

Cations λ_+^0		Anions λ_-^0	
H ⁺	349.8	OH ⁻	198.3
Na ⁺	50.1	F ⁻	55.4
K ⁺	73.5	Cl ⁻	76.3
Li ⁺	38.7	Br ⁻	78.1
NH ₄ ⁺	73.4	I ⁻	76.8
Ag ⁺	61.9	NO ₃ ⁻	71.5
N(CH ₃) ₄ ⁺	44.9	ClO ₄ ⁻	67.3
Ca ²⁺	119.0	C ₂ H ₃ O ₂ ⁻	40.9
Mg ²⁺	106.2	HCO ₃ ⁻	44.5
Cu ²⁺	107.2	AcO ⁻	40.9
Zn ²⁺	105.6	SO ₄ ²⁻	160.0
Ba ²⁺	127.7	CO ₃ ²⁻	138.6
Pb ²⁺	139.0	C ₂ O ₄ ²⁻	148.4
Fe ³⁺	204.0	PO ₄ ³⁻	240.0
La ³⁺	208.8	Fe(CN) ₆ ⁴⁻	442.0

The equipment needed for measuring the conductivity includes an electric power source, a cell containing the solution, and a suitable measuring bridge. The electric power source consists of an alternating current source that produces signals of about 1 kHz in order to eliminate effects of faradaic current. The measurement is performed by a Wheatstone bridge arrangement. Modern *conductivity meters* supply the alternating current and allow the measurement in a wide range of conductivities (0,001 $\mu\text{S cm}^{-1}$ to 1300 mS cm^{-1}). Additional electronics eliminate disturbing capacitance effects and offer automatic range switching. An integrated temperature sensor corrects automatically conductivities to their value at 25°C. The conductivity cell consists of a pair of electrodes placed in a defined geometry to each other. Usually, the electrodes are platinized to increase their effective surface (high capacitance). Thus, disturbing faradaic currents are minimized. For accurate conductivity determination, the precise area of the electrodes A and their distance apart d , the *cell constant* K , must be known exactly. Therefore, the cell constant ($K = A/d$) must be evaluated by calibration with a solution of accurately known conductivity (e.g., a standard KCl solution). Details of calibration standards and concepts of conductivity cells are given in Reference 36.

Applications of Conductometry

Direct Conductometric Measurement.

In spite of the insufficient selectivity of *direct conductometric measurements*, the high sensitivity of this procedure makes it an important analytical tool for certain applications. The specific conductivity of pure water (distilled or deionized) is about $5 \times 10^{-8} \text{ S cm}^{-1}$, and the smallest trace of ionic impurity leads to a large increase in conductivity by an order of magnitude and more. Therefore, conductometric monitoring is employed where a high purity of water is required (e.g., laboratories, semiconductor processing, steam-generating power plants, ion exchanger). Conductometric measurements are widely used to control pollution of rivers and lakes, and in oceanography to control the salinity of sea water.

Conductometric Titrations.

In *conductometric titrations*, the reaction is followed by means of conductometry and is used for locating endpoints (i.e., the equivalence point (EP) in acid-base titrations (neutralization titration)). To define the titration curve, at least three or four measurements before and after the EP are required. The obtained data of the conductivity are plotted as a function of the titrant volume, and the EP is given as the intersection of the two linear extrapolated fractions. A characteristic titration curve of a strong acid (hydrochloric acid) with a strong base (sodium hydroxide) is depicted in [Figure 70.24](#). The solid line represents the resulting titration curve, whereas the broken lines indicate the contribution of the individual species. By adding NaOH to the solution, the hydrogen ions are replaced by the equivalent number

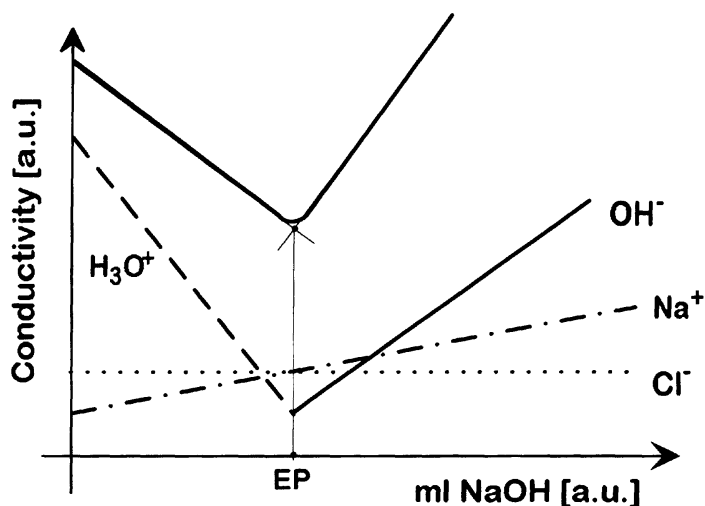


FIGURE 70.24 Conductometric titration of a strong acid (HCl) with a strong base (NaOH). The equivalence point is represented by EP.

of less mobile sodium ions (and $\text{H}^+ + \text{OH}^- \rightarrow \text{H}_2\text{O}$). As a result, the conductivity decreases to lower values. The solution exhibits its lowest conductivity at the equivalence point, where the concentrations of hydrogen and hydroxide ions are at the minimum. Further addition of NaOH reverses the slope of the titration curve, since both the sodium ion concentration and hydroxide ion concentration increase.

Due to the high linearity between the conductance and the volume of the added species, this method possesses a high accuracy and can be employed in dilute as well as in more concentrated solutions. In contrast to potentiometric titration methods, the immediate equivalence point region has no strong significance. Thus, very weak acids, such as basic acid and phenol can be titrated. Moreover, mixtures of hydrochloric acid or another strong acid and acetic (ethanoic) acid or any other weak acid can be titrated with a weak base (e.g., aqueous ammonia, acetate) or with a strong base (e.g., sodium hydroxide). Moreover, precipitation and complex-formation titrations of, for example, sodium chloride with silver nitrate are possible. For practical applications, the volume of the solution should not change appreciably during the titration. Therefore, the titrating reagent may be 20 to 100 times more concentrated than the solution being titrated, whereas the latter should be as diluted as practicable. For additional examples of analytical procedures and results of conductometric titrations, see Reference 37.

Oscillometry.

In order to investigate electrolyte solutions with high resistivities and dielectric constants, *high-frequency titration (oscillometry)* can be performed at 10^5 Hz to 10^7 Hz. For that, a specific measuring cell is required, where the metal electrodes encircle the outside of a glass container. In this arrangement, the electrodes are not in contact with the test solution, which is advantageous for dealing with corrosive materials. Oscillometric measurements can be employed for the determination of binary mixtures of nonionic species, where the dielectric behavior predominates (e.g., ethanol/nitrobenzene, benzene/chlorobenzene, and alcohol/water). Further practical examples are EDTA titrations and the determination of thorium (Th^{4+}) with sodium carbonate, beryllium (Be^{2+}) with sodium hydroxide, and hydrocarbons (e.g., benzene). However, the instrumentation as well as the interrelations are more complicated than for the classical conductivity method. Thus, oscillometry gets only significance for specific applications, where the presence of the electrodes interferes.

Conductometric Sensors.

Depending on the demanded size and geometry, miniaturized cells with two or more electrodes (e.g., a four-electrode conductivity meter) as well as contactless cells are commercially available as *conductometric*

sensors. The contactless methods use *capacitive* and *inductive conductivity cells*, which are advantageous to circumvent electrochemically caused electrode reactions. Conductivity cells can be coupled as detectors to ion chromatographic systems for measuring ionic concentration in the eluate. For this, special *micro-conductivity cells* with a volume of about 1.5 μL have been developed.

Within the last 10 years, two aspects of conductometric applications became important: *conductometric gas sensors* and the use of *conductometric chemiresistors* as sensors. In the former, a phase change that transfers the gaseous component into a solution is necessary (e.g., by a bubbler nebulizer). All methods deal with acidic gases, such as HCl, SO₂, or CO₃, or with alkaline gases like NH₃. Also, organic halogens can be detected after their conversion into HCl or HF. By means of integrated circuit technology, thin metal films can be photolithographically patterned as interdigital electrodes onto semiconductor substrates with insulating dielectric layers of SiO₂ or Si₃N₄. Both the thin metal films and additionally deposited organic layers on top of the metallic films can lead to a change of the total resistance by variation of the ionic composition of the reacting solution. For chemiresistors, the organic layer usually consists of an ion-selective polymer layer or a Langmuir-Blodgett membrane, for biosensors enzymatic layers are used (see the ISE section). Such sensors allow the determination of different gaseous components, such as CO, NO₂, H₂S, SO₂, or NH₃, as well as the detection of biologically relevant species like urea, glucose, penicillin, and choline chlorides. Although several companies offer such gas analyzer systems, conductometric sensors and chemiresistors are still in the state of research and development.

Coulometry

Coulometry represents an electroanalytical method, where the analyte is specifically and completely converted due to direct or indirect electrolysis. The quantity of electricity (in coulombs) consumed by this reaction, the charge, is measured. A fundamental requirement of coulometry is that the species in the solution interact with 100% current efficiency; that is, the reaction corresponds to Faraday's law. According to this condition, there exist two alternatives: the analyte participates in the electrode reaction (*primary or direct coulometric analysis*), and the analyte reacts with a reagent, generated by an electrode reaction (*secondary or indirect coulometric analysis*). Two general techniques — *controlled-potential coulometry* and *coulometric titration (controlled-current coulometry)* — are used for coulometric analysis.

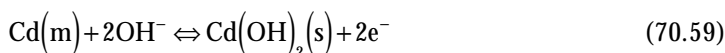
Controlled-Potential Coulometry

In this method, the potential of the working electrode is held at a constant value compared to a reference electrode. The resulting current is adjusted continuously to maintain the desired potential. The substance being determined reacts without involvement of other components in the sample. The reaction is completed when the current has practically decreased to zero. To measure the charge, a potentiostat, an instrument for measuring the time-dependent current, and a current-time integrating device are used. Modern potentiostats have a built-in electronic coulometer and allow extremely accurate determinations. Otherwise, one can use free-standing coulometers.

Controlled-potential coulometry has been widely employed for the determination of various metal ions, such as Cu, Bi, Cd, Zn, Ni, Co, Pu, and U. To apply this method, current-voltage diagrams must be available for the oxidation reduction system to be measured as well as for any reaction system at the working electrode. Current-voltage diagrams can be obtained by plotting the measured current versus the cathode-reference electrode potential. To fulfill the requirement of the 100% current efficiency in generation, it is necessary to control the potential of the working electrode. With regard to their determination, the metals are deposited at controlled potentials with a mercury cathode as working electrode and a silver wire or a platinum cylinder as anode. Typical applications are the electrolytic determination and synthesis of organic compounds like acetic acid and picric acid. Further, controlled-potential coulometry is frequently used for monitoring the concentration of constituents in gas or liquid streams, typically small oxygen contents. Here, the reduction of oxygen takes place within the pores of a porous silver cathode:



Using a cadmium sheet (m) as anode, the electrode reaction in solution (s) is:



The quantity of the electricity (current) is passed through a standard resistor and converted to a voltage signal. Hence, the oxygen concentration is proportional to the recorded potential drop. Controlled-potential coulometry needs relatively long electrolysis times, although it proceeds virtually unattended with automatic coulometers. With a multimeter, changes in the range from 1 ppm to 1% can be dissolved. Thus, controlled-potential coulometry permits analysis with an accuracy of a few tenths of a percent.

Coulometric Titration (Controlled-Current Coulometry)

Controlled-current coulometry maintains a constant current throughout the reaction period. Here, an excess of a redox buffer substance must be added in such a way that the potential does not cause any undesirable reaction. That means the product of the electrolysis of the redox buffer must react quantitatively with the unknown substance to be determined. *Coulometric titrations* need an electrolytically generated titrant that reacts stoichiometrically with the analyte to be determined. As in controlled-potential coulometry, 100% current efficiency is required. The current is accurately fixed at a constant value and the quantity of electricity can be calculated by the product of the current (in amperes) and the time (in seconds) using endpoint detection. In principle, any endpoint detection system that fits chemically can be used; for example, chemical indicators (color change), and potentiometric, amperometric or conductometric procedures. For coulometric titrations the instrumentation consists of a titrator (constant-current source, integrator) and a cell. As the constant-current source, an electronically controlled amperostat is preferably used. The integrator measures the product of current and time (i.e., the number of coulombs). The electrolysis cell, filled with the solution from which the titrant will be generated electrolytically and the solution to be titrated, is schematically shown in [Figure 70.25](#). The generator electrode, at which the reagent is formed, possesses a large surface area (e.g., a rectangular strip of platinum). The auxiliary electrode (e.g., a platinum wire) is in contact with an appropriate electrolyte of higher concentration than the solution to be titrated. It is isolated from the analyte by a sintered disk or some other porous media. This is required to avoid the interference of additional products generated at the second electrode. To circumvent these limitations of internal generation, an external generator cell is often used.

Typical applications of coulometric titrations are neutralization titrations, precipitation and complex-formation titrations, and oxidation-reduction titrations. Neutralization titrations can be employed for both weak and strong acids and bases. The former can be performed with hydroxide ions generated at a platinum anode by the reaction:



the latter one with hydrogen ions by the reaction:



A working (*generator*) electrode of silver as anode offers the determination of Cl^- , Br^- , I^- , and mercaptans in solution(s). For bromide, the reaction becomes:



Similar precipitation and complex-formation titrations as well as oxidation-reduction titrations are described in Reference 38.

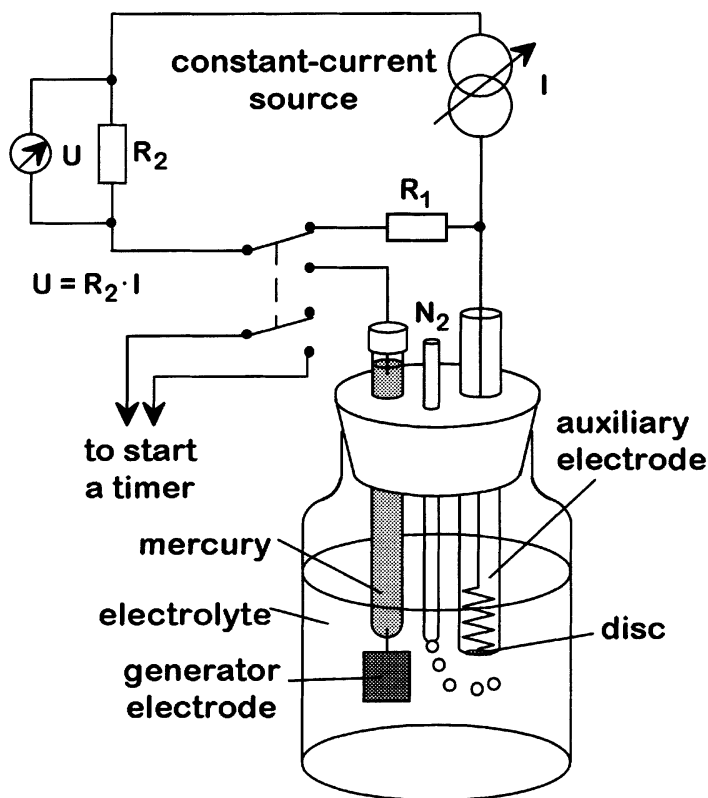


FIGURE 70.25 Coulometric titration cell with working electrode and auxiliary electrode, and equivalent circuit diagram (schematically).

Coulometric titrations possess some practical advantages: no standard solutions are required and unstable reagents can be generated or consumed immediately, small amounts of titrants can be electrically quantified with high accuracy, pretitration is possible, and the method can be readily adapted to automatic remote control. Thus, with respect to controlled-potential coulometry a wider field of practical applications exists. Often, automatic titrators for multipurpose and single analysis employ potentiometric endpoint detection. Examples are sulfur dioxide monitors and water titrators (*Karl Fischer*). For more detailed information concerning applications of coulometry, see Reference 39.

References

1. P. H. Rieger, *Electrochemistry*, Englewood Cliffs, NJ: Prentice-Hall, 1987, 70–80.
2. J. Wang, *Analytical Electrochemistry*, New York: VCH Publishers, 1994, 17–20.
3. J. Koryta and K. Šatulík, *Ion-Selective Electrodes*, Cambridge, UK: Cambridge University Press, 1983, 12–14.
4. R. C. Weast and M. J. Astle (eds.), *CRC Handbook of Chemistry and Physics*, Boca Raton, FL: CRC Press, 1982.
5. W. E. Morf, *The Principles of Ion-Selective Electrodes and Membrane Transport*, Amsterdam: Elsevier, 1981, 64–73.
6. J. Koryta, *Ions, Electrodes and Membranes*, Chichester, UK: John Wiley & Sons, 1991, 82–86.
7. P. L. Bailey, *Analysis with Ion-Selective Electrodes*, London: Heyden & Son, 1980, 15–18.
8. J. Koryta, J. Dvorák, and L. Kavan, *Principles of Electrochemistry*, Chichester: John Wiley & Sons, 1993, 176–177.

9. P. L. Bailey, *Analysis with Ion-Selective Electrodes*, London: Heyden & Son, 1980, 18–22.
10. R. N. Adams, *Electrochemistry at Solid Electrodes*, New York: Marcel Dekker, 1969, 19–29.
11. A. J. Bard and L. R. Faulkner, *Electrochemical Methods*, New York: John Wiley & Sons, 1980, 147.
12. A. J. Bard and L. R. Faulkner, *Electrochemical Methods*, New York: John Wiley & Sons, 1980, 316–366.
13. E. Gileadi, *Electrode Kinetics for Chemists, Chemical Engineers, and Materials Scientists*, New York: VCH Publishers, 1993, 428–443.
14. F. Oehme, Liquid electrolyte sensors: potentiometry, amperometry and conductometry, in W. Göpel, J. Hesse, and J. N. Zemel (eds.), *Sensors: A Comprehensive Survey*, Vol. 2, Weinheim: VCH Verlag, 1991, 302–312.
15. H. H. Willard, L. L. Merritt, J. A. Dean, and F. A. Settle, *Instrumental Methods of Analysis*, New York: D. Van Nostrand Company, 1981, 720–729.
16. A. J. Bard and L. R. Faulkner, *Electrochemical Methods*, New York: John Wiley & Sons, 1980, 186–190.
17. G. Henze, Analytical Voltammetry and Polarography, *Ullmann's Encyclopedia of Industrial Chemistry*, B5, Weinheim: VCH Verlagsgesellschaft, 1994, 705–742.
18. J. Wang, *Stripping Analysis*, Deerfield Beach, FL: VCH Publishers, 1985.
19. Kh. Z. Brainina, *Stripping Voltammetry in Chemical Analysis*, New York: Halsted Press, 1974.
20. C. H. Mastrangelo and W. C. Tang, Semiconductor Sensor Technologies, in S. M. Sze (ed.), *Semiconductor Sensors*, New York: John Wiley & Sons, 1994, 17–95.
21. K. Najafi, K. D. Wise, and N. Najafi, Integrated Sensors, in S. M. Sze (Ed.), *Semiconductor Sensors*, New York: John Wiley & Sons, 1994, 473 – 530.
22. A. K. Covington, Glass electrodes, in A. K. Covington (Ed.), *Ion-Selective Electrode Methodology*, Boca Raton, FL: CRC Press, 1979, 77–84.
23. Y. G. Vlasov, E. A. Bychkov, and A. V. Bratov, Ion-selective field-effect transistor and chalcogenide glass ion-selective electrode systems for biological investigations and industrial applications, *Analyst*, 119, 449–454, 1994.
24. A. K. Covington and P. Davison, Liquid ion exchange types, In A. K. Covington (Ed.), *Ion-Selective Electrode Methodology*, Boca Raton, FL: CRC Press, 1979, 85–110.
25. G. H. Jeffrey, J. Bassett, J. Mendham, and R. C. Denney, *Vogel's Textbook of Quantitative Chemical Analysis*, London: Longman Scientific & Technical, 1989, 572, 604.
26. G. H. Jeffrey, J. Bassett, J. Mendham, and R. C. Denney, *Vogel's Textbook of Quantitative Chemical Analysis*, London: Longman Scientific & Technical, 1989, 580–590.
27. M. J. Madou and S. R. Morrison, *Chemical Sensing with Solid State Devices*, San Diego, CA: Academic Press, 1989, 325–332.
28. M. J. Madou and S. R. Morrison, *Chemical Sensing with Solid State Devices*, San Diego, CA: Academic Press, 1989, 332–358.
29. D. N. Rheinhoudt, Application of supramolecular chemistry in the development of ion-selective ChemFETs, *Sensors and Actuators*, B6, 179–185, 1992.
30. M. J. Schöning, M. Sauke, A. Steffen, M. Marso, P. Kordoš, H. Lüth, F. Kauffmann, R. Erbach, and B. Hoffmann, Ion-sensitive field-effect transistors with ultrathin Langmuir-Blodgett membranes, *Sensors and Actuators*, B26-27, 325–328, 1995.
31. M. J. Madou and S. R. Morrison, *Chemical Sensing with Solid State Devices*, San Diego, CA: Academic Press, 1989, 361–366.
32. M. Josowicz and J. Janata, Suspended gate field-effect transistor, in T. Seiyama (ed.), *Chemical Sensor Technology*, Vol. 1, Amsterdam: Elsevier, 1988, 167–175.
33. S. M. Sze, *Physics of Semiconductor Devices*, New York: John Wiley & Sons, 1981, 332–379.
34. M. J. Schöning, D. Tsarouchas, A. Schaub, L. Beckers, W. Zander, J. Schubert, P. Kordoš, and H. Lüth, A highly long-term stable silicon-based pH sensor fabricated by pulsed laser deposition technique, *Sensors and Actuators*, B35, 228–233, 1996.
35. M. Armgarth and C. I. Nylander, Field-effect gas sensors, in W. Göpel, J. Hesse, and J. N. Zemel (eds.), *Sensors: A Comprehensive Survey*, Vol. 2, Weinheim: VCH Verlag, 1991, 509–512.

36. F. Oehme, Liquid electrolyte sensors: potentiometry, amperometry and conductometry, in W. Göpel, J. Hesse, and J. N. Zemel (eds.), *Sensors: A Comprehensive Survey*, Vol. 2, Weinheim: VCH Verlag, 1991, 317–328.
37. D. A. Skoog and D. M. West, *Principles of Instrumental Analysis*, Philadelphia, PA: Saunders College, 1980, 648–651.
38. D. A. Skoog and D. M. West, *Principles of Instrumental Analysis*, Philadelphia, PA: Saunders College, 1980, 598–599.
39. E. A. M. F. Dahmen, *Electroanalysis*, Amsterdam: Elsevier 1986, 218–224.

Further Information

- P. T. Kissinger and W. R. Heinemann, *Laboratory Techniques in Electroanalytical Chemistry*, 2nd ed., New York: Marcel Dekker 1996.
- P. J. Gellings and H. J. M. Bouwmeester, *The CRC Handbook of Solid State Electrochemistry*, Boca Raton, FL: CRC Press, 1997.
- J. Bockris and S. Khan, *Surface Electrochemistry: A Molecular Level Approach*, New York: Plenum Press, 1993.
- C. Brett and A. Brett, *Electrochemistry: Principles, Methods and Applications*, New York: Oxford University Press, 1993.

70.2 Thermal Composition Measurement

Mushtaq Ali, Behrooz Pahlavanpour, and Maria Eklund

Thermal analysis is the measurement of a physical parameter as a function of temperature. The area comprises several techniques where thermogravimetry, thermometric titrimetry, thermomechanical analysis, differential thermal analysis, differential scanning calorimetry, and some specialized techniques are among those described in this section. Applications are found in the characterization of organic materials, both solids and liquids. Materials of interest can be polymers, mineral and synthetic oils, lubricants, greases, paper (cellulose), and pharmaceuticals. The material to be analyzed (typically 10 mg) must be isolated and subjected to thermal treatment, hence the technique is destructive. The obvious advantage is that the thermal profile, or structure of a large specimen can be investigated. The disadvantage is that the small sample size can give rise to excessive statistical errors. However, recent advances in microcalorimetry techniques to look at slow degradation of pharmaceuticals allow thermal analysis to be performed at room temperature on samples up to a few grams without destruction of the sample. A general schematic of thermal analysis apparatus is shown in [Figure 70.26](#).

The history of the development of thermal analysis methods from the sixteenth century is the subject of a number of excellent papers by Mackenzie [1–3], Wendlandt [4], and Keattch [5]. Lavoisier and Laplace [6] were pioneers in the development of thermal analysis by their practical approach.

The International Confederation for Thermal Analysis and Calorimetry (ICTAC) has produced definitive guidelines regarding nomenclature and calibration [7–10].

Factors Affecting Results

The five factors affecting thermal analysis can be remembered by the acronym S.C.R.A.M. [11]. This refers to the **S**ample, **C**rucible, **R**ate of heating, **A**tmosphere, and **M**ass. See [Table 70.3](#).

Thermogravimetry

Thermogravimetry (TG) or TGA (thermogravimetric analysis) [8] is a technique in which the mass of the sample is monitored against time or temperature while the temperature of the sample, in a specified atmosphere, is programmed.

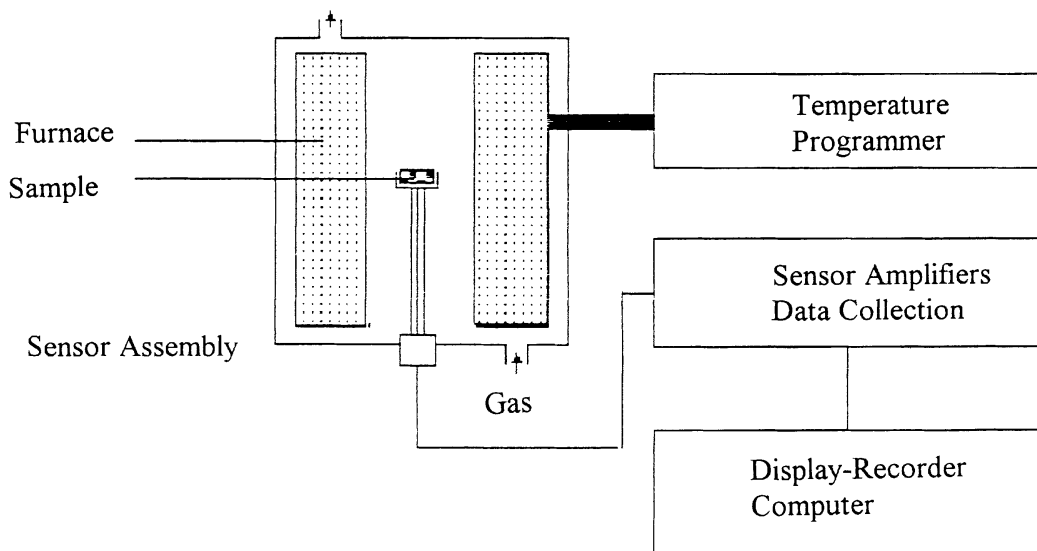


FIGURE 70.26 Schematic thermal analysis apparatus. The figure shows the essential components of a generalized thermal analysis apparatus.

TABLE 70.3 Factors Affecting Thermal-Analysis

Factor	Details
Sample	History of sample and preparative technique used can affect the curve and the presence of trace impurities (in some cases) may catalyze decompositions. Particle size can alter shape of curve (e.g., by surface reaction).
Crucible	The crucible (or sample holder) material should be such that it does not react with the sample or catalyze a reaction. The geometry of the sample holder may affect the results [12].
Rate of heating	Thermal lag: rate of heat transfer between furnace and all parts of the sample are not instantaneous. Therefore, care should be taken when working at different heating. Corrections can be applied [12].
Atmosphere	Various effects [12], including dissociation of sample.
Mass of sample	Size and packing density.

Note: Details the five main areas which would affect analysis of a sample via thermal experiments. The effects can be marked and would certainly affect repeatability also.

Derivative Thermogravimetry (DTG) shows the change in mass per unit time as a function of temperature.

Apparatus

The apparatus is referred to as a thermobalance or thermogravimetric analyzer. There are a number of configurations: horizontal, simultaneous (TGA-DTA), and vertical. The vertical design provides better sensitivity and weight capacity. The thermobalance consists of five essential components: furnace, temperature regulator, weighing mechanism, atmosphere controller, and recording system.

Calibration

Small furnaces can be calibrated by a method [8] using Curie points of a range of metals and alloys. The Curie point is the temperature at which a ferromagnetic material loses its ferromagnetism. At the Curie point, the magnetic force is reduced to zero and an apparent mass change is observed.

The study of the reactions can be divided into the stages: (1) intermediates and (2) products of reaction, (3) energetics of reaction, and (4) the reaction kinetics. Stages (1) and (2) can be readily studied by TG and DSC.

For example, the decomposition of calcium oxalate monohydrate shows three distinct steps. The first around 200°C with a loss of 12.4% corresponds to dehydration, while those at 500°C and 800°C match with a loss of CO and CO₂. These are confirmed by analysis of residues.

Kinetics of Reaction Including Measurement of α and $d\alpha/dt$.

The use of thermogravimetry as a means for the elucidation of the reaction kinetics is attractive. The nature of solid-solid interactions is quite complex [14] and will not be discussed in this section.

Consider an endothermic solid-state reaction:



During the course of the reaction, there is a mass loss, combined with the loss of gas. Heat absorption also occurs. This process can be modeled. However, it should be noted that the equation (although generally applicable) are not valid for all cases. Methods and mathematical treatment of results are given in the papers by Šatava, Šesták, and Škvára [15-18].

Static (isothermal) and dynamic methods can be used in a kinetic study of the weight change. The former is based on the determination of the degree of transformation at constant temperature as a function of time. The latter is the determination of the degree of transformation as a function of time during a linear increase of temperature. The static method is probably better suited for obtaining information about the slowest process, the reaction order, and reaction mechanism. The dynamic method is better if data on the kinetics of the reaction from a single curve for the whole temperature range is required. Comparisons between both methods have shown comparable results with respect to precision [19].

The extent of a reaction ξ may be defined [20] by Equation 70.64.

$$n_B = n_{B,0} + \nu_B \xi \quad (70.64)$$

where n_B = Amount of substance B

$n_{B,0}$ = Amount of substance B at $t = 0$

ν_B = Stoichiometric number of B (positive number if B is a product and negative if B is a reactant)

For solid-state reactions, the changes in the portion reacted α are followed with respect to time. Therefore, the rate of reaction can be defined by Equation 70.65.

$$\text{Rate} = d\alpha/dt \quad (70.65)$$

For solution reactions (referring to Equation 70.63), the change in concentration C_B of B is followed.

Since the rate of reaction varies with time (even at constant temperature) at a value of α Equation 70.66 is derived.

$$\text{Rate} = d\alpha/dt = k_T f(\alpha) \quad (70.66)$$

where k_T = the rate constant at temperature T

$f(\alpha)$ = mathematical expression in α

It should be noted that the form of $f(\alpha)$ sometimes alters part way through a reaction.

If hyphenated group-specific techniques are employed to study a reaction simultaneously (e.g., as in the case in TGA and FTIR), the IR-active species may not contribute the greatest mass loss and therefore the values of α will not be the same.

There are many equations relating the rate of solid-state reactions to α and they have been summarized by Sestak and Berggren [21].

A general *integrated* kinetic equation is given in Equation 70.67.

$$g(\alpha) = k_T t \quad (70.67)$$

where $g(\alpha) = \int d\alpha/f(\alpha)$.

The rate constant k_T can be calculated from the Arrhenius equation given in Equation 70.68.

$$k_T = A \exp(-E_A/RT) \quad (70.68)$$

where E_A = Activation energy (J mol⁻¹)

A = Pre-exponential factor

R = Molar gas constant, 8.314 J (K mol)⁻¹

Measurement of α and $d\alpha/dt$

Consider a thermogravimetric curve consisting of one step. α at a particular time can be found using:

$$\alpha = m_i / (m_i - m_f) - m_t / (m_i - m_f) \quad (70.69)$$

The differential is hence:

$$d\alpha/dt = -[dm_t/dt / (m_i - m_f)] \quad (70.70)$$

This states that the rate of reaction can be measured from the slope of the mass–time curve. Since dm_t/dt is already measured by the DTG curve, $d\alpha/dt$ can be found directly from the curve.

Combination of a number of the equations discussed [13] gives:

$$\ln d\alpha/dt - \ln(f(\alpha)) = \ln(A/\beta) - E_A/RT \quad (70.71)$$

where $\beta = dT/dt$.

Thermometric Titrimetry

Thermometric titration is the measurement of the temperature change in a system as a function of time or volume of titrant. The technique consists of the measurement of the change in temperature as the titrant is added to it, under near adiabatic or more commonly referred to as isoperibol conditions. The experiments are typically carried out in a small dewar flask submerged in a well-controlled constant-temperature bath. The method can be used to study oxidation-reduction, complexation, precipitation, and neutralization reactions in aqueous solvents. Publications by Zenchelsky [22] and Jordan [23] review the technique in detail.

The basic principle is that a free energy change occurs in the system [24], and is based on the measurement of the free energy-dependent term:

$$\Delta G^\ominus = -RT \ln K \quad (70.72)$$

where ΔG^\ominus = Change in free energy under standard conditions

R = Molar gas constant

T = Temperature in kelvin

K = Equilibrium constant for the system at the temperature T

A calorimetric method (entropy titration) for the determination of ΔG , ΔH , and ΔS from one thermometric titration has been described by Christensen et al. [24].

Thermomechanical Analysis

Thermomechanical analysis relates to techniques where deformation is measured as a change in either volume or length. The deformation is plotted against temperature when a sample is heated under a controlled temperature program. Thermodilatometry measures the dimensional changes as a function of time under negligible loads. Thermomechanical analysis (TMA) is similar to thermodilatometry, but also provides information regarding penetration, extension, and flexure using various types of loads on the test specimen. In dynamic mechanical analysis (DMA), the test specimen is subjected to a sinusoidally modulated stress under specified temperature. The viscoelastic response of a material is then monitored under tensile, compressive, shear, or torsional load [25].

Apparatus

A typical instrument for thermal mechanical analysis is called a dilatometer and is equipped with a linear variable differential transformer (LVDT). The displacement of the sample is transferred to the LVDT via a rod (probe) that is unaffected by heat and dimensional changes. A zero weight is accomplished for thermodilatometry by a float system so that a minimum of a load is subjected to the sample. The sample is placed on a sample holder in an oven. A force is applied through the probe in TMA and DMA. The sample cylinder and the probe are independently connected to the measuring device. The top of the probe is also connected to a balance arm. Probe movement and sample length changes are detected. The recorded signals are time, temperature, dimensional changes, and load. Various probes are available, depending on the analysis needs. Expansion, compression, and penetration probes are standard. Tension, three-point bending, and cubical expansion probes are available. Measuring temperature from -150°C to 600°C or even up to 1500°C is possible, depending on the instrument.

Calibration of Probe

The temperature is usually the measured quantity in thermomechanical analysis. Therefore, calibrating the temperature axis is important. Thermomechanical analyzers can be temperature calibrated according to ASTM standard test method E 1363 [26]. An equation is developed for a linear correlation of the experimentally obtained program temperature and the actual melting temperature for known melting standards (i.e., mercury, water, tin, benzoic acid). A penetration probe is used to obtain the onset temperatures for two melting standards. The two-point calibration assumes the relationship Equation 70.73 between the actual specimen temperature (T_i) and the observed extrapolated onset temperature (T_0). S and I are the slopes and intercept, respectively, in the TMA thermal curve (Figure 70.27).

$$T_i = (T_0 \times S) + I \quad (70.73)$$

Thermomechanical methods are generally applied on solid, shaped samples like polymeric products. Special clamps are used for testing of soft samples made of rubbers, adhesives, fats, etc. Films and fibers can be tested using clamps. Liquid polymers are tested on support. DMA is used for detecting α , β , and γ transitions in cured epoxy systems [25]. Thermomechanical analysis, TMA, is used for measuring the volume change of bitumen. Scratching and crack propagation at low temperatures is simulated. This is useful when investigating asphalt paving materials [27]. The thermal expansion coefficient of linear expansion is calculated from the slope of the expansion-temperature curve. This is obtained under zero load in thermodilatometry mode. Thermodilatometry can also provide information on phase changes, sintering, and chemical reactions. Softening temperatures are measured using small-diameter tips on the probe under a load (TMA). This sensitive technique is also used for the measurement of heat distortion temperatures and glass transition temperatures of polymers [28].

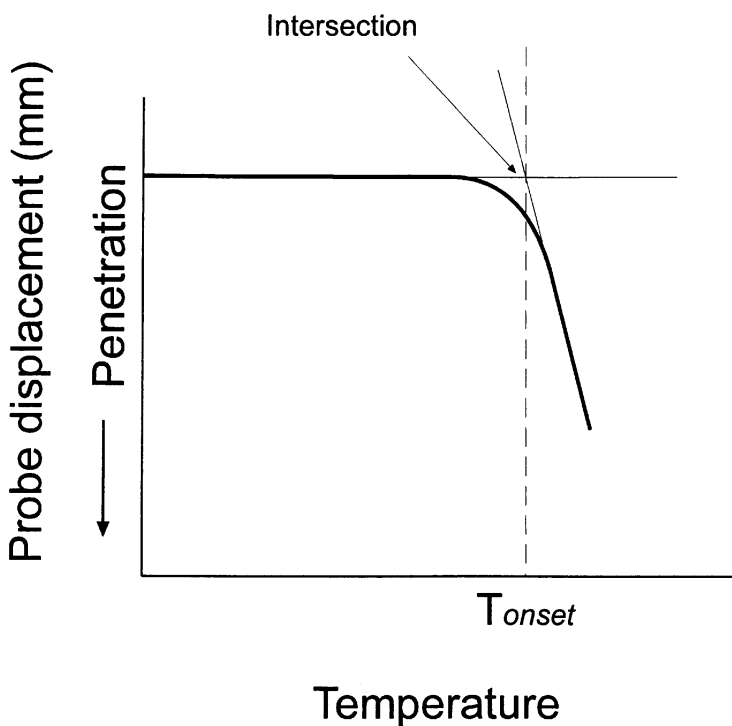


FIGURE 70.27 The calibration of a TMA instrument is a two-point method. There is an assumption that there is a relationship $T_i = (T_o \times S) + I$ between the actual specimen temperature and the onset temperature (Equation 70.73).

Differential Thermal Analysis and Differential Scanning Calorimetry

DTA is the detection of the temperature difference between the sample holder and the reference holder using the electromotive force of the thermocouples, which are attached to the holders. The sample and reference are subjected to a controlled temperature program. The **differential** is output as the DTA signal. DSC is similar to a DTA in construction, but the DSC measures the difference in heat flow rate to the sample and the reference. Consequently, more information is received on the thermodynamic behavior of the material using DSC. Quantitative DTA is also addressed as a DSC. This definition results in that the major part of all differential thermal analyses performed today uses DSC. An application is found for combined TGA/DTA analysis for kinetic evaluation of petroleum products [29].

Apparatus

The DTA apparatus has a sample and a reference cell subjected to the same temperature program. The measuring device consisting of a thermocouple or any temperature measurement device placed in each cell, measuring the difference in temperature. Operating temperature range is ambient to 1000°C or higher depending on the construction of the instrument and sample pan material. Differential scanning calorimetry is originally defined as individually heated cells. Equal temperature is maintained in the cells, giving an electrical signal proportional to the power needed. The DSC curves represent the rate of energy absorption. Today, most DTA units that can be calibrated to give calorimetric response are called DSC [25]. For qualitative applications, both classical DTA and DSC are equally good. In quantitative work, the DSC is claimed to be better at low heating rates [30].

Calibration and Reference Materials

The dynamic nature of thermal analysis requires a calibration and standard compound to be able to relate results obtained by different instruments. Temperature calibrations can be done using a range of selected materials. Different materials are chosen depending on the temperature range. Common standards are 1,2-dichloroethane, indium, silver sulfate, and quartz. Other organic compounds, metals, inorganic nitrates, sulfates, or chromates are also used [25].

Theory of DTA and DSC

The measured quantity is ΔT , the difference between the temperature of the sample and the reference material. In Equation 70.74, T_S is the temperature of the sample and T_R is the temperature of the reference material.

$$T_S - T_R \equiv \Delta T \quad (70.74)$$

The result is presented as a plot of ΔT against T under a stated temperature program, the differential thermal curve. An endothermic process is then shown as a negative signal. A quantity of material decomposition or the enthalpy of the process is obtained from the area of the peak. It is then, in fact, a calorimetric analysis and the technique is referred to as differential scanning calorimetry.

In DTA, heat transfer to a sample and reference causes a difference in temperature ΔT , which can be related to the energy of any transition of the sample.

$$\Delta H = K (\text{peak area}) \quad (70.75)$$

For heat flux DSC, a similar process occurs, whereas in power compensated DSC, electric heating is supplied to the sample and reference to keep their temperatures as close as possible. For best calorimetric accuracy, the constant K should vary little with T .

Specialized Techniques

Thermoelectrometry

Electrical properties such as resistance/conductance and capacitance can be measured as a function of temperature. A variation that can measure the generated EMF is called thermovoltic detection [8].

Modulated DSC

In MDSC, the heating rate is modulated. This is performed using a small alternating power supply in combination with the standard programmed heating. The heating program is given by the equation:

$$T = T_0 + \beta t + B \sin(\omega t) \quad (70.76)$$

and the heat flow is given by:

$$dq/dt = C_p [\beta \omega \cos(\omega t) + f(t, T) + C \sin(\omega t)] \quad (70.77)$$

- where T_0 = Initiation temperature
 B = Amplitude of temperature modulation
 ω = Angular frequency = $(2\pi f)$
 C_p = Heat capacity
 $f(t, T)$ = Kinetic response (average)
 C = Amplitude of response to sine-wave modulation

Simultaneous Techniques

Each of the techniques discussed above provides information about the sample. However, a synergistic effect exists, in that, the total amount of information obtained (by using techniques simultaneously) regarding the sample is greater than the sum of the information from the individual techniques.

Evolved Gas Analysis.

This allows the identification of gases evolved during thermal analysis and is performed by replacing the detector with a mass spectrometer or FTIR. An alternative technique is to precede the detector by passing gases evolved during the thermal analysis through a gas chromatograph.

Thermomicroscopy.

This can be incorporated under thermooptometry (a family of techniques that measure changes of an optical property with temperature change). Thermomicroscopy uses observations under a microscope.

Applications (Including the Analysis of Electrical Insulating Materials)

Oxidative Stability of Oils and Greases and Polymers.

Oxidative degradation of oils upon heating can be monitored using a DSC apparatus. The detected onset *time* or *temperature* of the exotherm can be taken as a measure of the thermal/oxidative stability of the oil. The detected onsets are a strong function of the sample size, instrument sensitivity, kinetics, and scan rate. This enables DSC to be used in an oxidation test. Isothermal high-pressure DSC (PDSC) has been used to characterize the oxidative stability and the oxidation mechanisms of lubricants [34,35]. A PDSC works at pressures up to 3.5 MPa of a selected gas, using a wide temperature range. The technique is useful in the development of new lubricants with improved thermal and oxidative properties. The influence of metal catalysis on oil oxidation can be determined using PDSC. The volatile degradation products have been determined using combined PDSC–GC/MS (gas chromatography–mass spectrometry) [36]. PDSC gives information about relative oxidation stability used for comparing the lifetime of oils [37,38]. It has been a good technique for evaluating the thermal and oxidative stability of lubricating oils [34,39]. PDSC has also been used for evaluating deposit-forming tendencies of liquid lubricants [39].

Volatilization occurs when a low-boiling oil is heated, especially at high temperatures. This leads to uncontrolled changes in composition. It also affects the size and shape of the DSC exotherm, causing imprecise determination of the oxidation onset [34]. Use of high pressure in the DSC cell reduces volatility and evaporation interference with it. Added to this, the onset value is shifted to lower temperatures [34]. The onset becomes better defined and the peak size increases [40].

DSC is a fast technique for oxidation stability testing. This is a great advantage in the quality control of electrical insulating oils. Experimental evaluations of transformer insulating oils have shown ranking to be possible. The remaining lifetime of inhibited oils may correlate to the oxidation induction time [41]. Important parameters in PDSC are sample weight, pressure, and temperature program and have to be carefully considered before applying the technique. The sample pans must not be overlooked. Results are significantly influenced by variations in metallurgy, due to the catalytic and inhibiting effects of various metals. Oxidation induction time of lubricating greases can be determined by ASTM method D5483-93.

Predicting the Lifetime of a Product.

Estimating the lifetime of a product typically uses some form of accelerated testing. TGA decomposition kinetics can be used to arrive at aging stability information and lifetime predictions in relatively short timescales (hours compared months in conventional oven aging). The sample (e.g., insulating paper, etc.) can be heated through its decomposition at several heating rates and the weight loss as a function of temperature recorded. The activation energy is calculated from a plot of log heating rate versus the reciprocal of the temperature for a constant decomposition level. The activation energy is subsequently used to calculate kinetic parameters such as specific rate constant (k) or half-life times, as well as to estimate the lifetime of the material at a given temperature. DTA and DSC have been employed in the

electric industry to study polymeric insulation and for the determination of dielectric stability and lifetime prediction.

Thermal Analysis and Stability of Materials.

TGA is widely employed in the determination of thermal stability of materials and analysis of their composition. The thermal history of electric cable insulation has been determined using DSC [42]. Thermal analysis techniques have greatly improved the quality control and inspection of electric cables. Hyphenated techniques have been employed in the analysis of trace components in electrical insulation [42-44]. ASTM method D3386-84 standardizes measurement of coefficient of linear thermal expansion of electrical insulating materials, while D3850-84 refers to the rapid determination of thermal degradation of solid electrical insulating materials by thermogravimetric methods.

Mechanical Stress Determinations.

Longitudinal mechanical stresses, frozen into electric cable insulation during the fabrication process, can produce "shrink back." This causes the insulation to shrink away from freshly cut cable ends, to varying degrees. TMA can be used to determine these stresses and has been found more versatile than the traditional BS6469 shrinkage measurement [45,46].

Evolved Gas Detection and Evolved Gas Analysis.

The main use of EGD is to distinguish between phase transitions and endothermic decompositions (e.g., coordination chemistry). It has been used for the analysis of effluents [47]. Thermogravimetric analysis coupled with FTIR has been used to establish the failure mechanisms of electrical insulating materials [48]. EGA is also used for assessing the thermal endurance of polymeric materials and is of particular value in thermosetting polymers used in the electric industry [49].

Investigation of Polymeric Systems.

Thermogravimetry can be applied to the study of polymer processes (pyrolysis, oxidative degradation, volatilization, absorption, adsorption, and polymerization) in which a change in weight occurs. The degree of crystallinity provides information regarding the thermal history of a polymer and can be measured by DSC. Physical and mechanical properties of polymers are related to the degree of crystallinity [50]. Thermophysical property measurements and analysis of additives in polymers can also be performed using thermal analysis techniques [51]. ASTM method D4000-89 can be used for the identification of plastic materials.

Pharmaceutical Applications.

Calorimetric purity determinations are used in the pharmaceutical industry. The concentration of the impurity is regarded as inversely proportional to its melting point. Therefore, an increase in the sample's impurity content decreases the melting point and broadens the melting range. DTA can also be used but DSC is preferred since it also gives the ΔH_f (heat of fusion) of the melt [52]. The DSC method is based on the van't Hoff equation. A compound may exist in various crystal forms DSC and TG are used to characterize polymorphs and assess the stability of the compounds. DSC has been used for investigating the effect of inhibitors with model membranes [53]. Drug incompatibility is defined as "an interaction between two or more components to produce changes in the chemical, physical, microbiological, or therapeutic properties of the preparation" [54]. DTA and DSC are used to record reactions as a function of temperature and investigate drug compatibility [55]. Recent advances in microcalorimetry have allowed nondestructive analysis at room temperature [56,57]. The technique is gaining popularity in the pharmaceutical industry and also in the study of ballistics.

Characterization of Greases and Lubricants.

Greases and lubricants are, in application, exposed to high temperatures in both inert and in oxidizing atmosphere. Material losses due to evaporation and loss or alteration due to thermal cracking or oxidation of the molecular structure are possible. The various aging reactions are usually inhibited by additives. Thermogravimetry, differential thermoanalysis, and differential scanning calorimetry are used as test

instruments, but the overall difficulty is to find methods that correlate with real thermal aging of the greases and lubricants.

The peak onset and peak maximum temperatures from DTG, DTA, and DSC curves are used or the peak onset from TGA curve. The evaporation behavior of greases is the most used parameter, but wax content, glass temperature, and cloud point are other characteristics of greases that are studied using thermoanalytical techniques [27].

In the Noack test of evaporative loss (DIN 51 581), the sample is held at 250°C for 60 min in an air flow. The sample is weighed before and after treatment. The cause of the weight loss is not clear, whether it is evaporation of parts of the original sample or evaporation of oxidative degradation products. The question has arisen whether isothermal thermogravimetry could replace the Noack test. This would provide continuous loss information during the thermal exposure. It has been shown that there is a higher weight loss in the thermobalance than in the Noack test at equal test conditions. The deviation is caused by the difference in surface:volume ratio between the two methods [27].

Oxidation studies of low boiling lubricant or lubricating oils do not give representative results. This is due to the evaporation of the oil and low boiling oxidative degradation products. A TGA curve of a lubricant produced in an air atmosphere does not always represent the oxidation reaction. The use of an elevated oxygen or air pressure in DSC has been shown to reduce sample evaporation due to an increased evaporation temperature and increase the rate of the oxidation. Several papers deal with this technique, which has found application in the characterization of lubricants [27,34-41,58].

Insulation Paper/Cellulose.

The rate of weight loss on pyrolysis of cellulosic materials has applications to engineering problems in many industries. On heating, cellulose undergoes a number of linked physical and chemical changes [59]. Properties such as weight, strength, crystallinity, and enthalpy are affected.

Thermogravimetric analysis can be used to perform a collective measurement of the weight loss due to the production of H₂O, CO, and CO₂ during degradation. Of course, the measurement will include evaporation of other pyrolysis products. The enthalpy changes can also be measured by DSC. These methods are very useful in determining the temperature range at which physical and chemical processes occur. The rate of these processes can be determined by using DTG (derivative thermogravimetry).

Acknowledgments

The authors would like to thank P. Haines, Chapman and Hall, and TA Instruments for their advice and permission.

Defining Terms

Thermal analysis: A group of techniques in which a property of the sample is monitored against time or programmed temperature (in a specified atmosphere).

Derivative: Techniques where a measurement or calculation of the first derivative is performed.

Differential: Techniques where a difference in a property is measured.

References

1. R.C. Mackenzie, A history of thermal analysis. *Thermochim. Acta*, 73, 249, 1984.
2. R.C. Mackenzie, Origin of thermal analysis. *Israel J. Chem.*, 22, 203-205, 1982.
3. R.C. Mackenzie, Early thermometry and differential thermometry. *Thermochim. Acta*, 148, 57-62, 1989.
4. W.W. Wendlandt, The development of thermal analysis instrumentation 1955-1985. *Thermochim. Acta*, 100, 1-22, 1986.
5. C.J. Keatch and D. Dollimore, *Introduction to Thermogravimetry*, Heyden, London, 1975.
6. A.L. Lavoisier and P.S. de Laplace, *Mem. R. Acad. Sci., Paris*, 355, 1784.

7. R.C. Mackenzie, C.J. Keattch, D. Dollimore, J.A. Forrester, A. Hodgson, and J.P. Redfern, Nomenclature in thermal analysis II. *Talanta*, 19, 1079-1081, 1972.
8. J.O. Hill, *For Better Thermal Analysis and Calorimetry III*. ICTA, 1991.
9. R.C. Mackenzie, Nomenclature in thermal analysis III. *J. Thermal Anal.*, 8(1), 197-199, 1975; *Thermochim. Acta*, 28, 197, 1975.
10. R.C. Mackenzie, Nomenclature in thermal analysis, in *Treatise on Analytical Chemistry*, P.J. Elving, (Ed.), Part 1, Vol. 12, John Wiley & Sons, New York, 1983, 1-16.
11. P.J. Haines, *Thermal Methods of Analysis*, Blackie/Chapman and Hall, London, 1995.
12. E.L. Charsley, J.P. Davies, E. Gloeggler, N. Hawkins, G.W.H. Hoehne, T. Lever, K. Peters, M.J. Richardson, I. Rothmund, and A. Stegmayer, *J. Thermal Anal.*, 40, 1405-1414, 1993.
13. G.M. Lukaszewski, Accuracy in thermogravimetric analysis. *Nature*, 194, 959, 1962.
14. W.E. Garner, *The Chemistry of the Solid State*, Butterworths, London, 1955.
15. V. Šatava, *Silikáty*, Pouziti Terografických Metod ke Studiu Reakcí Kinetiky, 5(1), 68, 1961. (The Thermographic method [sic] of Determination of Kinetic Data).
16. V. Šatava and J. Šesták, Kinetika Analýzy Termogravimetrických Da, *Silikáty*, 8(2), 134, 1964. (Kinetic Analysis of Thermogravimetric Measurements), Source: un-numbered English-language contents page preceding p.93 in *Silikaty*, 8(2), 1964.
17. V. Šatava and F. Škvára, Mechanism and kinetics of the decomposition of solids by a thermogravimetric method. *J. Amer. Ceram. Soc.*, 52, 591-595, 1969.
18. J. Šesták, A review of methods for the mathematical evaluation kinetic data from nonisothermal and isothermal thermogravimetric measurements. *Silikáty*, 11, 153-190, 1967.
19. J. Šesták, Errors of kinetic data obtained from thermogravimetric curves at increasing temperature. *Talanta*, 13, 567, 1966.
20. M.L. McGashan, *Physico-Chemical Quantities and Units*, RSC, London, 1968, 39.
21. J. Šesták and G. Berggren, Kinetics of the mechanism of solid state reactions at increasing temperatures, *Thermochim. Acta*, 3, 1-12, 1971.
22. S.T. Zenchelsky, Thermometric Titration, *Anal. Chem.*, 32, 289R, 1960.
23. J. Jordan, *Handbook of Analytical Chemistry*, L Meites, Ed., McGraw-Hill, New York, 1963, Sec. 8-3.
24. L.S. Bark and S.M. Bark, *Thermometric Titrimetry*, International series of monographs in Analytical Chemistry, Vol. 33, Pergamon Press, 1969; J.J. Christensen, R.M. Izatt, L.D. Hansen, and J.A. Partridge, Entropy titration. A calorimetric method for the determination of ΔG , ΔH , ΔS from a single thermometric titration. *J. Phys. Chem.*, 70(6), 1966 and 40(1), 1968.
25. D. Dollimore, Thermoanalytical instrumentation, in G.W. Ewing (Ed.), *Analytical Instrumentation Handbook*, Marcel Dekker, New York, 1990.
26. ASTM Designation: E 1363-90, Standard test method for Temperature Calibration of Thermomechanical Analyzers. 1990.
27. H. Kopsch, *Thermal Methods in Petroleum Analysis*, VCH, Verlagsgesellschaft mbH, Weinheim, 1995.
28. H.H. Willard, L.L. Merritt Jr., J.A. Dean, and F.A. Settle Jr., *Instrumental Methods of Analysis*, 6th ed., Wadsworth Publishing Company, Belmont CA, 1981.
29. ASTM Designation E 698-79, Standard Test Method for Arrhenius Kinetic Constants for Thermally Unstable Materials. 1979.
30. M.I. Pope and M.D. Judd, *Differential Thermal Analysis*, Heyden & Sons Ltd., London, 1980.
31. W.W. Wendlandt, Thermoelectrometry — a review of recent thermal analysis applications. *Thermochim. Acta*, 73, 89-100, 1984.
32. P.D. Garn and G.D. Anthony, Repetitive gas chromatographic analysis of thermal decomposition products. *Anal. Chem.*, 39, 1445-1448, 1967.
33. M.R. Holdiness and R. Mack, Evolved gas analysis by mass spectrometry: a review, 1 *Thermochim. Acta*, 75, 361-399, 1984.
34. S.M. Hsu, A.L. Cummings, and D.B. Clark, Society of Automotive Engineers SAE, Technical Paper 821252, 1982.
35. R. Schumacher, Practical thermoanalysis in tribology, *Tribology International*, 25(4), 259-270, 1992.

36. A. Zeman, DSC cell — a versatile tool to study thermooxidation of aviation lubricants. *Journal of Synthetic Lubricants*, 5, 133-148, 1988.
37. E. Gimzewski, A multi-sample high pressure DTA for measuring oxidation induction times. *Thermochim. Acta*, 170, 97-105, 1990.
38. R.E. Kauffman and W.E. Rhine, *Journal of the Society of Tribologists and Lubrication Engineers*, 44, 154-161, 1988.
39. Y. Zhang, P. Pei, J.M. Perez, and S.M. Hsu, *Journal of the Society of Tribologists and Lubrication Engineers*, 48, 189-195, 1992.
40. R.L. Blaine, Thermal-analytical characterization of oils and lubricants, *American Laboratory*, Reprint, January, 22, 18-20, 1974. Vol. 6; No. 1.
41. M. Eklund, Literature review of DSC oxidation tests on petroleum products. Report to International Electrotechnical Commission Technical Committee, April 10, 1996.
42. J.W. Billing, Thermal history of cable insulation revealed by DSC examination. *IEEE DMMA Conference*, 289, 309-312, June 1988.
43. R.L. Hutchinson, Thermal analysis to spectroscopy, an overview of analytical instrumentation for electrical insulating materials. *Proceeding of the 17th Electrical/Electronics Insulation Conference*, Boston, MA, 1985.
44. M.T. Baker, S. O'Connor, and J.F. Johnson, Hyphenated analysis for trace components in electrical insulations. *Proceeding of the 17th Electrical/Electronics Insulation Conference*, Boston, MA, 1985.
45. J.W. Billing and D.J. Groves, Treeing in mechanically strained h.v. cable polymers using conducting polymer electrodes. *Proc. Institution Elec. Eng.*, 121, 1451-1456, 1974.
46. BS6469 1992 Insulating and sheathing materials of electric cable Part 1 section 1.3 (equivalent to IEC 811-1-3. 1985 + A1:1990).
47. W. Lodding (Ed.), *Gas Effluent Analysis*, Edward Arnold, London, 1967.
48. M. Ali, J.M. Cooper, S.J. Fitton, and S.P. McCann, The Development of techniques for the analysis of materials, *The 7th INSUCON 1994, BEAMA International Electrical Insulation Conference*, 131-135.
49. M. Ali, J.M. Cooper, S.G. Swingler, and S.P. Waters, Simultaneous thermal and infrared analysis of insulating resins, *IEE 6th International Conference on Dielectric Materials measurements and Applications*, Manchester, 363, 77-80, 1992.
50. E.L. Charsley and S.B. Warrington (Eds.), *Thermal Analysis — Techniques and Applications*, RSC Special Publication No. 117, 1992.
51. E.A. Turi (Ed.), *Thermal Characterization of Polymeric Materials*, Academic Press, New York, 1981.
52. L. Kofler and A. Kofler, *Thermomikromethoden zur Kennzeichnung Organischer Stoffe und Stoffgemische*, Verlag Chemie, Weinheim, 1954.
53. D.R. Reid, L.K. MacLachlan, R.C. Mitchell, M.J. Graham, M.J. Raw, and P.A. Smith, Spectroscopic and physicochemical studies on the interactions of reversible hydrogen ion. *Biochim. Biophys. Acta*, 1029, 24-32, 1990.
54. A. Wade (Ed.), *Pharmaceutical Handbook, 19th edition*, Pharmaceutical Press, London, 1980, 28.
55. J.L. Ford and P. Timmins, *Pharmaceutical Thermal Analysis*, Academic Press, New York, 1989.
56. R.J. Willson, A.E. Beezer, J.C. Mitchell, and W. Loh, Determination of thermodynamic and kinetic parameters from isothermal heat conduction microcalorimetry: applications to long-term-reaction studies. *J. Phys. Chem.*, 99, 7108-7113, 1995.
57. D.L. Hansen, Instrument selection for calorimetric drug stability studies, *Pharm. Technol.*, 20(4), 64-65, 68, 70, 72, 74, 1996.
58. ASTM Designation D 5483-93, Standard Test Method for the Oxidation Induction Time of Lubricating Greases by Pressure Differential Scanning Calorimetry.
59. D. Dollimore and J.M. Hoath, The preparation and examination of partially combusted cellulose chars, *Thermochim. Acta*, 45, 103-113, 1981.

70.3 Kinetic Methods

E.E. Uzgiris and J.Y. Gui

Kinetic methods involve the measurement of chemical reactions or processes in a time-dependent manner. Rates of dynamic processes are measured rather than the properties of a system at equilibrium. Of course, this approach is a central one for the study of chemical reactions and reaction mechanisms; however, it has much value in analytic chemistry; that is, in the determination of the composition of materials. This fact has been recognized for some time, but in recent years there has been a resurgence in interest in the use of kinetic methods in analytic chemistry. There have been several world congresses on this subject, numerous monographs [1,2], and the number of papers on kinetic methods has dramatically increased in the last decade [3].

Why is there such an interest? After all, there are many analytic procedures that are quite general and sensitive. As a specific example, consider the analysis for various metals in environmental samples. Metal ions can be detected by numerous means such as by ion selective electrodes, atomic flame spectroscopy, or ion coupled plasma spectroscopy, yet there is abundant literature on metal detection by catalyzed reactions in a kinetic manner [1-3]. In this case, the method of choice is dictated by cost of analysis, speed, sensitivity, and convenience. Furthermore, certain molecular species may be difficult to discriminate from others in conventional analysis. In this case, with a proper reaction, the kinetic approach is a powerful tool in detecting such constituents. Finally, the kinetic approach is the only method capable of elucidating the nature of binding sites in molecular binding because the determination of an equilibrium association constant alone is insufficient to elucidate mixed binding sites [4]. It is also the principal means of identifying short-lived intermediate species in a reaction [5].

Thus, kinetic methods comprise an important group of methods available for the analysis of substances. In some cases, kinetic methods offer unique advantages as in the study of mixed binding sites, in the delineation of competing species, and in the determination of short-lived intermediates. In other cases, kinetic methods offer speed and convenience, and low cost, as for example in such applications as clinical analysis and environmental field analysis.

In a broader sense, time-dependent changes in chemical, physical, and biological processes are universal. Because equilibrium may not be achieved in certain processes, time-dependent effects must be considered and accounted for in a satisfactory manner for analytic determinations to be accurate and reproducible. In some instances, for reasons of speed of analysis, kinetic rates are measured rather than equilibrium values. The range of time dependencies can range from picoseconds, studied with mode-locked lasers, to seconds or minutes, studied with batch mixing procedures. Kinetic methods encompass a broad range of processes and time domains. The methods of simple chemical reactions can often be applied to complicated biological processes. This is possible because often one reaction in a group of coupled reactions controls the overall rate of the process.

Kinetic methods have been classified according to different criteria. The most common classification is based on whether the method involves a catalyst. This is so because reactions are frequently quite slow. In such cases, a catalyst must be added to speed up the reactions and make rate determinations practical. In other instances, the catalyst is the analyte itself. There are two major groups of catalysts: enzymatic and nonenzymatic. Another common classification of kinetic methods is based on whether the reaction proceeds in a homogeneous or heterogeneous system. Most of the discussion will be focused on homogeneous liquid and heterogeneous liquid–solid systems because these comprise the majority of kinetic analytical methods that have been developed. Presented in [Table 70.4](#) are classifications based on the above criteria along with example reactions.

Theoretical Aspects

A reaction involving species A and B proceeds to a product with a rate constant, k , such that the rate of change of species A is given by

TABLE 70.4 Classification of Kinetic Methods Based on System and Catalyst

System	Catalyst	Reaction examples
Homogeneous	Enzymatic	Hydrolysis Electron transfer
	Nonenzymatic	Redox Complexation Chemiluminescence
	No catalyst	Redox Chemiluminescence
Heterogeneous	Enzymatic	Immunoenzymatic Electrode reactions Electrocatalysis Fluorescence
	Nonenzymatic	Electrode reactions Electrocatalysis Fluorescence
	No catalyst	Fluorescence Radioimmunoassay

$$-dA/dt = k' [A] [B] \quad (70.78)$$

where the brackets denote concentration. If the species A is of interest, then the reactant B can be in excess, in which case changes in [B] can be ignored. A pseudo-first-order reaction can be written:

$$-d[A]/dt = k [A] \quad (70.79)$$

where $k = k' [B]$ and the time evolution of [A] is just:

$$[A] = [A]_0 e^{-kt} \quad (70.80)$$

The product, P, which is the species that is usually detected, evolves as:

$$[P] = [A]_0 (1 - e^{-kt}) \quad (70.81)$$

The species A can be expressed in terms of product by:

$$[A] = [P]_{\infty} - [P] \quad (70.82)$$

where $[P]_{\infty} = [A]_0$. By measuring [P] as a function of time, the initial concentration of A can be deduced from a plot of:

$$\ln [A] = \ln [A]_0 - kt \quad (70.83)$$

In this way, a calibration curve can be generated against which an unknown sample can be measured for the content of species A.

In case the reaction is of a different order, the time-dependent plots for determining $[A]_0$ take on a different form. For example, in a second-order reaction, the rate of change of $[A]$ is given by:

$$-d[A]/dt = k[A][A] \quad (70.84)$$

where, as before, the reactant $[B]$ is considered in excess and its time dependence can be assumed to be negligible. The calibration curve is now:

$$1/[A] = 1/[A]_0 + kt \quad (70.85)$$

Clearly, the order of the reaction under study must be known for a correct analysis. There are straightforward ways to determine the order by varying the initial concentration of $[A]$ and noting the initial velocity of the reaction. A plot of the initial velocities versus initial $[A]$ will reveal the order of the reaction [1].

One of the strong points of kinetic methods is that closely related species that may be difficult to resolve by other means can be resolved by kinetic measurements. This is particularly true when enzyme reactions are employed. Enzymatic reactions are extremely sensitive to molecular structure and closely related structural analogs may have significantly different kinetics. For example, consider species A and B going through a reaction to a product but each having a different rate constant, k_a and k_b . The detected product is given as a sum of the two components by:

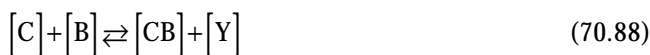
$$[P]_{\infty} - [P] = [A]_0 \exp(-k_a t) + [B]_0 \exp(-k_b t) \quad (70.86)$$

Then, by computer fitting or graphical analysis of a semilog plot of

$$\ln \{ [P]_{\infty} - [P] \} = \ln [A]_0 - k_a t + \ln [B]_0 - k_b t \quad (70.87)$$

one can extrapolate to $t = 0$ and determine, $[A]_0$ and $[B]_0$.

The important case of catalyzed reactions must be considered separately as there are important differences from the case of uncatalyzed reactions considered above. The catalyst is usually the species to be determined as it often is a metal ion or nonorganic ion of interest. Usually the catalyst combines with the reactant species $[B]$ in a very fast reaction with a given equilibrium constant to give:



Here, CB , the reactant B bound to C , reacts with A with a much faster rate than if B is unbound. This develops because of the reduction of the activation energy provided by the catalyst C in combination with B as discussed below. Thus,



This more complex kinetics simplifies to pseudo-first-order if one considers only the initial rates of the reaction. The initial velocity of the indicator product, P , takes the simple form:

$$V_0 = d[P]/dt = K'[C]_0 + K'' \quad (70.90)$$

where K' and K'' are constants. A calibration curve for C can thereby be generated through initial velocity measurements.

Enzyme Reactions

Enzymes are a class of proteins that catalyze reactions with exquisite specificity. The activity of certain enzymes is in itself of great importance in clinical diagnosis, but enzymes can be useful in determining **substrate** concentration — also very important for clinical applications and for environmental analysis. The rates of enzyme reactions are directly proportional to enzyme concentration; however, there is a saturation of reaction rates with increasing substrate concentration. This saturation effect must be considered when analyzing such reactions. The essential feature of enzyme reactions involves the enzyme, the substrate, the enzyme–substrate complex, and the product. It is the formation of the enzyme–substrate complex that leads to the saturation kinetics [5]. The reaction can be represented as follows:



where the reaction to form the enzyme–substrate complex is reversible as indicated by the arrows and k_1 is the forward rate and k_2 is the backward, dissociation rate, and there is no reversion of product to substrate in the initial stages of reaction.

With the condition that initially $P \sim 0$, and setting $d[ES]/dt = 0$, it is easy to show that:

$$[ES]/[E][S] = 1/K_M \quad (70.92)$$

where K_M is the Michaelis–Menton constant. Now, since the velocity of the reaction (and here one considers the initial velocity only) is given by:

$$V_i = k_3 [ES] \quad (70.93)$$

and one can define a maximum velocity such that:

$$V_{\text{imax}} = k_3 [E]_{\text{tot}} \quad (70.94)$$

The velocity is maximum when all of the enzyme binding sites are filled with substrate. Solving for $[ES]$ and using $[E] = [E]_{\text{tot}} - [ES]$, one obtains:

$$V_i = k_3 [E]_0 [S] / (K_M + [S]) \quad (70.95)$$

This is the functional form that expresses saturation kinetics with respect to substrate concentration. Generally, for determination of activities, enzyme reactions are performed in a fully saturated regime (i.e., $[S] \gg K_M$); otherwise, the kinetic rates need corrections and the Michaelis–Menton constant must be known or needs to be determined. For determination of substrate concentration, the analysis must account for the nonlinearity of V_i with respect to $[S]$.

Enzyme activity is defined in terms of units, rate of formation of product under given conditions, since the protein content in the enzyme preparation can be misleading — not all of the enzymes in a preparation need be active. Because enzymes are proteins, and in some cases rather delicate ones, great care must be exercised in handling and storing. The activities of enzymes are very sensitive to pH, salinity, and temperature. All of these factors must be precisely controlled for reliable kinetic determinations.

Temperature Dependence

Rate constants obey the Arrhenius relation:

$$k = A \exp \left\{ -E_a / RT \right\} \quad (70.96)$$

where E_a is the activation energy, R is the gas constant, T is absolute temperature, and A is a prefactor term. Knowledge of the activation energy allows for the extrapolation of a kinetic rate to any temperature. It is the lowering of this activation energy that is at the heart of catalysis and enzymatic reactions. Because of the exponential dependence, a reduction of the activation energy can lead to a rate constant increase of many orders of magnitude.

The prefactor A is determined by some collision frequency. However, in general, reactions proceed slower than the collision theory would predict. This is because, in addition to collisional frequency, there are also configurational and entropic terms that play a role in determining A . Nevertheless, it is useful to consider the concept of diffusion-controlled reactions. Here, it is the collisional frequency that dominates the reaction. In that situation, it is possible to utilize the diffusion theory of random motion in a medium to derive A such that:

$$A_{\text{diff}} = 4\pi \left(r_{ij} \right) \left(D_i + D_j \right) N_0 / 1000 \quad (70.97)$$

where N_0 is Avogadro's number, D_i , and D_j , are the diffusion constants for species **i** and species **j**, and r_{ij} is the encounter distance. For D of the order of $1.5 \times 10^{-5} \text{ cm}^2 \text{ s}^{-1}$, which is a value appropriate for small molecules, A_{diff} is $10^{10} \text{ M}^{-1} \text{ s}^{-1}$. Reactions involving protonation or the OH^- ion proceed at this rate, but only a few enzyme-substrate complex formation reactions approach the diffusion limited rate [6].

Experimental

The kinetic methods can be further classified according to experimental approaches as presented in [Table 70.5](#).

TABLE 70.5 Classification of Kinetic Methods Based on Mixing Technique or Equilibrium Perturbation

Technique	Methods
Batch mixing (for slow reactions)	Stirring in cuvette or flask
Flow mixing (fast reactions)	Continuous flow Accelerated flow Pulsed flow Stopped flow
Thermodynamic jump	Temperature jump Pressure jump Electric current jump Concentration jump
Periodic relaxation	Cyclic voltammetry Dielectric relaxation
Pulse relaxation	Time resolved fluorescence Time resolved phosphorescence Flash photolysis Pulse NMR Pulse EPR

The principal instrumental elements of a kinetic apparatus are the mixing chamber, timing device and control of data acquisition, and detector. Automation and computer controls have allowed kinetic measurements to be done routinely and with great accuracy for even very fast reactions. We consider those aspects of instrumentation unique to the problem of mixing and proper fast sampling — the essential issues of the experimental method. The other components of instrumentation are beyond the scope of this chapter; the readers may refer to the monographs for more details on those topics [1,2].

Although the nature of kinetic measurements does not require absolute quantitation of a product, it does require care in accurate timing and fast mixing of reactants. For slow reactions, the mixing chambers can be closed systems without any need for elaborate devices or techniques to initiate the reaction of interest. So called “batch mixing” can be done in ordinary optical cuvettes with a suitable magnetic stirring rod or mixing plunger. These straightforward experimental techniques are not discussed here; rather, the time domain for which kinetic methods require specialized equipment will be considered. This domain is in the region of 1 ms to 1 s, for example. Reactions with time constants in this domain are very common in current applications of kinetic methods.

Mixing Methods

In the so-called open systems, there are three approaches to initiating and monitoring reactions: (1) continuous flow, (2) pulse and accelerated flow; and (3) stopped-flow.

In method (1), the reactants are brought together into a capillary under fast flow conditions and the product is monitored (by a photodiode for example) along the length of the capillary, thus tracing out the kinetics in so far as the time dependence of the reaction is transformed into distance along the capillary by:

$$t = d/v \quad (70.98)$$

where v is the flow velocity, and d is the distance along the capillary after the junction in which the reactants are introduced. A high flow rate ensures a high Reynolds number condition and the achievement of turbulent flow and good mixing in the capillary. This method has the disadvantage of requiring rather high molar extinction coefficient for the product to achieve sensitivity and the high consumption of sample and reactant. In addition, multiple measurements along the tube are required to trace out the kinetics.

Method (2), pulsed and accelerated flow, was devised to address these deficiencies. By accelerating the flow, it is possible to do a single point measurement: the kinetics can be deconvoluted from the known change of flow as a function of time. In addition, integrated detection can be used in which the light path of the detector and source look down the flow tube, thus affording much greater sensitivity by virtue of a long absorption path length. Rather small quantities of analyte and reactant are consumed by this method because the flow is not continuous and a single point measurement is sufficient for the measurement of the kinetic parameters.

Method (3), the stopped-flow method has all the advantages of method (2), is simpler analytically, and can measure even faster kinetics. In this method, reactant and analyte are combined from two syringes driven simultaneously by a push block as shown schematically in [Figure 70.28](#). As the stop syringe plunger hits a precalibrated stop position, the flow is halted. Data are accumulated after the flow is stopped, free from effects of flow turbulence and other time-dependent interferences. Dead times (i.e., the time between inception of mixing and start of measurements) can be as short as 0.5 ms. The steps involved in the measurements can be automated for multi-sample, high throughput applications. A particularly simple stopped-flow system has been described by Harvey [7]. The drive syringes are standard 10-mL syringes that are manually pushed by a plunger. The mixing chamber is at the bottom of a 3-cm² observation cell. As the mixed solution enters the cell, it pushes up a float past the level of the light beam by which the reaction is monitored. After the measurement, the spent solution is displaced by pushing down on the float. This very simple approach is adequate for reactions slower than some 100 ms or so.

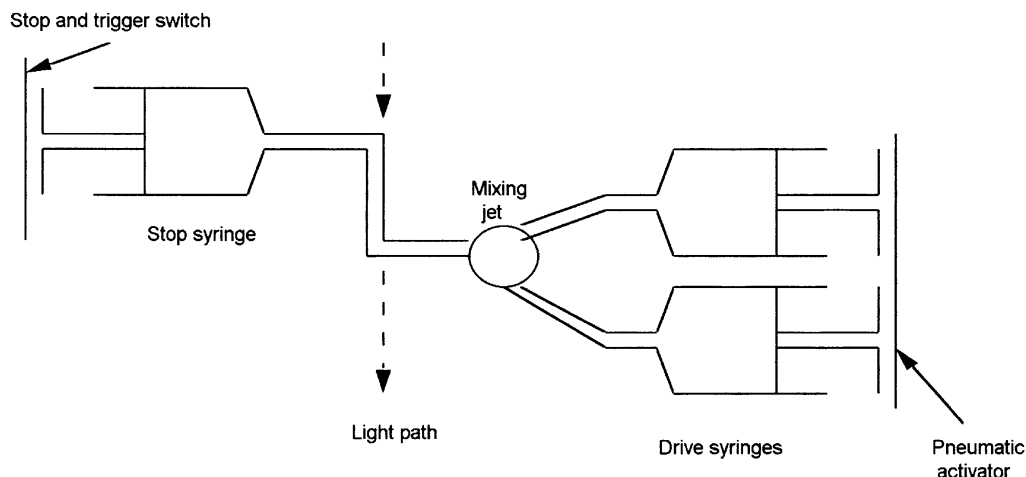


FIGURE 70.28 Schematic diagram of stopped-flow system. The reactant solutions are taken up into the two drive syringes as shown. The charging of the syringes is accomplished by valves and reservoirs not shown in the schematic for simplicity. As the activator plunger pushes the solutions through the mixing chamber, which is designed for efficient and fast mixing through tangential injection and turbulent flow (as in the Dionex Corp. system, for example), the old spent solution in the observation chamber is forced out into the stop syringe. The stop syringe plunger hits a stop, which causes immediate cessation of flow and activates the data acquisition system, which may be an oscilloscope, strip chart, or computer. The observation chamber shown here is oriented parallel to the light beam path for maximum pathlength and maximum sensitivity to absorption changes. The deadtime of such a system can be as low as 0.5 ms and the quantity of solutions required can be as low as 100 to 500 μL . At the end of a measurement, the stop syringe is purged and the drive syringes are recharged for another measurement cycle.

Reactions as fast as 1 ms can be measured by the stopped-flow technique. Fully automated sampling and data acquisition systems have been implemented [8]. Computer-controlled, three-wave valves are used to charge up the drive syringes and to flush them clean between measurements. Very fast reactions such as those involved in the folding of proteins have been studied in this way [9].

Relaxation Methods

An entirely different approach to kinetics is to probe the reactions of two reacting species that are in equilibrium by perturbing the equilibrium by a sudden change of temperature or pressure. These methods, known as relaxation methods, have as their virtue the ability to resolve kinetics in the very fast time regime much shorter than 1 ms [10]. If the equilibrium is disturbed, the relaxation to the new equilibrium state will proceed with a time constant τ given by:

$$1/\tau = k_1 + k_{-1} \quad (70.99)$$

where k_1 and k_{-1} are the forward and back reaction rate constants between the two species, respectively. The magnitude of the response depends on the enthalpy change with temperature or volume change with pressure of the particular reaction under study.

In the temperature jump method, a pulse of energy is supplied to the sample, either by a current pulse if the solution is conducting or by a light pulse if the solution is absorptive at a suitable wavelength. Light pulses can be made extremely short with a suitable laser source — nanoseconds to picoseconds — and this approach lends itself to the examination of the very fast molecular processes such as the intermediate states in photoreception [11].

These methods are well suited for the study of fast reactions but less useful for compositional analysis. However, a type of relaxation that is well known (i.e., fluorescence and phosphorescence) have become very valuable analytical tools. In such methods, a light pulse populates and excited state of molecules

under study and the rate of decay of that state provides an identifying signature of the species, even in a background of other emissions at the same wavelength. This holds as long as the signal of interest decays with a different time constant from the background signals.

The steady-state aspect of fluorescence and phosphorescence spectroscopy is a well-established “equilibrium” analytical technique that relies on the spectral differences for identification and intensity differences for quantitation. Its application, however, becomes invalid when an analytical sample contains multiple species that have indistinguishable luminescence spectra. However, it is frequently the case that the different species have different luminescence lifetimes. Thus, time-resolved spectra may produce a resolution of the species. For example, some tetracyclines have overlapping phosphorescence spectra that prevent characterization of each individual tetracycline. By using time-resolved, room-temperature phosphorescence, simultaneous determination of these tetracyclines was achieved based on their decay times in a continuous-flow system [12]. Even if two species have similar lifetimes, one can attach luminescence groups with different lifetimes to differentiate them. For example, different antigens tagged with different dyes with different lifetimes [13] were used to allow simultaneous detection of the antigens.

There are many benchtop fluorescence instruments capable of measuring lifetimes as short as nanoseconds. However, most of them are capable of monitoring only one specific wavelength as a function of time. Recently, fast optical spectrometers have been developed that have nanosecond time resolution over the entire visible spectrum [3].

Catalytic Reactions

Catalytic methods are based on the kinetic determination of catalyzed reactions. Such reactions can be extremely sensitive when the **catalyst** is the analyte. For example, chemiluminescence reactions of the oxidation of luminol by hydrogen peroxide catalyzed by metal ions provides extremely low detection limits for Co(II), Cu(II), Ni(II), Cr(III), and Mn(II). It should be pointed out that the term “catalyst” is loosely defined here as a substance that modifies the rate of a reaction without altering its equilibrium. Thus, the term “catalyst” includes the notion of promotion, inhibition, and, of course, true catalysis in which the catalyst remains chemically unchanged at the end of the reaction. Catalysts are usually categorized into two groups: enzymatic and nonenzymatic. Discussed below are overviews of catalytic-based kinetic methods applied in both homogeneous and heterogeneous systems.

Homogeneous Systems

Most applications of homogeneous kinetic methods are based on rate determination of catalyzed indicator (or substrate) reactions. Most frequently, the catalyst is the analyte to be determined, although, occasionally, it may serve simply as a reagent. Enzymes are one special type of catalyst. They are proteins possessing a very high degree of specificity. For example, certain enzymes can only exert catalytic actions on particular chemical bonds or steric isomers. Homogeneous enzymatic methods are widely used in clinic diagnoses to determine enzyme activity as well as enzyme substrate concentrations. The theoretical aspects of enzyme kinetics have been discussed in the previous section. Analytical applications for both enzyme activity determination and enzyme substrate detection can be found in the literature [3,14].

Homogeneous nonenzymatic catalytic methods are mainly applied for detection of metal ions, and other simple inorganic and organic species [3,15]. There are three major types of indicator reactions: redox, chemiluminescence, and complexation. One popular redox indicator reaction is the reduction of hydrogen peroxide by iodide catalyzed by metal ions (Fe, Mo, W, and Zr) that are also the analytes. The most common chemiluminescence indicator reaction is the decomposition of luminol (5-amino-2,3-dihydrophthalazine-1,4-dione) accompanied by the generation of luminescence at 425 nm. This decomposition is achieved through the oxidation of the doubly charged anion by the oxidant in this reaction (metal ions in most cases.) Although the oxidant in this case is consumed during the reaction, it is often termed a “catalyst” in the literature because its consumption is negligible in the time frame of the initial rate measurement, principally because of the ultrasensitivity of the chemiluminescence measurement. For complexation reactions, there are two main groups: ligand-exchange and complex-formation reactions. They are less studied compared with the above two indicator reactions but have promising application in

the determination of non-transition metals. For example, a reaction involving ligand exchange can be used to detect 0.4 ppm Ca. The most widely used detection technique for the complexation indicator reaction is UV/VIS absorbance.

Heterogeneous Systems

Many kinetic methods depend on the application of different heterogeneous catalysis processes where the catalytic reaction takes place at the interface between two immiscible phases, usually between the liquid–solid phases. The discussion here focuses on two main areas of heterogeneous catalysis that are important in chemical analysis. The first encompasses immobilized enzymes in which the labeled enzymes are either physically or chemically attached onto a solid surface. The measurement of surface enzyme activity is then related to the analyte concentration. The second is the area of electrocatalysis, in which chemical reactions occur at the interface of an electrode and an electrolyte solution. The catalyst in this case is the charged electrode surface in either the intrinsic state or in a chemically modified state. The analyte concentration in the solution is determined by the electrode dynamic current.

The most widely used format for immobilized immunoenzymatic techniques is known as ELISA (enzyme-linked immunosorbent assay). This type of assay combines the great selectivity provided by specific antibody–antigen recognition, the high sensitivity provided by enzymatic amplification, and general applicability provided by the use of common detection methods. It has proven to be a very powerful technique for simple, rapid, and cost-effective trace analysis and is widely used today in clinical diagnosis [16], drug screening [17], food safety inspection [18], and environmental analysis [19,20].

ELISA can be operated in several different modes, depending on the nature of analyte, sample environment, and requirements on speed, cost, and detection limits. Different assays are usually classified according to their operating procedure (competitive or noncompetitive), to the signal detection technique used (calorimetric, luminescent, electrochemical, or radioactive), or to the physical arrangement of the antibody–antigen binding structure (single layer or sandwich layers). For a more detailed description, the reader is referred to several references [21,22].

A typical immunoassay procedure involves three steps: (1) immobilization of antibodies onto a solid surface, (2) competitive binding of analytes and enzyme-tagged conjugates to the antibody sites, and (3) rate measurement of a substrate reaction catalyzed by the enzyme. In most cases, only the latter two steps operate in a kinetic mode. Illustrated in [Figure 70.29](#) is the chemiluminescence ELISA developed for rapid field analysis for PCBs (polychlorobiphenyls) in which the kinetic response of the enzymatic reaction enables the quantitative determination of PCB concentration [19]. First, a solid support of specified material and format is chosen based on the analysis requirement. The support surface is then treated with protein-A, a procedure to allow for the immobilization of antibodies in the proper orientation as shown in [Figure 70.29](#). The third step is to immobilize the antibodies onto the protein-A coated surface. Then an enzyme–antigen conjugate (specifically the bromobiphenyl–alkaline phosphatase) is introduced to the well so as to saturate all of the antibody binding sites. After thorough rinse with pH 7 buffer solution, these conjugate treated well-plates are ready for use in analysis of samples. The analysis of PCB-containing samples proceeds simply by adding the PCB-containing solution into the well for a fixed time to allow the PCBs to displace the previously bound enzyme conjugates. The higher the PCB concentration in solution, the higher will be the displacement of the enzyme conjugates in a given amount of time. After a fixed time, the well is then thoroughly rinsed and a chemiluminescence substrate is added. Under the catalysis of alkaline phosphatase, the substrate is transformed into a luminescent species that is then detected. The initial luminescence generation rate or the total intensity within a fixed time is proportional to the surface alkaline phosphatase, and thus inversely related to the PCB concentration, as shown by the results in [Figure 70.30](#).

Electrocatalytic reactions have been widely used for measuring chemical variables for electroactive species. However, not all electroactive species can be measured by electrochemical methods because for some species the electrode reaction kinetics may be very slow. A simple example is the reduction of molecular oxygen (O_2) at bare Pt electrodes in an aqueous solution. Oxygen cannot be reduced at the thermodynamic potential of the electrode. In this case, one can apply a large overpotential to drive the O_2 reduction. Unfortunately,

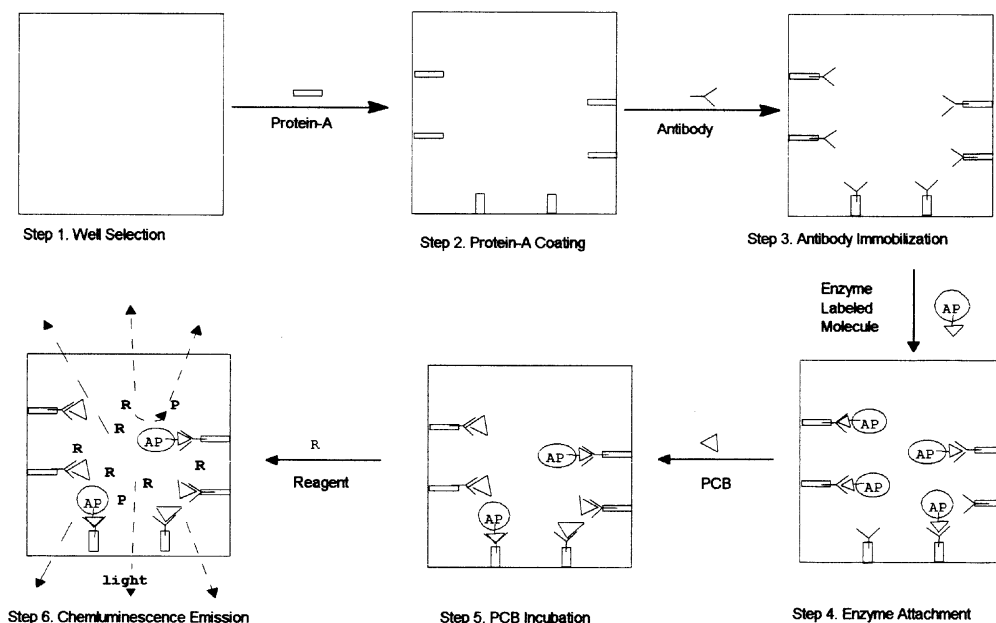


FIGURE 70.29 Pictorial presentation of chemiluminescence immunoassay.

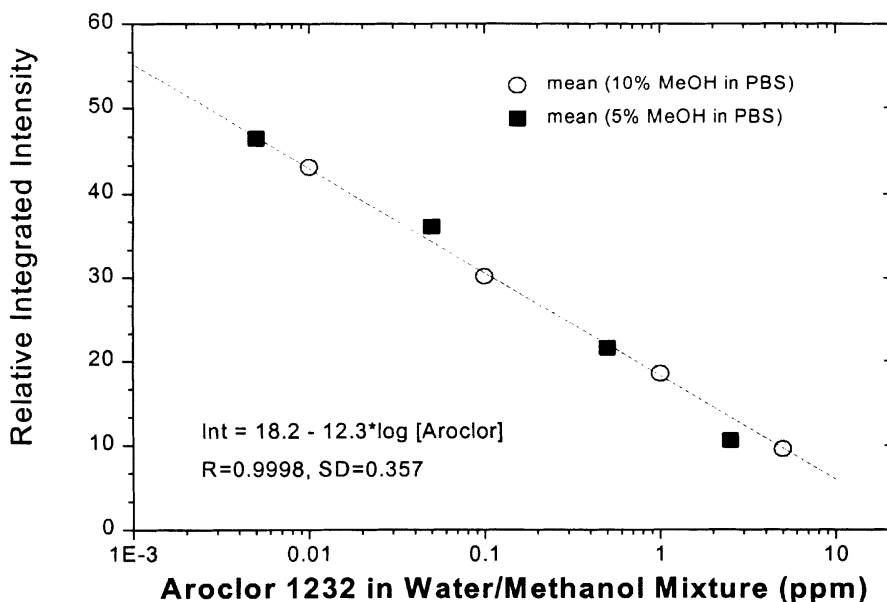


FIGURE 70.30 Dependence of chemiluminescence relative intensity on PCB Aroclor concentration. Plotted are chemiluminescence signals integrated during the first minute of enzymatic reaction (adamantyl dioetane decomposition catalyzed by alkaline phosphatase in pH 10 buffer.) Samples contain various amount of Aroclor 1232 in pH 7 PBS buffer solution containing 5% (open circles) or 10% (solid squares) methanol.

in many cases, a large overpotential cannot be used because of the limited available potential window or because of the interference from other electroactive species. Thus, to overcome this problem, electrochemists have chemically modified electrode surfaces in order to accelerate electron transfer rates at the electrode-solution interface [23].

Chemical modification is produced by coating a monolayer of atoms, molecules, or thin layers of polymers onto the electrode surface. These surface-attached molecules may or may not be electrochemically active, but they can accelerate electrode kinetics for the target analyte. When the surface species is electrochemically active, it is termed a mediator; when inactive, it is called a promoter. For example, cytochrome-c, like many other large macromolecules, has a large electron transfer rate in a homogenous solution phase, but it exhibits extremely slow electron transfer kinetics at many metal electrode surfaces. Eddowes and Hill, as well as Gui and Kuwana [24], have successfully demonstrated that by adsorbing a monolayer of heteroaromatic molecules such as 4,4'-bipyridyl and *trans*-1,2-bis(4-pyridine)ethylene onto Au or Pt electrode surfaces, electron transfer kinetics of cytochrome-c is significantly promoted. Recently, Dong, Cotton, and co-workers [25] have used a halide-modified Au electrode to study cytochrome-c electrode kinetics. They adsorb different halides onto the Au electrode and find that they all can accelerate the electron transfer rate for cytochrome-c and the promoting effort is of the order of $F^- < Cl^- < Br^- < I^-$. Various theories for the above phenomenon have been proposed. One possible explanation is that cytochrome-c and related electron transfer molecules can adsorb onto bare electrode surfaces in undesired orientations. Besides the above atomic and molecular modified electrodes, lipid modified electrodes [26] have also shown some promoting effect for cytochrome-c electron transfer. Direct immobilization of cytochrome oxidase in a lipid bilayer at an Au electrode has resulted in electrochemical reactivity of cytochrome-c in solution [27].

Electrochemical methods can also be applied to analyze electrochemically inactive species. The electrochemical immunoassay is a typical example. It combines the great selectivity provided by specific antibody-antigen recognition, the sensitivity provided by catalytic amplification, and the simplicity of electrochemical detection. It has proven to be a useful technique for measuring chemical variables for biological, clinical, and environmental samples. There are many forms of electrochemical assays: homogeneous vs. heterogeneous, competitive vs. noncompetitive, enzymatic vs. nonenzymatic, simple vs. sandwich. Details can be found in References 21, 28, and 29.

The great advantage of the electrochemical immunoassay compared with enzyme modified electrode methods is that it is a universal method and can be configured to analyze wide range of analytes, regardless of their electrochemical reactivity. For example, Heineman and co-workers have used this technique to detect dioxin, with a detection limit of one attomole using alkaline phosphatase as enzyme to convert 4-aminophenyl phosphate to the electroactive species 4-aminophenol [28]. They also used multiple metal labels rather than enzyme labels for simultaneous detection of multiple analytes [29].

Noncatalytic Reactions

As stated earlier, most kinetic-based analytical methods are catalytic systems. Noncatalytic systems have more limited applications because equilibrium methods are usually adequate in providing the necessary accuracy and sensitivity, and the noncatalytic kinetic methods do not provide any advantages of sensitivity. However, kinetic methods have been found to be more valuable or even the only choice in some special cases, as illustrated by the following examples:

1. When a sample contains hard-to-separate interference species that demand laborious and time-consuming separation before final measurement with a classic equilibrium method. A kinetic method may provide a simpler and faster determination by not requiring a prior separation.
2. When the equilibrium method is based on a very slow reaction or a reaction cannot proceed to completion due to side reactions. In this case, an initial rate measurement is much preferred and may be the only method of analysis.
3. When the species of interest has an extremely short lifetime, such as in the case of a reaction intermediate.

Table 70.6 lists some vendors of appropriate apparatus and assay kits for performing kinetic determinations.

TABLE 70.6 Companies Providing Kinetic Instrumentation or Kinetic Assay Materials

Instrument	Company
ELISA apparatus	Dynatech Laboratories 14340 Sullyfield Circle Chantilly, VA 22021
Immunoenzymatic assays	Becton Dickinson Microbiology Systems P.O. Box 243 Cockeysville, MD 21030
Enzyme assay kits, ELISA kits	Pierce Chemical Co. 3747 N Meridian Rd. P.O. Box 117 Rockford, IL 61105
Electroanalytic instruments	EG&G Princeton Applied Research P.O. Box 2565 Princeton, NJ 08543
Stopped-flow apparatus	Dionex Corp 1228 Titian Way Sunnyvale, CA 44088
Spectrometer with stopped-flow attachment	On-Line Instruments, Inc. 130 Conway Drive Bogart, GA 30622
Time-resolved spectrometers	Perkin-Elmer Corp. 761 Main Ave. Norwalk, CT 06859

Note: As examples, one company is listed for each category. For more complete listings, the reader is referred to the latest buyer's guide of *Analytic Chemistry*.

Defining Terms

Antibody: One of a class of immunoglobins produced by an animal's immune response to antigens (i.e., substances foreign to the body). Antibodies bind to molecular determinants of the antigen with great specificity.

Catalyst: A substance that accelerates a chemical reaction but is not itself consumed by the reaction.

Enzyme: A protein molecule that catalyzes reactions with great specificity.

Substrate: That which is being transformed by an enzyme-mediated reaction.

References

1. D. Perez-Bendito and M. Silva, *Kinetic Methods in Analytic Chemistry*, England: Ellis Horwood, 1988.
2. A. Mottola, *Kinetic Aspects of Analytical Chemistry*, New York: John Wiley & Sons, 1988.
3. (a) H. A. Mottola and D. Perez-Bendito, Kinetic determinations and some kinetic aspects of analytical chemistry, *Anal. Chem.*, 66, 131R-162R, 1994; (b) Kinetic determinations and some kinetic aspects of analytical chemistry, *ibid.*, 68, 257R-289R, 1996.
4. S. F. Feldman, E. E. Uzgiris, C. M. Penny, J. Y. Gui, E. Y. Shu, and E. B. Stokes, Evanescent wave immunoprobe with high bivalent antibody activity, *Biosensor & Bioelectronics*, 10, 423-434, 1995.
5. R. J. H. Clark and R. E. Hester, *Time Resolved Spectroscopy*, New York: John Wiley & Sons, 1989.
6. I. Tinoco, Jr., K. Sauer, and J. C. Wang, *Physical Chemistry, Principles and Applications in Biological Sciences*, 2nd edition, Englewood Cliffs, NJ: Prentice-Hall, 1985.
7. R. A. Harvey, A simple stopped-flow photometer, *Anal. Biochem.*, 29, 58, 1969.
8. S. R. Crouch, F. J. Holler, P. K. Notz, and P. M. Beckwith, Automated stopped-flow systems for fast reaction-rate methods, *Appl. Spectrosc. Rev.*, 1, 165, 1977.

9. M. S. Briggs and H. Roder, Early hydrogen-binding events in folding reaction of ubiquitin, *Proc. Natl. Acad. Sci. USA*, 89, 2017-2021, 1992.
10. P. Fasella and G. G. Hammes, A temperature jump study of aspartate aminotransferase, *Biochemistry*, 6, 1798-1804, 1967.
11. H. Shichi (Ed.), *Biochemistry of Vision*, New York: Academic Press, 1983.
12. F. Alava-Moreno, Y.-M. Liu, M. E. Diaz-Garcia, and A. Sanz-Medel, Kalman filtering-aided time-resolved solid-surface room temperature phosphorimetry for simultaneous determination of tetracyclines in solution, *Mikrochim. Acta*, 112, 47-54, 1993.
13. J. Choo, E. Cortez, J. Laane, R. Majors, R. Verastegui, and J. R. Villarreal, Far-infrared spectra and ring-puckering potential energy functions of two oxygen-containing ring molecules with unusual bonding interactions, *Proc. SPIE-int. Soc. Opt. Eng.*, 2089, 538-539, 1993.
14. Chapter 3 of Reference 2.
15. (a) Chapter 2 of Reference 1; (b) G. G. Guilbault, in *Treatise on Analytical Chemistry*, I. M. Kolthoff and P. Elving (Eds.), 2nd ed., Part I, Vol. 1, Chapter 11, New York: John Wiley & Sons, 1978.
16. D. S. Hage, Immunoassays, *Anal. Chem.*, 65, 420R-422R, 1993.
17. T. A. Brettell and R. Saferstein, Forensic science, *Anal. Chem.*, 65, 293R-310R, 1993.
18. S. K. C. Chang, P. Rayas-Duarte, E. Holm, and C. McDonald, Food, *Anal. Chem.*, 65, 334R-363R, 1993.
19. (a) J. Y. Gui, S. F. Feldman, E. Y. Shu, D. R. Berdahl, and E. B. Stokes, Chemiluminescence immunoassay for rapid PCB analysis, *Real-Time Analysis*, 1, 45-55, 1995; (b) J. Y. Gui, D. R. Berdahl, E. Y. Shu, J. J. Salvo, S. F. Feldman, and E. B. Stokes, *Chemiluminescence Immunoassay for PCB Detection*. U.S. Patent No. 5,580,741, Dec. 3, 1996.
20. J. M. Van Emon and R. O. Mumma (Eds.), *Immunochemical Methods for Environmental Analysis: 198th National Meeting of the American Chemical Society, ACS Symposium Series*, Miami Beach, FL, Sept. 10-15, 1989.
21. (a) C. P. Price and D. J. Newman, *Principles and Practice of Immunoassay*, New York: Stockton Press, 1991; (b) T. T. Ngo (Ed.) *Electrochemical Sensors in Immunological Analysis*, New York: Plenum Press, 1987.
22. (a) E. Harlow and D. Lane, *Antibodies — A Laboratory Manual*, New York: Cold Spring Harbor Laboratory, 1988; (b) A. L. Ghindilis, P. Atanasov, and E. Wilkins, Enzyme-catalyzed direct electron transfer: fundamentals and analytical applications, *Electroanalysis*, 9, 661-674, 1997; (c) B. Liedberg, C. Nylander, and I. Lundstrom, Biosensing with surface plasmon resonance — how it all started, *Biosensors and Bioelectronics*, 10, i-ix, 1995.
23. M. D. Ryan, E. F. Bowden, and J. Q. Chambers, Dynamic electrochemistry: methodology and application, *Anal. Chem.*, 66, 360R-427R, 1994.
24. (a) M. J. Eddowes and H. A. O. Hill, Novel method for the investigation of the electrochemistry of metalloproteins: cytochrome c, *J. Chem. Soc. Chem. Commun.*, 771, 1977; (b) Y. Gui and T. K. Kuwana, Electrochemistry and spectroelectrochemistry of cytochrome c at platinum, *J. Electroanal. Chem.*, 226, 199-209, 1987.
25. (a) T. Lu, X. Yu, S. Dong, C. Zhou, S. Ye, and T. M. Cotton, Direct electrochemical reactions of cytochrome c at iodine-modified electrodes, *J. Electroanal. Chem.*, 369, 79-86, 1994; (b) X. Qu, J. Chou, T. Lu, S. Dong, and C. Zhou, T. M. Cotton, Promoter effect of halogen anions on the direct electrochemical reaction of cytochrome c at gold electrodes, *J. Electroanal. Chem.*, 381, 81-85, 1995.
26. (a) Z. Salamon and G. Tollin, Chlorophyll-photosensitized electron transfer between cytochrome c and a lipid-modified transparent indium oxide electrode, *Photochem. Photobiol.*, 58, 730-736, 1993; (b) P. Bianco, and J. Haladjian, Control of the electron transfer reactions between c-type cytochromes and lipid-modified electrodes, *J. Electrochim. Acta*, 39, 911-916, 1994.
27. J. K. Cullison, F. M. Hawkridge, N. Nakashima, and S. Yoshikawa, A study of cytochrome c oxidase in lipid bilayer membranes on electrode surfaces, *Langmuir*, 10, 877-882, 1994.

28. N. Kaneki, Y. Xu, A. Kumari, H. B. Halsall, W. R. Heineman, and P. T. Kissinger, Electrochemical enzyme immunoassay using sequential saturation technique in a 20 ml capillary: dioxin as a model analyte, *Anal. Chim. Acta*, 287, 253-258, 1994.
29. (a) W. R. Heineman, H. B. Halsall, K. R. Wehmeyer, M. J. Doyle, and D. S. Wright, Immunoassay with electrochemical detection in methods of biochemical analysis, *Methods of Biochemical Analysis*, 32, 345-393, 1987; (b) M. J. Doyle, H. B. Halsall, and W. R. Heineman, Heterogeneous immunoassay for serum proteins by differential pulse anodic stripping voltammetry, *Anal. Chem.*, 54, 2318-2322, 1982.

70.4 Chromatography Composition Measurement

Behrooz Pahlavanpour, Mushtaq Ali, and C. K. Laird

During the early development of modern analytical chemistry, the study of natural materials was a primary concern of organic chemists and biologists. A major problem facing these scientists was the formulation of methods to separate and analyze the complex mixtures encountered in biological research.

Chromatography (literally "color-writing") is a physical or physicochemical technique for separation of mixtures into their components on the basis of their molecular distribution between two immiscible phases. One phase is **stationary** and is in a finely divided state to provide a large surface area relative to volume. The second phase is mobile and is caused to move in a fixed direction relative to the stationary phase. The mixture is transported in the mobile phase, but interaction with the stationary phase causes the components to move at different rates.

Origination of the technique, early in the 20th century, is generally attributed to Tswett, who separated plant chlorophylls by allowing solutions in petroleum ether to percolate through a vertical glass tube or column, packed with calcium carbonate. The separated components formed colored bands that were later isolated. Chromatography was adapted for qualitative or quantitative analysis of mixtures by inclusion of a suitable detector at the downstream end of the column and allowing the separated components to pass completely (elute) through the column and detector.

To analyze a sample, a suitable volume is injected into the stream of mobile phase or onto the upstream end of the column and the output of the detector is continuously monitored. The composition of the stream (eluent) passing through the detector then alternates between the pure mobile phase and mixtures with each of the components of the sample. The output record of the detector (chromatogram), plotted as a graph of response vs. time, shows a series of deflections or peaks, spaced in time and each related to a component of the mixture. For a given column, mobile phase, and set of operating conditions, the time for a component to pass through the column (retention time) is characteristic and can be used to identify the component. The peak area is proportional to the concentration of the component in the mobile phase.

In modern instrumental applications of chromatography, the stationary phase is either a solid or a liquid, and the mobile phase either a liquid or a gas. The various types of chromatography are classified according to the particular mobile and stationary phases employed. The solid stationary phase may be a granular solid packed in a tube (column), or coated as a thin layer on a suitable supporting plate (thin layer chromatography, TLC). Liquid stationary phases may be coated onto granular solids or bonded as a thin film to the inner wall of a capillary tube. In gas chromatography, the mobile phase is a gas (carrier gas), and the stationary phase is either a high-boiling liquid (gas-liquid chromatography, GLC) or a solid (gas-solid chromatography, GSC). In liquid chromatography (LC), the mobile phase is a liquid and the stationary phase is either a solid (liquid-solid chromatography) or a second liquid, immiscible with the mobile phase, coated on a granular solid (liquid-liquid chromatography).

Principles

Chromatographic theory is given in general textbooks [1,2], and also in specialized texts on different types of chromatography [3,4]. Chromatographic separation involves continuous interchange of solute

molecules between the mobile and stationary phases. Four principal processes are involved: **adsorption**, liquid-liquid partition, ion exchange, and size exclusion. In gas chromatography, the predominant processes are adsorption, while liquid chromatography may involve all four processes. Where liquid-liquid partition is the predominant separation mechanism, the sample components are **eluted** in order of increasing boiling points.

Since the **analyte** is transported in the mobile phase, chromatography is limited to solutes that are distributed between the two phases. In practice, this means that gas chromatography is limited to substances that are thermally stable in the vapor phase and are volatile at temperatures up to the maximum operating temperature of the GC column (about 350 to 400°C for most columns and packings, although some metal columns can be operated at higher temperatures). Liquid chromatography can be used for analysis of thermally labile and high molecular weight materials such as polymeric materials and proteins, at temperatures below their boiling point and that of the **eluent**.

The separating power of a chromatographic column is described by analogy with distillation separation processes. It is given as the number of theoretical separation plate (either per meter of column length or in total for the column), and depends on its length, internal diameter, and on the stationary phase employed. The height equivalent to a theoretical plate (HETP) value may also be quoted. Separating power is enhanced by use of long, narrow-bore columns with packings of the finest possible mesh size to allow intimate contact between the mobile and stationary phases, but these columns require higher operating pressures to overcome the column resistance, and analysis times increase with column length.

The chromatographic separation process is highly dependent on the temperature of the column, and temperature effects can be related to the temperature dependence of the distribution or adsorption equilibria of the solute between the stationary and mobile phases. However, in practice, the choice of column operating temperature involves a compromise between resolution and speed of analysis. Liquid chromatography is commonly carried out with the column at ambient temperature, although applications requiring operation at temperatures up to 100°C are becoming more common. In gas chromatography, the column temperature has a major influence on the speed of elution and the separation of sample components. Gas chromatography can be carried out at a single controlled temperature (isothermal) or the oven temperature can be increased during the analysis in one or more linear ramps (temperature programming). Temperature programming speeds the elution of later components relative to early ones and enables mixtures containing a range of components to be separated more quickly than would be possible with isothermal operation. The broadening of later peaks due to diffusion in passing through the column is also minimized by temperature programming.

Gas Chromatography

A block diagram of a gas chromatograph is shown in [Figure 70.31](#). The essential components are the column or columns; the carrier gas supply and flow and pressure controllers to enable carrier gas to be delivered to the column at a constant, controlled, and known rate; and the detector or detectors and associated electronics and data recording and processing system. An injector or facility for introducing suitable volumes of sample must be provided at the upstream end of the column. The column must be contained in an environment whose temperature can be held at a constant known value or heated or cooled at known rates. Temperature control in the range 25°C to 400°C (–0.1°C) and heating and cooling rates of 0.1°C to 40°C min^{–1} are typically required. Subambient operation at temperatures down to about –30°C may be required for separation of some volatile materials or for certain specialized eluents such as liquid carbon dioxide. Both injectors and detectors must be temperature controlled to allow rapid volatilization of the sample in the injector and to prevent condensation in the detector.

Columns

In gas chromatography, the processes involved in separation are predominantly adsorption and liquid-liquid partition when the eluent is liquid CO₂. Separation is almost entirely dependent on the nature of the stationary phase, with the gas phase acting mainly as an inert carrier. Separations of permanent gases

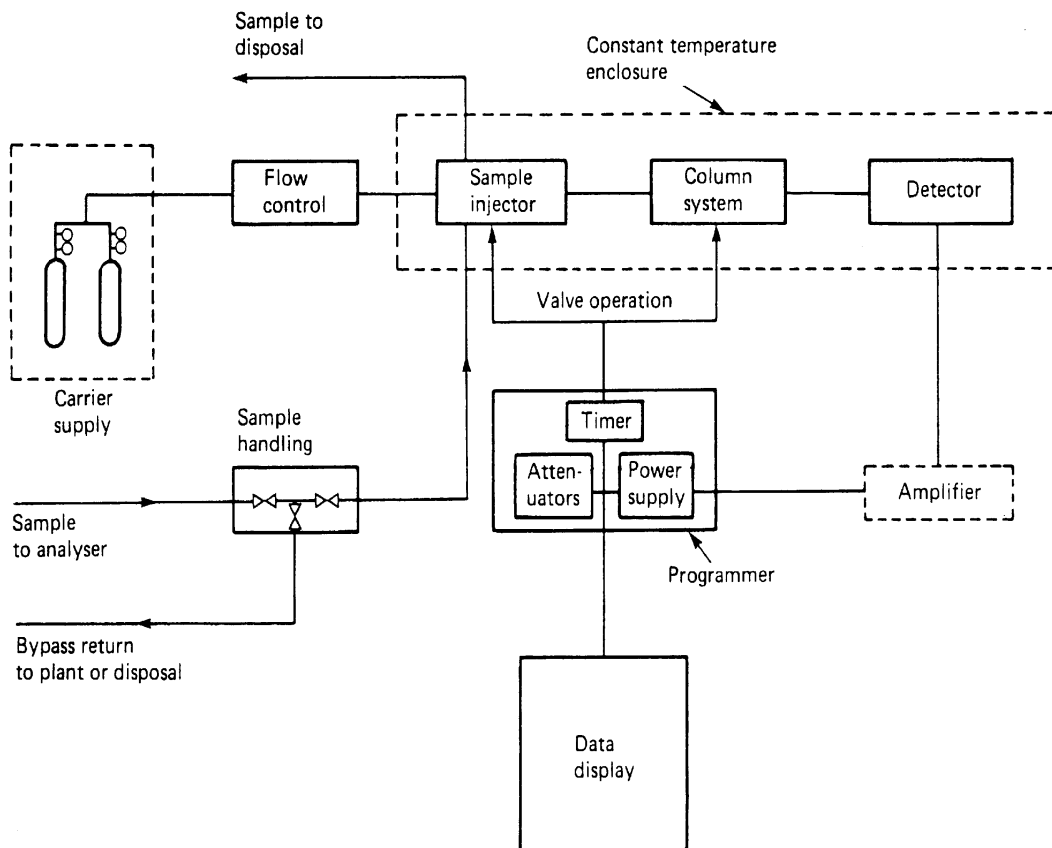


FIGURE 70.31 Functional diagram of process gas chromatography. The system consists of gas flow control, sample injection, separation of the components through the column, and a detector. Carrier gas at high pressure is used to move the sample through the column.

are carried out by gas-solid chromatography (GSC) using adsorbents such as silica gel, alumina, or synthetic zeolites (molecular sieves, particularly MS 5A and MS 13X) as the stationary phase. Proprietary porous polymers, such as Porapak (styrene-divinylbenzene copolymer), Chromosorb, and Tenax (polymer of 2,6-diphenyl-*p*-phenylene oxide), and various “carbon molecular sieves” are also used, and some of these materials are also used in separation of liquid samples.

In gas-liquid chromatography (GLC), the stationary phase is a high-boiling liquid, coated to a few percent by weight on an inert granular support such as silica, firebrick, diatomaceous earth, or Teflon. A wide range of liquids, gums, and waxes have been employed that provide stationary phases which are usable over different temperature ranges and with different polarities. Examples include silicone oils and gums, hydrocarbons, polyphenyl ethers, high molecular weight polymeric alcohols, etc.

Originally, in both GLC and GSC, the stationary phase or coated support was packed into a column, typically a glass or stainless steel tube, 1 to 3 m long, and coiled to fit the chromatograph oven. Developments in column technology have led to the gradual, but not yet complete, replacement of the packed GC columns by capillary columns. These columns are usually formed from drawn silica tubing, typically 10 to 100 m long, 0.2 to 0.5 mm o.d. with an outer protective coating of polyimide or, for operation above about 350°C, aluminium. The stationary phase is often a silicone oil — for example, polydimethylsiloxane, which instead of being coated on a granular support is present as a film, 0.1 to 5 μm thick, chemically bonded to the inner wall of the column (wall-coated, open tubular or WCOT column). Such open tubular columns operate at lower carrier gas pressures [typically 34 to 69 kPa (5 to

10 psig) instead of 138 to 340 kPa (20 to 50 psig) and carrier gas flow rates (1 mL min⁻¹ or less instead of 20 to 30 mL min⁻¹) than packed columns. Capillary GC columns can typically have 3000 theoretical plates per meter (50,000 plates per column), compared with 1000 plates per meter or 2000 plates per column for a typical packed column. The capacity of the column (i.e., the size of sample that can be separated) depends on the thickness of the film of stationary phase, but is of course smaller than for a packed column and is typically in the microgram to nanogram range. Columns with thicker films have higher capacity, but lower resolving power, than thin film columns. Chemical bonding reduces the loss of stationary phase (“column bleed”), especially during temperature programming, and bonded columns are almost essential for critical applications such as coupled gas chromatography–mass spectrometry. Although low- or medium-polarity general-purpose capillary columns have high performance and can be used with a variety of samples, customized columns are available with stationary phases developed and optimized for particular analyses.

As an alternative to coating the inner wall of the capillary column with liquid stationary phase, the column wall can be coated with finely divided support, which is itself coated with stationary phase (support-coated open tubular or SCOT column). SCOT columns are one category of the more general group of porous-layer, open-tubular (PLOT) capillary columns where the inner wall of the capillary is coated or bonded with the stationary phase. PLOT columns are available with a range of solid adsorbents, including Porapak, molecular sieve, carbon molecular sieve, and alumina suitable for separation of mixtures of permanent gases and gaseous hydrocarbons, and bring the separating power of capillary columns to gas-solid chromatography. However, the difficulty of reproducibly injecting gas samples into these columns has meant that packed columns are often still favored for separation of gaseous samples.

Carrier Gas

The theory of the influence of carrier gas on the separation process was given by van Deemter, Zuidweg, and Klinkenberg [5]. The van Deemter equation combines rate theory and plate theory and gives the relation between carrier gas velocity, u , and HETP, H , for a given carrier gas and column. The equation has the form

$$H = A + B/u + Cu \quad (70.100)$$

where A , B , and C are constants. A depends on the particle diameter and irregularity of column packing; B depends on the tortuosity of the channels and the first power of the diffusion coefficient of solute molecules in the gas phase; and C depends on the distribution coefficient of the solute, the ratio of stationary-phase and gas-phase volumes, the effective film thickness, and inversely on the diffusion coefficient of the solute in the gas phase.

Plots of H versus u show a minimum value for H corresponding to an optimum carrier gas flow rate, where:

$$u_{\text{opt}} = (B/C)^{1/2} \quad (70.101)$$

The van Deemter equation shows that, for a given column, a carrier gas of higher molecular weight can give a more efficient separation (lower value of H_{min}) than one of lower molecular weight, and H_{min} occurs at higher gas velocities for carrier gases of lower molecular weight. However, the equation refers to a single solute, and since chromatography involves separation of several solutes, the optimum carrier gas velocity is necessarily a compromise. The van Deemter equation also shows that for low molecular weight carrier gases, particularly hydrogen and helium, the minimum is less pronounced; that is, that carrier gas flow is less critical to column performance, and these two gases are the preferred choice, especially for capillary chromatography. Where hydrogen or helium are not suitable for the detector in use, a separate “make-up” gas supply is provided at the downstream end of the column; for example, nitrogen make-up is necessary for capillary operation of an electron capture detector.

The H vs. u curve is not symmetrical, carrier gas flow rates being more critical at values below u_{opt} than above. Thus, analyses may be speeded by increasing carrier gas flow rates above the optimum without much deterioration in column performance, but operating at flow rates that are too low leads to a relatively rapid loss of separating power.

Detectors

Detectors for gas chromatography should ideally have high sensitivity, rapid and reproducible response, and a wide range of linear response to concentration. Early detectors had universal or near universal response to all solute molecules; more recently, the emphasis has been on development of detectors with some selectivity to particular groups of compounds.

Thermal Conductivity Detector (TCD).

The thermal conductivity detector or katharometer was one of the earliest GC detectors and utilizes the change in thermal conductivity of a gas mixture with composition. The detector consists of either two or four electrically heated filaments, or for highest sensitivity especially at low temperatures, thermistors. The filaments or thermistors are connected in a Wheatstone bridge circuit, with external resistors to complete the bridge if there are only two sensing elements. The filaments or thermistors are mounted in a metal block to provide thermal stability, and provided with channels to allow the effluent from the GC column, and a separate, controlled "reference" flow of pure carrier gas to pass over the sensors or pairs of sensors. The loss of heat from the filaments depends on the filament temperature and on the conductivity of the surrounding gas. The katharometer can be operated under constant current or constant voltage conditions, or feedback circuitry can be used to maintain the filament resistance constant; but in each case, changes in gas composition lead to an out-of-balance voltage in the Wheatstone bridge circuit.

The TCD is a universal detector; however, it is less sensitive than other detectors such as the FID, and is principally used for detection and measurement of permanent gases such as oxygen, argon, nitrogen, carbon monoxide, and carbon dioxide, which either cannot be measured by the FID or require special pretreatment of the effluent gas (see below). It can be shown that the sensitivity is greatest when the filaments are operated at the maximum possible current, and when the difference in conductivity between the carrier gas and sample components is greatest. Both these conditions are fulfilled by use of helium or, better, hydrogen as the carrier gas, as these two gases have higher thermal conductivities than other common gases.

Flame Ionization Detector (FID).

The flame ionization detector (FID) is one of a group of gas detectors in which changes in the ionization current inside a chamber are measured. The ionization process occurs when a particle of high energy collides with a target particle that is thus ionized. The collision produces positive ions and secondary electrons that can be moved toward electrodes by application of an electric field, giving a measurable current, known as the ionization current, in the external circuit.

The FID utilizes the fact that, while a hydrogen–oxygen flame contains relatively few ions, it does contain highly energetic atoms. When trace amounts of organic components are added to the flame, the number of ions increases and a measurable ionization current is produced. The effluent from the GC column is fed into a hydrogen–air flame. The flame jet serves as one electrode, and a second collector electrode is placed above the flame. A potential is applied between the electrodes. When sample molecules enter the flame, ionization occurs — yielding a current that can be amplified and recorded.

The main reaction in the flame is:



However, the FID also gives a small response to substances not containing hydrogen, such as CCl_4 and CS_2 . It is probable that the reaction above is preceded by hydrogenation to form CH_4 or CH_3 in the

reducing part of the flame. In addition to the ionization reactions, recombination also occurs, and the response of the FID is determined by the net overall ionization process.

The FID is a mass-sensitive detector; that is, the response is proportional to the amount of organic material entering the detector per unit time. For many substances, the response is effectively proportional to the number of carbon atoms present in the flame, and the detector sensitivity can be expressed as the mass of carbon per second required to give a detectable signal. A typical figure is 10^{-11} g C s⁻¹.

The FID responds to practically all organic molecules. It is robust, has high sensitivity, good stability, and wide range of linear response, and is widely used.

The FID is insensitive to inorganic molecules and water. However, it can be used for measurement of carbon oxides (CO and CO₂) by mixing the effluent from the GC column with a controlled stream of hydrogen. The mixed gas is passed over a heated catalyst to convert the CO or CO₂ to methane (methanation), followed by FID measurement of the methane generated. This allows GC determination of these gases at lower concentrations than can be detected by the thermal conductivity detector.

Photoionization Detector (PID).

The photoionization detector has some similarities to the FID, and like the FID, it responds to a wide range of organic and also to some inorganic molecules. An interchangeable sealed lamp produces monochromatic radiation in the UV region. Molecules having ionization potentials less than the energy of the radiation can be ionized on passing through the beam. In practice, molecules with ionization potentials just above the photon energy may also be ionized, due to a proportion being in excited vibrational states. The ions formed are driven to a collector electrode by an electric field, and the ion current is measured by an electrometer amplifier.

The flame in the FID is a high-energy ionization source and produces highly fragmented ions from the molecules detected. The UV lamp in the PID is of lower energy, leading to the predominant formation of molecular ions. The response of the PID is therefore determined mainly by the ionization potential of the molecule, rather than the number of carbon atoms it contains. In addition, the ionization energy in the PID can be selected by choice of the wavelength of the UV source, and the detector can be made selective in its response. Commonly available UV lamps for the PID have energies of 11.7, 10.2, and 9.5 eV. The ionization potentials of N₂, He, CH₃CN, CO, and CO₂ are above the energy of all the lamps, and the PID does not respond to these gases. The 10.2-eV lamp is particularly useful as it allows ionization, and thus detection of alkynes and alkenes (except ethene), but not alkanes.

The PID is highly sensitive, typically to picogram levels or about 1 order of magnitude more sensitive than an FID, and has a wide linear range. Any of the commonly used carrier gases is suitable, although some gases (e.g., CO₂) absorb UV radiation and their presence may reduce the sensitivity of the detector. The main disadvantage of the detector is the fragility of the UV lamp, the need for periodic cleaning of the UV window, and the difficulty in cleaning the window if the detector becomes heavily contaminated.

Electron Capture Detector (ECD).

The electron capture detector is an ionization chamber in which molecules of electronegative species are allowed to attach to or "capture" electrons that have been slowed to thermal velocities by collision with inert gas molecules. The detector consists of a cell containing an emitting radioactive source (usually ⁶³Ni) and purged with inert gas. Electrons emitted from the source are slowed to thermal velocities (thermalized) by collision with the gas molecules and are eventually collected by a suitable electrode, giving rise to a standing current in the cell. If molecules with greater electron affinity are introduced into the cell, some of the electrons are "captured," forming negative ions that are more massive and less mobile than the free electrons, and the current in the cell is reduced. This effect is the basis of the electron capture detector.

Originally, the ECD was operated under dc conditions, potentials up to 5 V being used; but under some conditions, space charge effects produced anomalous results. Modern detectors operate under constant current conditions and use a pulsed supply, typically 25 V to 50 V. The pulse width and/or frequency are varied by feedback circuitry to maintain the ionization current in the cell at a constant level. This extends the linear range of the detector response and ensures optimum response for a range

of molecules. The ECD must be used with a suitable inert gas, usually either an argon–methane mixture or nitrogen, either as the chromatograph carrier gas or (more usually) as an auxiliary gas supply.

The ECD is extremely sensitive to electronegative species, particularly halogenated molecules. It is widely used in the analysis of pesticides and some trace atmospheric components such as halocarbons, halogenated solvents, and nitrous oxide. The selectivity and extreme sensitivity is valuable, but the use of a radioactive source is a disadvantage. In certain cases, the detector response is highly sensitive to the cell temperature. The cell may be contaminated by “dirty” samples, and cleaning can be difficult or impossible.

Flame Photometric Detector (FPD).

In the flame photometric detector (FPD), the column effluent is passed through a fuel-rich hydrogen–air or hydrogen–oxygen flame, where the sample molecules are broken into simple molecular species and excited to higher electronic states. Under these conditions, most organic and other volatile compounds containing sulfur or phosphorus produce chemiluminescent species. The excited species return to their ground state, emitting characteristic molecular band spectra. The emission is monitored by a photomultiplier through a suitable filter, thus making the detector selective to either sulfur or phosphorus.

The FPD is most commonly used as a detector for sulfur-containing species. In this application, the response is due to the formation of excited S_2 molecules, S_2^* , and their subsequent chemiluminescent emission. The original sulfur-containing molecules are decomposed in the hot inner zone of the flame, and sulfur atoms are formed, which combine to form S_2^* in the cooler outer zone. As the S_2^* revert to their ground state, they emit light in a series of bands in the range 300 to 450 nm, with the most intense bands at 384.0 nm and 394.1 nm. The 394-nm band is monitored.

The FPD is highly sensitive (typically 10^{-11} g S s^{-1} or 10^{-12} g P s^{-1}), selective, and relatively simple. However, the response is nonlinear, given by:

$$I_s = I_0[S]^n \quad (70.103)$$

where I_s is the observed emission intensity (photomultiplier tube output), $[S]$ is the mass-flow rate of sulfur atoms, and n is a constant (value of 1.5 to 2, depending on flame conditions). Some systems incorporate circuitry to produce a linear output over 2 or 3 orders of magnitude concentration range.

Other Detectors.

A number of other GC detectors are available, but are less frequently used than those listed above. Examples include the nitrogen phosphorus detector, which is selectively sensitive to analytes containing those elements, and is used in pesticide analysis; and the helium ionization detector, in which the ionization process is due to highly energetic metastable helium atoms. The helium ionization detector is the only GC detector that permits analysis of the permanent gases at ppb levels. However, it is difficult to use, as the response is highly susceptible to the presence of trace impurities in the helium carrier gas. Additionally, gas chromatographic separation can be combined with detector systems specifically developed to measure a particular analyte. For example, trace levels of carbon monoxide in air can be measured by passing the effluent of the GC column through a heated bed of mercuric oxide. Carbon monoxide reduces the mercuric oxide, liberating mercury vapor, which is detected with high sensitivity by UV atomic absorption spectrometry.

Sample Injection

The purpose of the injection system is introduce defined and reproducible aliquots of sample into the chromatograph column. To minimize loss of resolution by diffusion, the sample must be injected as quickly as possible, and as a sharply defined slug. For analysis of liquids using packed columns, the injector is usually a zone heated to a temperature to ensure rapid volatilization of the sample, swept by carrier gas and fitted with a silicone rubber septum cap. Liquid injections are made by microsyringe through the septum cap. The syringe can be manual or controlled by an autosampler. Gas injections can

also be made by syringe, but this is unsatisfactory for quantitative work as the compressive effect of the column head pressure in the injector makes syringe injections of gas unreproducible, and valve injection is preferable.

The injection valve is a six-port changeover valve that allows a fixed volume of gas, defined by a length of tubing (the sample loop), to be connected in either one of two gas streams with only momentary interruption of either stream. The valve is connected in the carrier gas stream just upstream of the column. The sample loop is filled with sample gas and the valve is operated to connect the loop into the carrier gas stream.

Injection into capillary columns is more difficult than into packed columns due to their smaller sample capacity. An internal standard (i.e., a compound similar to the analyte but separated from it by the chromatograph) is often added to the sample to enable correction to be made for random differences in injection volume. The most widely used injection technique is the so-called split-splitless injector. In the "split" mode, an aliquot of liquid sample is injected into a heated zone at the head of the column. The injector is swept by carrier gas at constant pressure. A valve allows a variable but known proportion of the carrier gas to flow to waste. Carrier gas flow rates through the column are typically 1 to 2 mL min⁻¹ and the "split" flow is typically 30 to 50 mL min⁻¹. Thus, only a few percent of the aliquot of sample injected actually passes through the column. In the "splitless" mode, the valve controlling the waste stream of carrier gas is momentarily closed for a fixed time after injection, thus increasing the amount of sample transferred to the column for increased sensitivity.

Split-splitless injectors are relatively simple and can be used with conventional syringes. However, the injector must be carefully designed to obtain reproducible results, and there may be some discrimination (particularly loss of high boiling components) in samples containing components with a wide range of boiling points. Techniques where the sample is injected directly onto the column, without splitting, can give less discrimination and better sensitivity and reproducibility, but are more difficult to use. Examples include cold on-column or programmed temperature injectors. In this technique, a length of column at the head is cooled to trap the sample. The injector is subsequently flash-heated to a high temperature to release the sample.

Alternative injection techniques include headspace analysis, where the vapor in equilibrium with a volatile liquid is sampled, and purge-and-trap techniques, where volatile components are purged from a liquid sample by a stream of inert gas. The purged components are trapped in a cooled zone at the head of the GC column and subsequently released by rapid heating for chromatographic separation and determination.

Liquid Chromatography

In early applications of liquid chromatography, the adsorbent was contained in a vertical column through which the liquid phase was passed under gravity. The performance of such systems is limited by the tortuosity of the passage of the liquid phase through the column and by the efficiency and speed of solute exchange between the mobile and stationary phases. Column performance is enhanced by use of micro-particulate packings; but to achieve reasonably rapid separations in such systems, the mobile phase must be pumped through the column under pressure. The technique is known as high-performance (or sometimes high-pressure) liquid chromatography (HPLC).

High-Performance Liquid Chromatography (HPLC)

Figure 70.32 provides an illustration of process high-performance chromatography.

Columns.

HPLC columns are formed from precision-bore stainless steel tubing, 30 cm to 3 cm long, with 25 cm and 12.5 cm being the most common lengths. Standard columns have bores in the range 3.0 mm to 4.6 mm. Narrow-bore (2 mm) or microbore (1 mm) columns give increased sensitivity and higher chromatographic performance, together with reduced consumption of mobile phase, but require higher operating pressures and specially designed detector systems. The columns are packed under controlled

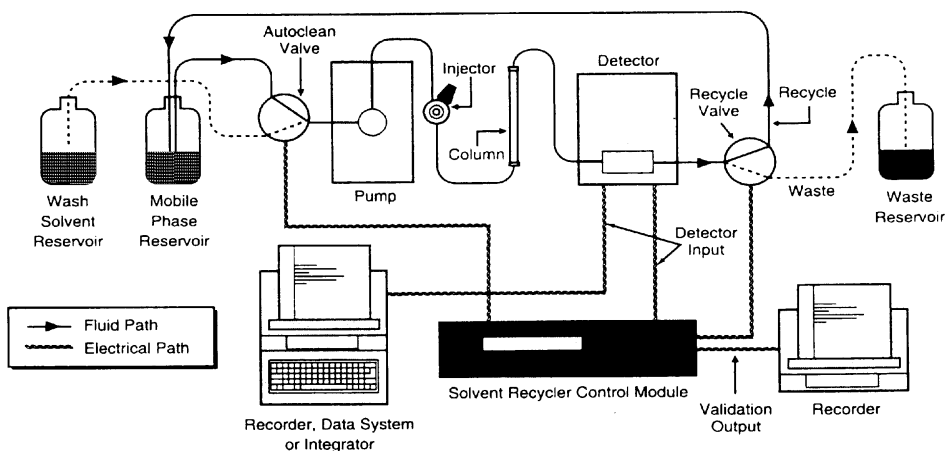


FIGURE 70.32 Functional diagram of process high-performance chromatography. The system consists of pump, sample injector, separation column, and detector. Mobile phase is liquid and wash solvent is used for cleanup. The used solvent can be recovered.

conditions with granular packing material of controlled size range, particle shape, and porosity. The “standard” particle diameter for packing materials is $5\ \mu\text{m}$, as it allows good column performance at moderate operating pressures, but columns packed with $10\ \mu\text{m}$ or 3 to $4.5\ \mu\text{m}$ particles can also be used.

A wide range of general-purpose and specialist packing materials have been developed for HPLC. The most widely used base material is silica, as it has high efficiency and physical rigidity, good solvent compatibility, and can be bonded with organosilanes for reversed-phase chromatography (see below). Other base materials include ceramics such as alumina, polymers, and graphitic carbon. Alumina has better pH stability than silica, but cannot be bonded with organosilanes. Polymers have limited organic solvent compatibility but tolerate strong alkali; they are less robust than silica and cannot be used at high operating pressures.

In liquid–solid chromatography, the samples are retained by adsorption on the support surface. The support may be coated with a liquid phase (liquid–liquid chromatography). In bonded phase HPLC, the support (usually silica, although alumina has also been used) is derivatized with a functional group covalently attached to the surface. In both coated and bonded phases, the separation is predominantly by partition; but like their counterparts in gas chromatography, bonded phases are inherently more stable than coated phases and can be used with a range of solvent and buffer systems.

In “normal” or traditional liquid chromatography, the stationary phase is polar and the mobile phase relatively nonpolar. The polar surface may be silica, or may be modified by chemical bonding of a suitable functional group. In reversed-phase chromatography, the stationary phase is nonpolar and the mobile phase is relatively polar. Reversed-phase chromatography is almost always carried out on modified silica columns, with octadecylsilyl (ODS or C18) or C8 groups being most commonly used, and the development of these systems has been largely responsible for the present popularity of HPLC.

Mobile Phase.

In contrast to gas chromatography, the mobile phase in HPLC plays a vital role in the separation process, with the rate and order of elution being determined by the relative polarities of the mobile and stationary phases, and by the nature of the sample components. In normal phase chromatography, the eluting power of the mobile phase increases with polarity; while in reversed-phase chromatography, the reverse situation applies, and eluting power decreases with increasing solvent polarity. Most of the common solvents can be used as mobile phase, but *n*-hexane is a common nonpolar solvent, while polar solvents in reversed-phase chromatography are often mixtures of water and methanol or acetonitrile. When a single solvent or mixture of fixed composition is used throughout a separation, the process is referred to as isocratic. In gradient elution procedures, the composition of the solvent is changed continuously during the separation

process. The change in solvent composition can be either linear with time or according to a predetermined profile. Gradient elution has some similarities in its effects to temperature programming in gas chromatography.

In HPLC, the mobile phase is pumped through the column. Flow rates for mobile phase are 0.5 to 10 mL min⁻¹ for conventional columns and 50 μ L to 5 mL min⁻¹ for narrow-bore columns at pressures up to 48263 kPa (7000 psi). The flow rate must be precisely controlled and the outlet stream must be pulse-free. Metered mixing of up to four solvent streams may be required for gradient elution and column washing. HPLC pumps must be capable of delivering a pulse-free stream of mobile phase, at pressures up to 48263 kPa (7000 psi). Variations in mobile phase flow rate lead to irreproducibility in chromatographic retention times, and pulses in the flow give noise in the detector baseline.

To ensure optimum pump performance and to remove dissolved oxygen, the mobile phase must be degassed. Degassing can be by vacuum, but periodic purging with helium is more usual. Dissolved oxygen causes noise and drift in UV detectors, quenching in fluorescence detectors, and high background currents and noise in electrochemical detectors.

Detectors.

Performance requirements for HPLC detectors are similar to those in GC, and the detector system should be sensitive, have a rapid and reproducible response, and have a wide linear range of response. The following types are most commonly used:

1. **Refractive index:** Detectors based on measurement of the refractive index of the mobile phase are applicable to a wide range of solutes. However, they are temperature sensitive, are generally less sensitive than UV or fluorescence detectors, and cannot easily be used with gradient elution systems.
2. **UV-VIS:** UV or visible detection is the most common detection technique. Photometers or spectrophotometers measure the absorption of UV or visible radiation in the range 190 nm to 700 nm by the solute molecules. Detectors can be either fixed or variable wavelength. Fixed-wavelength detection at 254 nm is suitable for many solutes. The response is linear according to the Beer Lambert law and detection limits are subnanogram in favorable cases. "HPLC grade" solvents that have been specially purified to remove UV-absorbing impurities may be required.
3. **Diode array:** The diode array, or photodiode array (PDA), detector allows the UV or UV-VIS spectrum of the mobile phase to be repeatedly scanned during the elution. The resulting spectra are stored by the data system and are useful for checking or monitoring peak purity during elution and may provide some information on the identity of the analyte. Diode array detectors are typically two or three times less sensitive than conventional, single-wavelength UV or visible detectors.
4. **Fluorescence:** Detection of suitable molecules by fluorescence is typically one or two orders of magnitude more sensitive than UV-VIS detection, allowing detection down to low picogram levels in favorable cases. The fluorescence cell volume can be made as small as 5 μ L, making fluorescence detection suitable for use with narrow-bore columns.
5. **Electrochemical:** Electroactive (oxidizable or reducible) substances can be detected by electrochemical techniques. The flow-cell volume may be as low as 1 μ L, making the detectors suitable for narrow-bore columns. By choice of working conditions, the detector can be made specific to particular compounds or groups of compounds. Examples of suitable compounds for electrochemical detection include aromatic amines, phenols, and chlorinated phenols.

Injectors.

The injection process is critical in obtaining good performance in HPLC. Injection may be made directly by syringe; but for optimum results, valve injection is essential and is now almost universal. The injection valve is a six-port changeover valve, which allows a defined volume of liquid sample, contained in a sample loop, to be injected into the mobile phase. The sample loop typically has a volume in the range of 10 to 100 μ L for conventional HPLC columns, and is loaded by a syringe.

Ion Chromatography (IC)

Ion chromatography (IC) is a variant of HPLC in which inorganic and some organic cations and anions are separated on columns packed with high-efficiency pellicular ion-exchange resins. Anion separator columns are resin-based with positively charged fixed ionic sites, usually quaternary amines. The eluent is commonly dilute aqueous sodium hydroxide or sodium carbonate/sodium bicarbonate mixture. Cation separator columns have negatively charged fixed ionic sites, usually sulphonic acid groups, with methane sulphonic acid as eluent. Although conductimetric, amperometric (polarographic), UV–VIS photometric, and fluorescence detectors can all be used in ion chromatography, conductimetric detection is the most commonly used technique. When conductimetric detection is used, the sensitivity of the measurement is increased by reduction of the conductivity of the mobile phase (suppression) before detection. The conductivity is suppressed by conversion of the eluent to the corresponding acid or base form in a suppressor column, or membrane suppressor, downstream of the separation column. Thus, for anion analysis, the suppressor is a cation exchanger that replaces sodium ions in the eluent with hydrogen ions. Ion chromatography allows detection and measurement of anions and cations in solution, typically down to ppb ($\mu\text{g L}^{-1}$) levels. The common inorganic anions can be determined in a single sample aliquot. The technique is particularly useful for routine analysis of water and environmental samples.

Gel Permeation and Size Exclusion Chromatography

Gel permeation chromatography (GPC) and size exclusion chromatography (SEC) separate sample molecules on the basis of their effective molecular size in solution in aqueous or nonaqueous media. Column packings are porous materials with pores in controlled size ranges and can be either resin (e.g., styrene-divinylbenzene copolymers) or silica based. The solute molecules interact with the column packing. Small molecules are “trapped” in the pores and pass through the column more slowly than larger molecules that do not interact so strongly. GPC was developed for polymer chemistry and is useful for the determination of the molecular weight distribution of polymers, but the techniques are also finding other applications; for example, size separation of small organics and petrochemicals and in sequential analysis and sample cleanup of environmental samples.

Hyphenated Techniques

Chromatographic methods give powerful techniques for separation of mixtures. However, the commonly used detectors give little information about the identity of the separated components, and identification from retention times may be incomplete or ambiguous. The so-called “hyphenated techniques,” in which chromatographic separation is combined with another, usually spectrometric, technique, have been developed to combine chromatographic separating power with spectrometric identification.

Gas Chromatography–Mass Spectrometry (GC–MS)

Developments in column, mass spectrometer, and computer technology have made GC–MS the most widely used of the hyphenated techniques. Modern systems commonly incorporate the following features:

1. Capillary column gas chromatograph, with the column effluent fed directly to the ion source of the mass spectrometer through a heated transfer line
2. Miniaturized quadrupole or quadrupole-type mass spectrometer, optimized for use as a GC detector, and limited to this application. The mass spectrometer may have a limited mass range (maximum mass 650 or 700), corresponding to the maximum molecular weight of compounds that can commonly be analyzed by gas chromatography.
3. Control of the mass spectrometer and gas chromatograph, data recording, and mass spectral library searching by dedicated computer.

Such so-called “benchtop” GC–MS systems typically have sensitivities in the nanogram to picogram range, and unit mass spectral resolution. They give a valuable means of identification and quantitative determination of a variety of analytes, particularly in complex matrices such as biological or environmental

samples. However, for applications requiring the highest sensitivity or mass spectrometric resolution, gas chromatographs coupled to high-resolution magnetic sector mass spectrometers must still be used. If it is necessary to use a packed chromatograph column, the carrier gas flow rate is likely to be too high for direct coupling to the mass spectrometer, and an interface, which allows selective removal of carrier gas, will be required.

Gas Chromatography–Infrared Spectrometry (GC–IR)

Coupling a gas chromatograph with an infrared spectrometer is an alternative to GC–MS. The effluent from the GC column is fed to a miniaturized flow-through absorption cell (light pipe) where the infrared spectra are measured. Fourier transform infrared (FTIR) spectrometry is used to achieve the combination of high spectral scan rates and resolution required to measure spectra from peaks eluting from capillary columns. Computer control and data processing are used, together with computer matching with stored libraries of IR spectra. The IR spectra are vapor-phase, and differ in some respects from liquid- or solid-phase spectra. GC–IR is to some extent complementary to GC–MS in that some molecular properties, particularly those relating to overall structure or shape, which may be lost in the fragmentation process in the mass spectrometer, may be identified in the IR spectra. However, the technique is some three or more orders of magnitude less sensitive than GC–MS, and has received less attention. GC-IR-MS can be used for particularly complex mixtures.

Liquid Chromatography–Mass Spectrometry (LC–MS)

Coupling a mass spectrometer to a liquid chromatograph, in principle, offers the advantages of GC–MS to the greater range of materials that can be analyzed by liquid, compared to gas, chromatography. However, interfacing a liquid chromatograph to a mass spectrometer is more difficult than a gas chromatograph; and while GC–MS is a well-established technique, LC–MS is only now becoming a useful routine method.

The principal difficulty in interfacing LC and MS lies in the very different physical conditions required for operation of the two techniques. Liquid chromatography uses relatively large quantities of liquid mobile phase, which may include inorganic buffers, while the mass spectrometer operates under vacuum. An interface must be used to selectively remove mobile phase before sample can be introduced to the mass spectrometer. Direct liquid injection and moving belt interfaces have been used but are unreliable. Three main types of interface are currently in use:

1. **Thermospray.** The LC effluent is passed through a probe, heated to 350°C to 400°C, in an evacuated region just outside the source of the mass spectrometer. The mobile phase, which often includes a volatile buffer such as ammonium ethanoate, is vaporized, and the sample molecules are ionized by a chemical ionization (CI) process. A series of lenses focuses a proportion of the ions into the mass spectrometer, while the solvent is pumped away. Under these conditions, the ionization is soft, i.e., there is little fragmentation in the mass spectrometer and the principal peak in the mass spectra is the molecular ion, M^+ , MH^+ , or MNH_4^+ . This can be useful for molecular weight determination, but fragmentation may be increased; and in some cases, sensitivity enhanced, by including a filament in the ion source to give electron impact (EI) mass spectra. The thermospray interface is suitable for ionic and nonvolatile compounds. However, it requires the use of volatile buffers and the spectra are dependent on the solvent matrix.
2. **Particle beam interface.** The particle beam interface utilizes the principle of momentum to separate the solvent from the heavier solute molecules. The column effluent, mixed with helium in some designs, is passed through a series of chambers under pressure, exiting through a nozzle. As the effluent emerges, the solvent is vented while the solute molecules continue on their original trajectory and pass into the ion source of the mass spectrometer. The interface allows the use of a standard ion source in either EI or CI modes. It can therefore be used to produce standard library-searchable mass spectra, and is the only commonly used interface where this facility is routinely available. The interface requires some sample volatility, and some compounds (such as complex sugars) do not give satisfactory spectra.

3. **Electrospray.** In the electrospray interface, the column effluent is mixed with a nebulizing gas and passed through a jet nebulizer into a high-voltage electric field. Drop formation and ionization, by a chemical ionization process, occur. The ions enter the mass spectrometer through a capillary tube charged to a different voltage from the remainder of the interface, while the solvent is pumped away. Electrospray interfaces have, thus far, mainly been used for very high molecular weight analytes, although systems for lower molecular weights are being developed. Atmospheric pressure chemical ionization (APCI) is somewhat similar to electrospray except that the ionization process takes place at atmospheric pressure. Both systems can be used for polar compounds, molecular weights up to 100,000 Daltons, and are highly sensitive. However, ionization and separation involve a complex series of mechanisms, and setup and operation of the system, and interpretation of the spectra produced, may be difficult.

Applications in the Electricity Industry

Dissolved Gas Analysis (DGA)

Gas chromatography analysis of gases dissolved in transformer oil has been used for condition monitoring since the early 1970s [6–8]. The large volumes of gas often generated during a transformer fault have been used to trip mechanical relay for some 60 years [9]. It was later realized that if gases are evolved from the oil in sufficient quantities to operate a Buchholz relay, then slowly developing faults would also produce decomposition gases that would be dissolved in the oil. They only appear in the Buchholz at the end of a complicated system of interchange between the gases contained in bubbles rising to the surface and the less soluble atmospheric gases dissolved in the oil. It should therefore be possible to detect any incipient faults which may be present in the transformer early by analysis of the gases dissolved in the oil, using a gas chromatograph. Thermal and electric faults in a transformer produce various characteristic gases that are, to some extent, soluble in the oil. Extraction and GC analysis of dissolved gases can be used for monitoring of transformer condition. Dissolved gas analysis has been accepted as an important and vital condition monitoring technique for power transformers [10–12].

Oil samples can be collected from the equipment using syringes, bottles, or other sampling techniques, as described in IEC 567 [13]. The analysis requires extraction of the dissolved gases from the oil and then injection into a GC. The details of extraction of the gases from the oil are given in IEC 567. Generally, gases are extracted under vacuum using a mercury Toepler pump and the total volume of the extracted gas is measured by bringing to atmospheric pressure. The gases are then separated and determined by gas chromatography. An automated mercury-free instrument can also be used for extraction of dissolved gases [14] and other techniques have been used for extraction of the gases from the oil [15]. A static headspace sampling technique has been combined with capillary gas chromatography to allow dissolved gases and furan-related compounds to be determined in power transformer oils in a single GC run [16].

Regardless of the technique used for the extraction of the gases from the oil, gas chromatography is used for analysis of the gases. Alternative techniques such as mass spectrometry, although very sensitive, have not been used for routine analysis. Infrared spectrometry has been used for detection of gaseous hydrocarbons and carbon oxides [17]. The technique is rapid and accurate, and the detector is very stable. However, it cannot detect hydrogen and atmospheric gases. Hydrogen is a very important incipient gas for transformer condition monitoring. The ratio of oxygen to nitrogen dissolved in the oil is also used as an indication of oil or paper degradation in the transformer (the oxygen is used by reaction with the cellulose).

The gas chromatograph used for analysis of the gases is usually dual channel with FID and TCD detectors. A Poropak column is used for separation of hydrocarbons, and a methanizer is used for converting carbon oxides to methane followed by FID detector, while hydrogen, oxygen and nitrogen are separated on a molecular sieve column and measured by TCD. Other arrangements such as column switching, back flushing should be used if a single detector is going to be used. In such cases, a TCD is usually used as a detector. Infrared detection of hydrocarbons followed by TCD is an alternative arrangement.

A combination of Porapak and molecular sieve column is used for separation of hydrogen, oxygen, and nitrogen, followed by TCD detection. This arrangement requires a flash backflush system to prevent carbon dioxide from entering the molecular sieve column — where it would be so strongly adsorbed that it would require prolonged heating at a high temperature to remove it. The system is capable of detecting 1 ppm hydrocarbons and carbon oxides and 5 ppm hydrogen in the oil. Oxygen and nitrogen in the oil are usually present at high concentration and therefore their detection does not present any problem. High concentrations of acetylene gas in the oil may present some problems, such as poisoning the methanizer catalyst and it may stay in the column for a long time. In such cases, a longer isothermal time and higher oven temperature for cleaning of the column is the recommended technique.

Water has been determined in transformer oils with an accuracy better than 3%, precision better than 4% at the 10-ppm level and detection limit of 0.3 ppm, by headspace sampling and capillary chromatography with TCD detection. The technique could be automated using the headspace GC system proposed for dissolved gas analysis [18].

Furfuraldehyde Analysis (FFA)

Under normal operating conditions, the insulation system of transformers gradually deteriorates and produces various degradation byproducts. Thermal degradation, or aging of the paper insulation, is one of the most important factors in limiting the lifetime of a transformer. Detection and analysis of the degradation byproducts have been widely used to evaluate and monitor the degradation state of the insulation. The aging process of the paper is accompanied by the production of several byproducts — mainly carbon monoxide, carbon dioxide, and furfurals. Carbon oxides can be monitored by DGA, but their production is not specific to paper degradation. The measurement of furfurals could provide an early indication of paper degradation and their analysis by HPLC has been used as a tool for the monitoring of transformer performance [19-22]. A spectrophotometric method has also been used for analysis of furfuraldehyde [23]. The method is only capable of measuring furfuraldehyde and not other furanic compounds present in the oil.

The oil is dissolved in cyclohexane for HPLC analysis and passed through a solid-phase silica cartridge, where the furfurals, phenol, and *m*-cresol (which are products of degradation of phenol-formaldehyde resins in the transformer) are retained. The remaining oil in the cartridge is removed by washing with the solvent. The furfurals, phenol, and *m*-cresol are extracted from the cartridge with water:acetonitrile. The collected extracts are analyzed by HPLC. For separation of furfuraldehyde and other compounds, a C18 column is recommended. A UV detector at 276 nm is usually employed for detecting these compounds. The use of a UV photodiode array detector gives improved discrimination of products in what is often a complex chromatogram at the expense of some slight loss of sensitivity.

Analysis of Antioxidants in Oil

The presence of antioxidants is a key factor in controlling the oxidation of an insulating oil. Their use results in substantial savings by prolonging the oil service life and slowing down the transformer aging process. A large number of antioxidant additives are used, and HPLC is a useful technique for quantitative determination of their concentrations in insulating oil [24,25]. Thin-layer chromatography (TLC) has also been used for quantitative determination of antioxidant in insulating oil [29].

HPLC is also used for evaluation of the quality of mineral insulating oil [26,27]. The presence of certain characteristic chemical compounds is of considerable importance in the electric industry. This technique is also used to identify the presence of some byproducts of oil under electric stress, such as x-wax and fluorescence materials. Polar compounds, such as acids and aldehydes, are also products of oxidation of oil and they can also be determined by HPLC. Early detection of such products is important in transformer condition monitoring to provide prior warning of a developing fault and to enable appropriate corrective action to be taken.

HPLC is also used for health and safety monitoring of the polyaromatic hydrocarbon (PAH) content of transformer oils [28]. The toxic and carcinogenic nature of PAH compounds is well established.

Molecular Weight Distribution of Insulating Paper

Gel permeation chromatography has been used to measure the change in molecular weight distribution of insulating paper during aging [30]. This technique has been used for measurement of the degree of polymerization of the paper, but requires a sampling of the paper in the transformer, which is not generally practical. Measurement of paper degradation by analysis of products dissolved in the oil, such as FFA, although much easier, is indirect and therefore dependent on a knowledge of the history of the transformer and its components. GPC can provide direct information of the state of the paper and the average molecular weight of the cellulosic chains, and currently is mostly used as a forensic analysis tool for the investigation of failures.

Two techniques are available for getting the paper into solution for analysis. Direct dissolution into dimethylacetamide/8% lithium chloride is possible for most forms of cellulose, followed by dilution to 1% lithium chloride for analysis. However, high levels of lignin (3–4%) in the paper interfere with the dissolution process. The alternative is to derivatize the cellulose to the tricarbonylate in pyridine. The product can then be analyzed in solution in tetrahydrofuran, but there is evidence in the literature that the derivatization process itself degrades the paper.

Polychlorinated Biphenyls

Polychlorinated biphenyls (PCBs) are synthetic materials with dielectric and chemical properties that in the past made them attractive alternatives to petroleum-based products. However, they have since been identified as environmental pollutants and possible health hazards. PCBs are not used today, but their use in the past has led to widespread contamination of mineral oil with PCBs. Current legislation requires that oil in service shall have a PCB content of less than 50 ppm. Therefore, the PCB content of insulating oil in the transformer must be measured quantitatively and capillary GC is the technique currently used [31].

The sample is diluted in hexane and deoxygenated. A small volume of the resulting solution is injected into a narrow-bore capillary gas chromatographic column. The capillary column separates the PCBs into individual or small groups of overlapping congeners. Their presence in the effluent is measured by an electron capture detector (ECD).

Feedwater and Boiler Water Analysis

Ion chromatography (IC) is well suited to the analysis of highly pure water such as boiler feedwater, and often gives better precision, sensitivity, and speed of analysis than established techniques. For example, IC has been used for the determination of carbonic acid in steam-condensate cycles [32].

Morpholine is added to the thermal cycle of some CANDU reactors, and has been determined, together with its amine breakdown products, by reversed-phase HPLC on a C18 column with visible detection at 456 nm [33].

Other Applications

The size and scope of the electricity supply industry imply that it has a major effect on the environment. Chromatographic techniques are widely applied in environmental monitoring and research, and the electricity industry is both a major user of standard techniques and sponsor of research.

Defining Terms

Adsorption: The noncovalent attachment of one substance to the surface of another.

Analyte: The substance that is being analyzed.

Baseline resolution: Separation of components at the peak base (no overlap of any peak area).

Chromatography: The physicochemical technique for separation of mixtures into their components.

Column: A steel, glass, or plastic tube containing the stationary phase.

Detector: A device for monitoring the separated compounds from the chromatography by sensing chemical or physical properties of the sample.

Eluent: The moving solvent in a chromatographic column.

Elute: To travel through and emerge from the column.

Gel permeation chromatography (GPC): A mode of LC in which samples are separated according to molecular size.

HPLC: High-performance liquid chromatography.

IC: Ion chromatography.

Mobile phase: The following solvent.

Stationary phase: The material that is contained in the column and does not move during the chromatographic process.

Acknowledgments

The authors would like to thank Perkin-Elmer and Phenomenex for permission to reproduce diagrams.

References

1. C.F. Poole and S.A. Schuette, *Contemporary Practice of Chromatography*, Elsevier Science BV, Amsterdam, 1984.
2. R.L. Grob (ed.), *Modern Practice of Gas Chromatography, 3rd ed.*, New York; John Wiley & Sons, 1995.
3. G. Guiochon and C.L. Guillemin, Quantitative gas chromatography for laboratory analyses and on-line process control, *J. Chromatogr. Library*, Vol. 42, Elsevier Science, Amsterdam, 1988.
4. J. Weiss, *Ion Chromatography, 2nd ed.*, VCH Publishers, Cambridge, U.K., 1994.
5. J.J. van Deemter, F.J. Zuiderweg, and A. Klinkenberg, Longitudinal diffusion and resistance to mass transfer as causes of non-ideality in chromatography, *Chem. Eng. Sci.*, 5, 271, 1956.
6. P.S. Pugh and H.H. Wagner, Detection of incipient faults by gas analysis, *TAIEE*, 80, 189-195, 1961.
7. L.C. Aicher and J.P. Vora, Gas analysis — a transformer diagnostic tool, *Allis Chalmers Electrical Review*, 28, 22-24, 1963.
8. E. Dornenburg and W. Strittmatter, Monitoring oil-cooled transformers by gas analysis, *Brown Boveri Review*, 61(5), 238, 1970.
9. M. Buchholz, The Buchholz protection system and its application in practice, *E.T.Z.*, 49, 1257-1260, 1928.
10. R. Muller, K. Potthoff, and K. Soldner, The analysis of gases dissolved in the oil as a means of monitoring transformers and detecting incipient faults, *CIGRE*, paper 12-02, 1970.
11. E. Dornenburg and K. Schober, Determination and analysis of gases formed in transformers. Evaluation of gas analysis results, *CIGRE*, paper 15-01, 1972
12. J.R. Booker, Experience with incipient fault detection utilizing gas chromatographic analysis, *Doble Client Fortieth Annual International Conference*, 10-5.1, 1973.
13. IEC publication 567, *Guide for the sampling of gases and oil from oil-filled electrical equipment and for the analysis of free and dissolved gases*, 1992.
14. B. Pahlavanpour, Mercury-free extraction of dissolved gases in transformer oil, *AVO International Technical Conference*, Dallas, 1996.
15. T.J. McGarvey, An automated system for analysis of gases dissolved in electrical insulating oil by headspace gas chromatography, *Doble Client Fifty-Seventh Annual International Conference*, 10-8.1, 1990.
16. Y. Leblanc, R. Gilbert, J. Jalbert, M. Duval, and J. Hubert, Determination of dissolved gases and furan-related compounds in a single chromatographic run by headspace/capillary gas chromatography, *J. Chromatogr. A*, 657, 111-118, 1993.
17. J. Jalbert, S. Charbonneau, and R. Gilbert, A new analytical method for the determination of moisture in transformer oil samples, *Sixty Third Annu. Conf. Doble Clients*, Boston, MA, March 25-29, 1996.

18. B. Pahlavanpour, S. McCann, and M. Ali, Preliminary investigation into the use of Fourier transform infrared analysis of continuous monitoring of dissolved gases in transformer oil, *Natl. Grid Tech. Rep.*, TR(T)38, 1993.
19. P.J. Burton, J. Graham, A.C. Hall, J.A. Laver, and A.J. Oliver, Recent developments by CEGB to improve the prediction and monitoring of transformer performance, *CIGRE*, paper 12-09, 1984.
20. X. Chendong, Monitoring paper insulation aging by measuring furfural contents in oil, *Proc. 5th Int. Symp. High Voltage Engineering*, 139, 1991.
21. A. DePablo, R. Andersson, H.J. Knab, B. Pahlavanpour, M. Randoux, E. Serena, and W. Tumiatti, Furanic compounds analysis as a tool for diagnostic and maintenance of oil paper insulation system, *CIGRE*, 110-09, 1993.
22. J. Unsworth and F. Mitchell, Degradation of electrical insulating paper monitoring with high performance liquid chromatography, *IEEE Trans. Elec. Insul.*, 25, 737, 1990.
23. B. Pahlavanpour and G. Duffy, Development of a rapid spectrophotometry method for analysis of furfuraldehyde in transformer oil as an indication of paper aging, *CEIDP Annual Report*, 493, 1993.
24. C. Lamarre and A. Gendron, Analyse quantitative par chromatographie liquide haute performance du di-*tert*-butyl-2,6-*para*-cresol dans les huiles de transformateurs, *J. Chromatogr.*, 464, 448-452, 1989.
25. M. Duval, S. Lamotte, D. Gauchon, C. Lamarre, and Y. Giguette, Determination of low-improved additives in new and aged insulating oil by gel permeation chromatography, *J. Chromatogr.*, 244, 169-173, 1982.
26. M. Duval and C. Lamarre, The characterization of electrical insulating oils by high-performance liquid chromatography, *IEEE Trans. Electr. Insul.*, E12, 340-348, 1977.
27. M. Duval, C. Lamarre, and Y. Giguere, Reversed-phase high-performance liquid chromatographic analysis of polar oxidation products in transformer oils, *J. Chromatogr.*, 284, 237-280, 1984.
28. A.N. Gachanja, Analysis of polycyclic aromatic hydrocarbons by liquid chromatography, *Chromatography and Analysis*, February-March, 5-7, 1993.
29. IEC Publication 666, *Detection and determination of specified anti-oxidant additives in insulating oil*, 1979
30. D.J. Hill, T.T. Le, M. Darveniza, and T. Saha, A study of degradation of cellulosic insulation materials in a power transformers. Part 1. Molecular weight study of cellulose insulation paper, *Polymer Degradation and Stability*, 48, 79-87, 1995.
31. B. Pahlavanpour and G. Duffy, Analysis polychlorinated biphenyls in transformer oils by gas chromatography, *Natl. Grid Publication*, RDC/0045/R91, 1991
32. S. Charbonneau, R. Gilbert, and L. Lepine, Determination of carbonic acid in steam-condensate cycle samples using non-suppressed ion chromatography, *Anal. Chem.*, 67, 1204-1209, 1995.
33. C. Lamarre, R. Gilbert, and A. Gendron, Liquid chromatographic determination of morpholine and its thermal breakdown products in steam-water cycles at nuclear power plants, *J. Chromatogr.*, 467, 249-258, 1989.